THE UNIVERSITY OF CHICAGO

EXPLORING THE REGULATORY ROLE OF CELLULAR PRION PROTEIN (PRP^C) IN AMYLOID PRECURSOR PROTEIN (APP) PROCESSING AND TRAFFICKING: IMPLICATIONS FOR ALZHEIMER'S DISEASE THERAPEUTICS

A DISSERTATION SUBMITTED TO
THE FACULTY OF THE DIVISION OF THE BIOLOGICAL SCIENCES
AND THE PRITZKER SCHOOL OF MEDICINE
IN CANDIDACY FOR THE DEGREE OF
DOCTOR OF PHILOSOPHY

COMMITTEE ON NEUROBIOLOGY

BY

NIKITA MEHTA

CHICAGO, ILLINOIS

AUGUST 2024

To my parents, who gave me and Tani the best gift that you can give your children, and the most valuable commodity in the world - time.

“The credit belongs to the man who is actually in the arena, [...] who spends himself in a worthy cause; who at the best knows in the end the triumph of high achievement, and who at the worst, if he fails, at least fails while daring greatly, so that his place shall never be with those cold and timid souls who neither know victory nor defeat." - Theodore Roosevelt, "Citizenship in a Republic"

CONTENTS

LIST OF FIGURES

LIST OF TABLES

ACKNOWLEDGMENTS

Mastrianni laboratory: I want to thank the Mastrianni lab, especially my advisor, Jim Mastrianni. Observing your clinical empathy has inspired my own aspirations to pursue medicine. Thank you for your invaluable support and guidance through my graduate school experience, and for always making time to meet despite your schedule - I'm deeply grateful.

Thinakaran laboratory: I want to thank Gopal Thinakaran for giving me the opportunity of a lifetime to conduct research at the Byrd Alzheimer's Research Center. Gopal, your mentorship has been transformative, and your generosity has been invaluable. Thank you for sharing your time and resources with me so graciously. To the Thinakaran laboratory, especially Stas Stanislau, Melike Yuksel, and Lisa Collier, your willingness to share your expertise has been a gift.

My Thesis Committee: Peggy Mason, thank you for your enduring mentorship since my undergraduate days, for seeing potential in me, and steering me towards neuroscience. You have created a legacy through your mentorship of students that I feel very lucky to be a part of. Steve Meredith, our discussions have been pivotal in simplifying complex scientific problems. Thank you for always being willing to meet with me. Sam Sisodia, your scientific insights and generous sharing of resources have enriched my research experience immensely. Thank you for challenging me to think critically in evaluating my own science and the science of others.

Collaborators: Jonathan Aow, Eric Norstrom, and Russ Taylor, thank you for your scientific input, time, and friendship. Thank you to the The Duchoissois Family Institute, especially Ashley Sidebottom and Nick Dylla for all your experimental design input.

Scholarships: I'm very grateful for the Ralph W. Nichols International House Fellowship (International House, University of Chicago), Rita Levi Montalcini Award (Dompé Foundation), and BSD Donald Steiner Award (Steiner Family, University of Chicago).

Administrative Support: I want to thank the Neurology department, the Neuroscience Institute, and the Office of Graduate and Postdoctoral Affairs, particularly Erika Slaughter, Elena Rizzo, Dan McGehee, Lili Gonzalez Hernandez, David Kovar, Diane Hall, and Melissa Lindberg, for all your support and kindness.

Mentors: To Brooke Carrell, Jason Merchant, Jo Cai, Nick Seamons, and my Graduate Council and IGSAB teams, thank you for enriching my experience at UChicago, teaching me how to lead with grace, and for your friendship through everything.

Friends and Family: To all my friends, thank you for your unwavering love and support. Mira, Annika, Jelena, Sone, Linnea, Elle, Sandra, Grace, Ben, Cynthia, John, and Elise - I would not be here today without you. Thank you to the Lemp family for opening your doors to me on every family occasion and holiday, and making Chicago feel like home.
Forrest, thank you you for your never-ending encouragement, kindness, patience, and all the happiness you've brought into my life. Macus and Carmela, thank you for welcoming me into the Haydon and Alonso families, and for giving me another home in Chicago. Mom, Dad, and Tani, thank you for loving me unconditionally, and for believing I can do anything.

My heart is full of gratitude for everyone who made this journey possible.

ABSTRACT

Prion protein (PrP^C) interacts with 38 to 42 amino acid amyloid-β (Aβ) peptides released by proteolytic processing of amyloid precursor protein (APP). Our laboratory previously reported a direct relationship between PrP^C expression and the levels of secreted Aβ_{42}, but the underlying mechanisms were unclear. I sought to test whether PrP^C exerts its effect on Aβ by modulating APP processing. I quantified APP synthesis and Aβ secretion following siRNA-induced knockdown (KD) of PrP^C in mouse neuroblastoma (N2a) cells stably expressing human APPwt (N2a-APPwt) or human APP carrying the Swedish mutation (N2a-APPswe). PrP^C KD significantly reduced net Aβ peptide secretion in both cell lines without affecting APP expression or extracellular Aβ degradation. PrP^C KD also significantly reduced sAPPβ release in both cell lines and increased sAPPα production in N2a-APPwt but not in N2a-APPswe cells. Surface biotinylation and immunofluorescence labeling studies revealed an increase in the levels of surface APP and an increase in intracellular APP C-terminal fragments (CTFs) following PrP^C KD. Using a previously validated method to assess APP CTF levels *in vivo*, I found an increase in APP CTF levels in female transgenic mice lacking PrP^C compared to wild-type mice. These findings are consistent with a model whereby PrP^C expression limits APP delivery to the plasma membrane and APP internalization, facilitating amyloidogenic APP processing and Aβ secretion. Our results suggest that reducing PrP^C expression might be a therapeutic avenue for treating AD by limiting BACE1-cleavage of APP, an essential step in Aβ production.

CHAPTER 1

CHAPTER 1: GENERAL INTRODUCTION

1.1 Neurodegenerative Diseases are Linked by Protein Misfolding and Aggregation

Alzheimer's disease (AD), Prion Disease (PrD), Parkinson's disease (PD), Huntington's disease (HD), and amyotrophic lateral sclerosis (ALS) are neurodegenerative diseases characterized by the gradual loss of neuron function and structure [116, 160]. While the clinical manifestations of neurodegenerative disorders are diverse, many of these diseases are linked by their shared etiology of "misfolding" and aggregation of an otherwise normal protein in the central nervous system (CNS) [34], a mechanism of disease initially promoted by studies of PrD [34, 114, 115]. These disorders also share other common pathological features, including genetic mutations, mitochondrial dysfunction, oxidative damage, and protein aggregation [116, 160].

1.1.1 Mutations Leading to Protein "Misfolding" Diseases"

Mutations in specific genes have been linked to the familial forms of these diseases, providing insights into their pathogenesis. For example, mutations in the genes encoding amyloid precursor protein (APP), presenilin 1 (PS1), and presenilin 2 (PS2) are associated with early-onset AD, highlighting the role of amyloidβ (Aβ) peptide accumulation in disease progression [12]. The amyloid cascade hypothesis, originating from observations in AD, suggests that the accumulation of toxic Aβ peptides initiates a series of events leading to neuronal damage and cognitive decline [12, 56]. This process involves complex molecular pathways, including the abnormal processing of APP, leading to the production of neurotoxic Aβ peptides. These insights into AD's molecular basis have spurred research into mechanisms of other neurodegenerative diseases [12].

1.1.2 Mitochondrial Dysfunction and Oxidative Stress

Additionally, mitochondrial dysfunction and oxidative stress are central to the pathogenesis of these disorders, and contribute to neuronal damage. In AD, synaptic failure and neuronal loss precede the formation of amyloid plaques and neurofibrillary tangles, with early signs of disease involving synaptic function and dendritic structure alterations [12, 160]. Similar disruptions in cellular homeostasis, energy metabolism, and redox balance are implicated in PD, HD, and ALS, underlining the importance of mitochondrial integrity and oxidative stress management in neuronal survival [12, 160].

1.1.3 Protein Aggregation

AD is marked by the accumulation of amyloid plaques and neurofibrillary tangles, primarily composed of insoluble protein or peptide aggregates. Similar protein misfolding and aggregation phenomena are observed in PD, where α-synuclein accumulates in Lewy bodies, in HD with mutant huntingtin protein aggregates, and in ALS, where various protein aggregates (superoxide dismutase among others) disrupt normal cellular functions [12, 116, 160]. There is also a large body of evidence demonstrating that different disease-causing protein aggregates share structural features, such as polypeptide chain organization into cross-β spines, and in some cases, aggregation propensity [2, 39, 99, 123]. These factors may interact with each other in ways that either advance or attenuate overall disease progression. The cellular prion protein (PrP^C), the central protein linked to PrD, may interact with AD-related proteins, through poorly understood mechanisms. It is not known whether PrP^C promotes or mitigates AD toxicity, and under what circumstances either may occur [1, 34, 43, 45, 80, 118, 122, 134].

The primary goal of our research extends beyond genetic factors, and focuses on understanding the protein trafficking pathways common to various diseases, which may identify

convergent points that offer potential for broad-spectrum therapies.

1.2 The Molecular Basis of Prion Disease

1.2.1 Prion Diseases

The prion diseases (PrDs) are a family of transmissible and fatal neurodegenerative disorders. PrDs are rare, with an annual global incidence of 1-2 cases per million for sporadic, genetic, and acquired forms combined [26, 100, 124]. Descriptions of PrD were first documented in Spanish merino sheep being transported to England in the 18th century [159]. In these sheep, a key symptom of the PrD was an intense itching that compelled them to scrape against fences, which led to the disease being named "Scrapie" [159]. Other symptoms included abnormal behavior and progressive ataxia [159]. This disease can now be detected in the blood up to twelve months prior to symptom onset, once the sheep exhibited symptoms, they never recovered. Scrapie once spread rampantly among flocks, and resulted in the death of both imported and endemic flocks [159]. Histopathalogically, scrapie is characterized by diffuse gliosis, neuronal death, and vacuolation in nervous tissue (spongiform degeneration) and deposits of the PrP [48, 135, 158]. When its transmissible nature was demonstrated in goats via intraocular inoculation [68], Scrapie was defined as a transmissble spongiform encephalopathy, which is the term used to describe PrDs today. The primary human prion diseases include Creutzfeldt-Jakob disease (CJD), variant CJD, Gerstmann-Sträussler-Scheinker (GSS) disease, fatal familial insomnia (FFI), and variably protease-sensitive prionopathy (VPSPr) [66]. Distinct pathological features are used to categorize these diseases, especially anatomic distribution of lesions. In addition, CJD is characterized by the especially prominent spongiform degeneration, while in GSS extracellular deposits of PrP amyloid is more prominent, FFI is marked by thalamic neuronal loss and astrogliosis [11, 113– 115]. Common symptoms across prion diseases are progressive cognitive decline that leads to dementia, severe gait and coor-

dination deterioration, and muscle twitching [3]. The incubation period of PrD is long, but after the onset of clinical symptoms, most PrDs progress with alarming celerity, leading to early death [26, 100, 124].

1.2.2 PrP^C and PrP^{Sc} in Prion Disease

The cellular isoform of prion protein (PrP^C) is central to the development of PrDs, and as such, has been well characterized. PrP^C is encoded by the *PRNP* gene, which is located on the short arm of chromosome 20 in humans [84, 113]. PrP^C has the ability to misfold into a protease-resistant β-sheet-rich conformation, designated PrP^{Sc}. PrP^{Sc}, in turn, propagates itself by templating its conformation onto resident PrP^C, which generates new PrP^{Sc} oligomers, protofibrils, and fibrils that deposit as PrP amyloid [34, 124]. PrDs are distinguished from other protein misfolding disorders, such as AD, by their ease of transmissibility and their requirement for PrP^C [11, 32, 100, 124]. While the annual global incidence of PrDs is only one to two cases per million [26, 100, 124], understanding the role of PrP^C in other protein misfolding disorders could lead to breakthroughs in treatment for AD and other more common neurodegenerative diseases.

1.2.3 The Structure and Function of PrP^C

The function of PrP^C has not been completely elucidated. Studies have pointed to its involvement in regulating synaptic function, protecting the synapse from excitotoxicity-mediated cell death, cell differentiation, and $Cu^{(2+)}$ recycling and metabolism [15, 93, 96, 110, 140, 148]. Human PrP^C is translated as a 253 amino acid (aa) protein, whereas its mouse homolog is 254 aa. Upon translocation of PrP into the endoplasmic reticulum (ER), the 22 aa N-terminal secretory signal peptide is cleaved from PrP, and 23 C-terminal residues are removed after the addition of the glycosylphosphatidylinositol (GPI) anchor to the serine residue at position 231. As a result, the mature forms of mouse and human PrP contain 209 and 208

aa respectively [18, 30, 124]. Using the mouse numbering system, mature PrP is predicted to contain a flexible N-terminal segment from aa 23 to 122, in which a $Cu^{(2+)}$-binding octapeptide repeat region (aa 60-95) flanked by charge cluster 1 (aa 23-28) and charge cluster 2 (aa 100-109) resides. This segment is followed by a hydrophobic core (aa 112-133) and a globular C-terminal domain (aa 134-231) comprised of three alpha helices and two anti-parallel beta sheets [18, 96, 113, 124]. PrP is folded in the ER prior to transport to the Golgi apparatus, where it is differentially N-glycosylated at sites Asn180 and Asn196 [30]. PrP^C is anchored to the outer leaflet of the plasma membrane via the GPI anchor, although some forms of PrP^C may display a transmembrane topology [96]. PrP^C at the membrane can exist in unglycosylated, mono-glycosylated, or di-glycosylated forms (i.e., at the above Asn residues). There is some evidence for differential glycosylation states for varying prion strains [30, 95, 97].

1.3 The Production of Aβ from Amyloid Precursor Protein

Aβ is generated by the endoproteolysis of its parent protein, amyloid precursor protein (APP), by sequential cleavage of APP by groups of enzymes or enzyme complexes termed α-, β-, and γ- secretases (Figure 1.1) [79]. As described in more detail, below, cleavage first occurs by either α- or β-secretase. Cleavage by both of these secretases does not occur. This cleavage is a necessary precursor of cleavage by the γ-secretase complex.

1.3.1 α-, β-, and γ- Secretases

α-secretase

The α-secretases are a family of enzymes including metalloproteases. The latter are inhibitors of platelet aggregation and integrin-dependent cell adhesion [79]. The α-secretases play a role in the regulation of learning and memory formation [79]. The three primary enzymes with α-secretase activity are ADAM9, ADAM10, and ADAM17. α-secretase activity predominantly resides on the plasma membrane [79, 144].

β-secretase

β-secretase is better known as β-site APP-cleaving enzyme (BACE1). BACE1 is a Type I integral membrane protein in the family of aspartyl proteases, of which the prototype is pepsin [64, 79, 133, 149]. While mutations in the BACE1 gene are not directly linked to familial AD, individuals with AD have increased levels and activity of BACE1 [55].

γ-secretase

γ-secretase is a complex of proteins that includes presenilin 1/2 (PS1 and PS2), nicastrin, anterior pharynx defective (APD), and presenilin enhancer 2 (PSE2) [44, 83, 138, 161, 163]. In addition to APP, γ-secretase has over 140 known substrates and substrate candidates, including proteins involved in cell adhesion, signaling, and neuronal function [63]. Approximately 150 AD related mutations have been found in the PS1 and PS2 complexes to date [38, 150, 164].

1.3.2 APP Cleavage

Broadly, APP cleavage can be subdivided into the non-amyloidogenic pathway, which does not result in the production of Aβ peptides, and the amyloidogenic pathway, which does result in the production of Aβ peptides (Figure 1.1 and 1.2). In the non-amyloidogenic pathway (Figure 1.1), APP is first cleaved by α-secretase at a position 83 amino acids from C-terminus of the protein. This cleavage produces an N-terminal ectodomain sAPPα, which is secreted into extracellular space, leaving behind an 83 aa C-terminal fragment of APP, α-CTF. γ-secretase cleaves the resulting 83 aa C-terminal fragment of APP to produce p3, which is also released extracellularly, and a C-terminal fragment (CTF) - APP intracellular domain, or AICD; this domain remains intracellular.

In the amyloidogenic pathway (Figure 1.2), APP is first cleaved by β-secretase at a po-

sition 99 amino acids from C-terminus of the protein. This cleavage produces an N-terminal ectodomain, sAPPβ, which is secreted into extracellular space, resulting in a 99 aa C-terminal part of the protein that remains intracellular, β-CTF. β-secretase can cleave APP at the +1 or +11 site of Aβ, which generates C-terminal fragments of variable length [21]. γ-secretase then cleaves the 99 aa C-terminal fragment of APP between residues 38 and 43, to produce Aβ peptides of various lengths that are released into the extracellular space. Like in the non-amyloidogenic pathway, the resulting CTF, AICD, remains intracellular.

1.4 Amyloid-β in Alzheimer's Disease

1.4.1 The Amyloid Cascade Hypothesis

The amyloid cascade hypothesis, first proposed by Hardy and Higgins in 1992 [56, 126], is centered on the idea that β-sheet rich amyloid fibrils formed from extracellular Aβ deposits are the root cause of AD. Hardy and Higgins posited that other observed AD hallmarks - neurofibrillary tau tangles (NFTs), cell death, and dementia - are a direct result of these Aβ deposits [56, 126]. AD is characterized by brain deposition of extracellular amyloid plaques comprised of aggregates of Aβ, 38-42 aa peptides derived from amyloid precursor protein (APP) by sequential enzymatic cleavage (Figure 1.2), as described above. In addition, intraneuronal NFTs are comprised of aggregates of hyperphosphorylated tau protein are a second histopathological hallmark of AD [27, 79].

1.4.2 An Alternative Hypothesis to Describe AD Progression

The Inside-Out Amyloid Hypothesis offers an non-mutually exclusive alternative to traditional models of Alzheimer's disease progression, focusing on the internal accumulation of Aβ peptides within neurons rather than external aggregation that subsequently leads to plaque formation [47, 112]. In this model, intracellular Aβ can be generated when extracellu-

lar Aβ binds to specific cell surface receptors and is internalized into endosomes as an Aβ-receptor complex [47, 79, 112]. Alternatively, if C99 is not immediately cleaved by γ-secretase at the plasma membrane, it can be transported to other intracellular compartments where γ-secretase resides, and cleaved there instead [47, 79, 112]. In addition, γ-secretase has high processivity, which means that it catalyzes consecutive, short, reactions without releasing substrate, allowing for the release of shorter, more soluble forms of Aβ [79, 112]. The processivity of γ-secretase can be lost if one of the enzymes in its complex is mutated, resulting in an increase in intracellular C99 Aβ_{42} isoforms, an isoform of Aβ that is hydrophobic and prone to aggregation [79]. Moreover, studies have shown that partial inhibition of γ-secretase actually increases both C99 and Aβ_{42} isoforms, which may contribute to cellular toxicity [79].

This hypothesis is based on studies showing age-related increases in the overall concentration of Aβ in Alzheimer's Disease (AD) mouse and human brains and the accumulation of Aβ in endosomes near synapses [47, 112]. This intracellular accumulation is hypothesized to be an early event leading to progressive Aβ aggregation and pathology, particularly affecting neurites and synapses. It has also been observed that synaptic activity modulates Aβ-dependent synapse pathology in AD models independently of plaque formation, suggesting that intraneuronal Aβ may contribute to the development of AD [47, 112].

While the two main histopathologic features, neuritic plaques and neurofibrillary tangles, are often used to diagnose AD, evidence suggests that Aβ plaques and clinical disease severity are only weakly correlated [7, 51, 65, 67, 127**?**] . More specifically, cognitive symptoms of AD sometimes manifest years after Aβ deposition and detectable plaque formation. Clinical trials of Aβ plaque-clearing drugs have been largely unsuccessful. Taken together, these findings suggest that Aβ accumulation trigger degenerative processes that are irreversible long before plaques are visible and diagnostic [46, 62, 101]. In line with these studies, Aβ fibrils may be

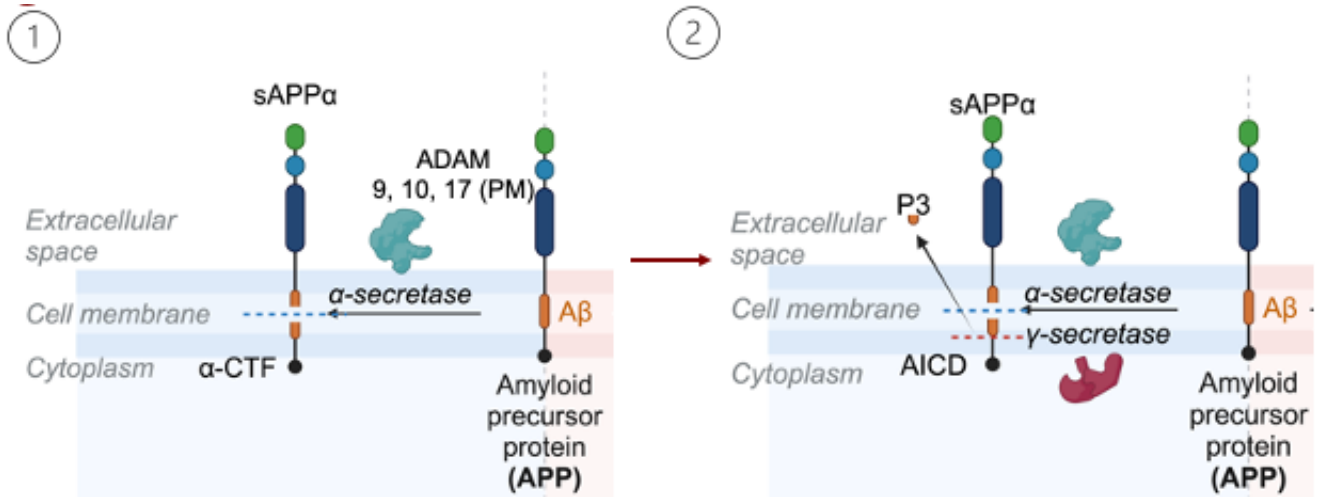

Figure 1.1: Amyloid precursor protein processing: The processing of amyloid precursor protein (APP) can follow two main pathways. **A.** In the non-amyloidogenic pathway, α-secretase cleaves APP within the Aβ region, releasing a soluble ectodomain, sAPPα into the extracellular place. The remaining intracellular C-terminal fragment (CTF), C83, is subsequently cleaved by γ-secretase, resulting in the release of both the p3 fragment and the APP intracellular domain (AICD), the latter of which remains intracellular.

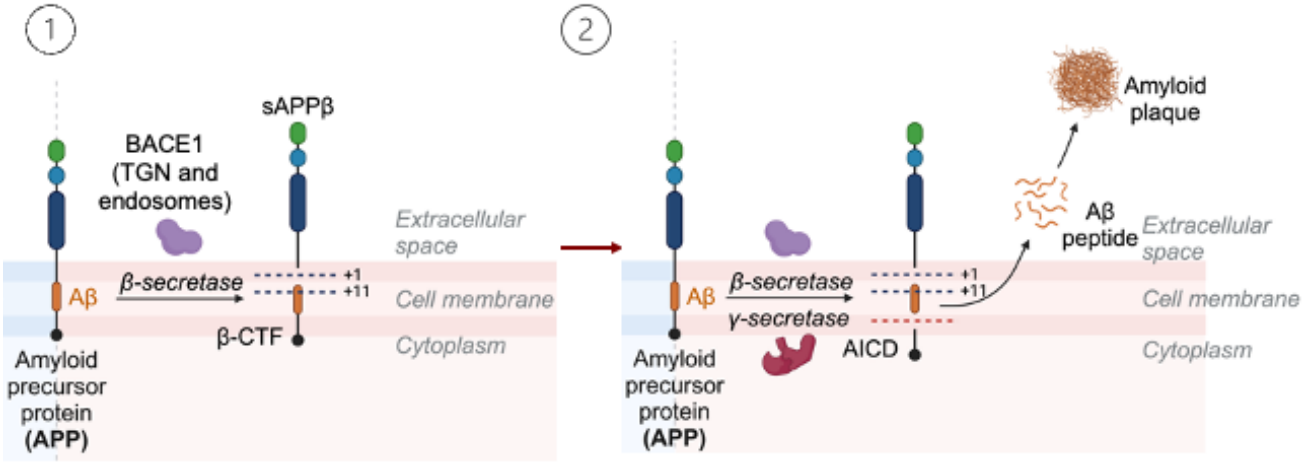

Figure 1.2: Amyloid precursor protein processing: The processing of amyloid precursor protein (APP) can follow two main pathways. In the amyloidogenic pathway, β-secretase cleaves APP to release the soluble sAPPβ fragment extracellularly. This leaves behind a CTF, C99, which γ-secretase further processes to create Aβ peptides of variable length, leaving behind AICD. The alternative hypothesis is that C99 does not get processed by γ-secretase immediately, but exerts intracellular toxic effects, and can later be cleaved to release Aβ intracellularly. Made with BioRender.com.

less directly neurotoxic than the soluble Aβ oligomers [31]. Studies have demonstrated that soluble Aβ oligomers can facilitate the formation of cofilin-actin rods that impair synaptic function and long-term potentiation (LTP), disrupt learned behaviors, affect spatial memory, reduce expression of critical receptors in the neuronal membrane, and markedly alter dendritic spine morphology [27, 31, 78, 82, 134, 154].

1.5 APP and PrP^C Share Similar Trafficking Pathways

APP and PrP^C are trafficked through similar intracellular pathways, and are expressed on the surface of neurons, endosomes, exosomes, as well as other membranes within the cell [23]. As a result, there are several potential locations where APP and PrP^C might interact. Broadly, APP and PrP^C trafficking can be subdivided into the secretory and endocytic pathways.

1.5.1 Secretory Pathway

In the secretory pathway, APP and PrP^C are synthesized in the endoplasmic reticulum (ER) and undergo post-translational modifications in the Golgi before being trafficked to the plasma membrane [111]. In neurons, APP and PrP^C are both transported to axons and dendrites through anterograde transport mediated by kinesin [34, 35, 54, 75, 152]. PrP^C is housed in bidirectional vesicles that undergo both anterograde and retrograde transport and require dynein and kinesin-1 light and heavy chain holoenzymes, depending on the type of transport [42, 152]. In contrast, APP moving towards the axon is housed in unique tubular unidirectional structures [35, 54]. In neurons, most APP remains localized to the Golgi or trans-Golgi Network (TGN), and only 10% of APP makes it to the cell surface, from where it is either shed after proteolytic cleavage or internalized through caveolin- or clathrin-dependent mechanisms [54]. PrP^C can also be shed into the extracellular space through proteolytic cleavage by zinc metalloproteases [107], but most PrP^C is internalized and recycled back to the plasma membrane in endosomes, transiting through the cell in $\sim$ 60 minutes [58, 130]. Once inter-

nalized, PrP and APP can either be recycled to the plasma membrane or TGN, or taken through the endocytic pathway [4, 54, 57, 141].

1.5.2 Endocytic Pathway

In the endocytic pathway, proteins targeted for degradation are sorted into intraluminal vesicles (ILVs) within late endosomes, which are then termed multivesicular bodies (MVBs) [111]. MVBs can either fuse with lysosomes, which results in degradation of ILV content, or they can fuse with the plasma membrane, which results in release of the ILVs into the extracellular space as "exosomes" [111]. There is evidence that Aβ and PrP^C may interact at one or more points in the secretory and endocytic pathways, which provides a basis for targeting shared trafficking pathways when designing therapeutics for AD [59, 118].

1.6 Bridging the Gap: Exploring Potential Roles for PrP^C in Alzheimer's Disease

PrP^C has been implicated in AD, although its role in mediating AD-related toxicity is still unclear. PrP^C binds with high affinity to Aβ peptides at human PrP^C residues 23–27 and 91–119 (aa 90-118 in mice), the latter of which has been reported by different groups with some variation in length, depending on the methodology, Aβ preparation, and model system used [27, 34, 45, 80, 157, 165].

1.6.1 A Neurotoxic Role for PrP^C in Alzheimer's Disease

Early evidence for its direct role in AD came from studies that found PrP^C to function as a possible suppressor of BACE1 [49, 50, 108], the enzyme involved in the initial cleavage of APP required for the generation of Aβ peptide in the amyloidogenic pathway [33] (Figure 1.1). Some groups have shown that the binding of Aβ oligomers to cell surface PrP^C is required for

AD-related toxicity, specifically by mediating hippocampal LTP impairment [45, 80, 122, 134], as Aβ-induced LTP impairment is not observed when PrP^C is mutated or deleted [45], all of which would suggest a neurotoxic role for PrP^C in AD.

1.6.2 A Neuroprotective Role for PrP^C in Alzheimer's Disease

On the other hand, in a recent study from our laboratory, intracellular Aβ levels were increased in mouse models of AD, in which the mice lack PrP^C expression, compared to the same type of mouse but expressing normal levels of wild-type (wt) PrP^C [118]. This same study also demonstrated that Aβ and PrP^C colocalize and are pulled down together in exosomes, suggesting that PrP^C might aid in the transport of intracellular Aβ to exosomes for secretion. Other groups have demonstrated that intracellular Aβ association with exosomal PrP^C could promote fibrilization of Aβ, which may be a less toxic aggregated form of the peptide than soluble oligomers [43]. These studies suggest a neuroprotective role of PrP^C in binding to Aβ and facilitating its export from the cell, possibly through exosome secretion [118], although other routes are currently being explored.

1.7 PrP^C Binds to Other Proteins Linked to Neurodegenerative Disorders

Recent work suggests that PrP^C can bind to other proteins believed to be involved neurodegeneration, such as tau and α-synuclein [34, 147]. Aβ, tau, and α-synuclein all appear to induce neuronal toxicity via a PrP^C-mediated mechanism. Some studies have demonstrated that PrP^C ablation prevents the LTP impairment and neuritic dystrophy caused by aggregation of all of these soluble proteins [34]. In possible conflict with these findings, other studies have shown that ablation or overexpression of PrP^C has no effect on the Aβ-induced LTP impairment in brain slice preparations from transgenic AD mouse models [22]. Apparent dif-

ferences between these findings might be related to differences in the aggregation state and solubility of their protein preparations. Most of the existing research has primarily focused on the interaction between plasma membrane-bound PrP^C and extracellular protein assemblies [34, 40, 45]. Interactions between PrP^C and intraneuronal disease-causing proteins and possible roles for PrP^C in intraneuronal accumulation of misfolded proteins remain unclear. Separating the function of extracellular PrP and intracellular pools of PrP^C may reveal key differences in their function and define opportunities for the selective modification of one pool over the other to mitigate the development of AD and potentially other neurodegenerative diseases. Overall, the studies highlighted in this section demonstrate the complexity of PrP^C's role in neurodegenerative disease.

CHAPTER 2

CHAPTER 2: THE EFFECT OF PRP^C EXPRESSION ON THE INTRACELLULAR PROCESSING AND TRAFFICKING OF APP, AND ON SUBSEQUENT Aβ RELEASE

2.1 Introduction

Early evidence for PrP^C's direct role in AD came from studies that found PrP^C to function as a possible suppressor of β-site APP Cleaving Enzyme 1 (BACE1) [108], which is responsible for the initial cleavage of APP required for the generation of Aβ peptide in the amyloidogenic processing pathway [33]. This work suggested that PrP^C may function to inhibit BACE1 activity when localized to lipid rafts, thereby reducing Aβ generation [108]. However, subsequent studies have found that PrP^C can affect APP processing independently of BACE1 and that the PrP^C-BACE1 interaction may be indirect [94].

Prior work from our laboratory established a direct relationship between PrP^C expression and Aβ_{42} secreted by mouse neuroblastoma (N2a) cells that stably express human APP carrying the Swedish mutation linked to familial AD (APPswe) [118]. The mechanism by which this occurs is unknown. Compared to cells expressing normal levels of PrP^C, the laboratory observed a reduction in Aβ_{42} in the media of cells following PrP^C knockdown [118].

The N2a-APPswe cell line, in which the "Swedish" mutation (K595N/M596L) in the amyloid precursor protein (APP) is expressed, serves as a crucial model for studying AD pathology [144]. This specific mutation significantly enhances the cleavage of APP by β-secretase, leading to an increased production of amyloid-β (Aβ) peptides, which are central to the development of AD [144].

In studies conducted using this cell line, it has been demonstrated that cells expressing APPswe secrete higher levels of Aβ peptides and β-secretase-generated soluble APP derivatives (APPsβ) compared to cells expressing wild-type APP (APPwt) [144]. There is a corresponding decrease in the levels of α-secretase-generated soluble APP derivatives (APPsα), indicating a shift in the cleavage process towards β-secretase pathways in the presence of the Swedish mutation [144].

The importance of using the N2a-APPswe cell line lies in its ability to mimic key aspects of the AD pathology. The cell line provides a system in which the metabolic processes leading to increased Aβ production can be studied in detail. This is crucial for understanding the intracellular mechanisms that contribute to the disease and for testing potential therapeutic interventions aimed at reducing Aβ levels.

In the present study, I examined how PrP^C might regulate steady-state Aβ levels - in particular, whether PrP^C alters the processing or trafficking of APP to normally promote the production or release of Aβ.

Our findings from N2a cells stably expressing either APPwt or APPswe show that KD of PrP^C increases APP steady-state levels at the plasma membrane and subsequent endocytosis. Furthermore, the increase in APP at the plasma membrane increases its access to and cleavage by α-secretase, with a concomitant increase in APP C-terminal fragments (CTFs). In the following chapter, I further show that Tg$Prnp^{-/-}$ mice that lack PrP^C expression have increased levels of endogenous APP CTF compared to wild-type mice. Our findings indicate that PrP^C affects APP trafficking. PrP^C's absence enhances APP localization to the plasma membrane and, in so doing, promotes α-secretase cleavage, associated with an overall reduction in Aβ secretion.

2.2 Materials and Methods

2.2.1 Cell Lines

N2a cell lines stably expressing either the APPwt (wild-type human APP695 with a c-Myc tag) or APPswe (human APP695 with the Swedish mutations K595N and M596L with a c-Myc tag) have been described previously [88, 144]. These cells were cultured in N2a growth medium (45% DMEM [high glucose w/L-glutamine], 50% OptiMEM I medium, 10% Fetal Bovine Serum (all v/v), and supplemented with Geniticin™).

2.2.2 Antibodies

Primary Antibodies

Detailed information on primary antibodies can be found in Tables A.1-A.3. The following primary antibodies were used: PrP antibodies, anti-PrP mouse mAb SAF-32 (Bertin Bioreagent, Montigny le Bretonneux, France), D-13 chimeric human-mouse Ab [121](kindly provided by Dr. Stanley Prusiner, UCSF, San Francisco, CA); APP, CTF, and Aβ antibodies, anti-ectodomain mouse mAb P2-1 (Invitrogen, Carlsbad, CA; Thermo Fisher Scientific, Inc.), anti-ectodomain mAb 22C11 (eBioscience, San Diego, CA), anti-ectodomain rabbit polyclonal antibody (pAb) NTH452 [5, 28] and pAb NTG449 [29](Thinakaran laboratory), C-terminal rabbit mAb, Y188 (Abcam, Waltham, MA), C-terminal mAb C1/6.1 (BioLegend, San Diego, CA), C-terminal pAb CTM1citeCheng2009S-Palmitoylation, Andrew2017Lack (laboratory), anti-β-amyloid, 1-16 antibody, clone 6E10 (BioLegend, San Diego, CA), anti-β-amyloid mAb AB9 (BioTechne, Minneapolis, MN); APLP1 antibodies, ectodomain rabbit pAb A1NT [5] (Thinakaran laboratory); APLP2 antibodies, ectodomain rabbit pAb D2II [142] and C-terminal pAb CT12 [143] (Thinakaran laboratory); BACE1 antibodies, BACE1 rabbit pAb PA1-757 (Invitrogen, Carlsbad, CA; Thermo Fisher Scientific, Inc.); ADAM10 antibodies, recombinant anti-ADAM10 antibody [EPR5622] (Abcam, Waltham, MA); Biotin antibodies,

Biotin Antibody (33) (SantaCruz Biotechnology, Dallas, TX); NrCAM antibodies, Anti-NrCAM (N-terminal) anti-rabbit pAb (Abcam, Waltham, MA), Anti-NrCAM (C-terminal) anti-rabbit pAb (Cell Signaling Technology, Danvers, MA); NCAM antibodies, human/mouse NCAM-1/CD56 antibody, anti-goat pAb (BioTechne, Minneapolis, MN), anti-neural cell adhesion molecule antibody, anti-rabbit pAb (Sigma Aldrich, St. Louis, MO); Loading control antibodies, β-Actin antibody (C4), anti-mouse mAb (SantaCruz Biotechnology, Dallas, TX), Anti-GAPDH antibody (6C5), anti-mouse mAb (Invitrogen, Carlsbad, CA; Thermo Fisher Scientific, Inc.).

AlexaFluor-conjugated secondary antibodies (Invitrogen, Carlsbad, CA; Thermo Fisher Scientific, Inc.) were used for immunofluorescence staining. IRDye- (NetaScientific, Marlton, NJ) or HRP-conjugated secondary antibodies (Invitrogen, Carlsbad, CA; Thermo Fisher Scientific, Inc. and SantaCruz Biotechnology, Dallas, TX) were used for Western blot analysis.

2.2.3 Cell Transfection

To transiently knock down expression of the endogenous mouse *Prnp* gene transiently, I used two siRNAs that target sequences within the 3' untranslated region (3'-UTR) of mouse *Prnp* were used: *Prnp*3, targeting sequence 5'CCC TAT GTT TCT GTA CTT CTA3', and *Prnp*4, targeting sequence 5'CTG ATT GAA GGC AAC AGG AAA3' (Qiagen, Valencia, CA). A non-interfering siRNA with no known homology to any gene (Qiagen, Valencia, CA) was used as a control [118].

Cells were seeded in 1 mL of N2a growth media on 6-well plates 24 hours prior to transfection, at which time the N2a growth medium was replaced with 800 µL of DMEM and 200 µL of OptiMEM I incubated with the siRNA and transfection reagent. Each well was transfected for 6 hours either with a mixture containing non-interfering siRNA and 5 µL

of RNAiMAX reagent (Invitrogen, Carlsbad, CA; Thermo Fisher Scientific, Inc.) or with 0.0163 µM of *Prnp3* and *Prnp4* siRNA and 5 µL of RNAiMAX reagent at concentrations previously determined to produce the highest level of PrP KD with the least cell toxicity. At the end of the incubation, the media was removed, cells were washed once with PBS, and the media was replaced with 1 mL of N2a growth media for 24 hours, at which time the conditioned media and cell lysates were collected and stored at 80°C for subsequent analysis.

2.2.4 Cell Lysate and Conditioned Media Preparation

Cells were lysed in Radio-Immunoprecipitation Assay (RIPA) buffer (50 mM Tris, 150 mM NaCl, 0.1% SDS, 0.5% sodium deoxycholate, 1% NP-40, 5 mM EDTA, pH 8.0) supplemented with protease inhibitors (Halt™ Protease Inhibitor Cocktail) and 0.25 mM phenylmethylsulphonyl fluoride (PMSF), incubated on ice for 30 minutes, and centrifuged at 10,000 x g for 10 minutes. The pellet was discarded, and supernatants were saved as the cell lysate fraction and stored at -80°C until analyzed. The protein concentration of each cell lysate fraction was determined using the bicinchoninic acid (BCA) assay (Pierce, Thermo Fisher Scientific Inc., Waltham, MA). Conditioned media from cells was collected and centrifuged at 500 x g for 5 minutes to clear cell debris. TCM proteaseArrest™ (G-Biosciences, St. Louis, MO) was added to the media after clearing the sample to protect secreted proteins from degradation, and aliquots were stored at -80°C.

2.2.5 Immunofluorescence Cell Staining

Cells were seeded on poly-L-lysine-coated coverslips placed in 12-well plates. After 24 h, cells were either transfected with control siRNA or siRNA to downregulate *Prnp* expression and used 24 h later for immunostaining (Thinakaran laboratory).

Surface PrP^C/APP

To visualize plasma membrane PrP or APP (Figure 2.1), cells were moved from 37°C to ice, washed in Neuroimaging (NIM) media (119 mM NaCl, 2.5 mM KCl, 2 mM $CaCl_2 \bullet 2H_2O$, 2 mM $MgCl_2 \bullet 6H_2O$, 30 mM D-Glucose, and 25 mM 1M HEPES, pH 7.4), and incubated with the mAb SAF-32 or pAb NTH452 for 1 hour on ice (1:1000). Unbound antibodies were removed with three NIM washes for 5 minutes each, followed by fixation in 4% PFA for 5 minutes, and quenching in 50 mM NH_4Cl. Between each step, cells were washed with PBS 3 times for 5 minutes each. Next, cells were incubated with secondary antibodies (1:1000) diluted in 3% BSA in PBS + 0.2% Tween-20 for 1 hour on ice. Cells were washed with PBS + 0.2% Tween-20 three times for 5 minutes each, incubated with a DAPI solution for 5 minutes, washed again with PBS + 0.2% Tween-20 three times for 5 minutes each, and then mounted onto slides with VectaShield mounting media (Thinakaran laboratory).

Surface PrP^C/APP and total APP

To simultaneously visualize the surface and total APP (Figure 2.2), surface PrP and APP were first labeled following the above staining protocol. After incubation for 1 hour with secondary donkey anti-mouse AlexaFluor 555 to label surface PrP and donkey anti-rabbit AlexaFluor 647 to label surface APP, cells were washed with PBS + 0.2% Tween-20 three times for 5 minutes each and then permeabilized with 0.2% Triton X in PBS for 5 minutes. Cells were then washed with PBS + 0.2% Tween-20 3 times for 5 minutes, then blocked for 1 hour on ice in a 3% BSA in PBS solution supplemented with glycine and NH_4Cl. To stain total APP, the cells were incubated with pAb CTM1, which recognizes the C-terminal of APP, that was diluted in 3% BSA and 0.2% Tween-20 in PBS (1:1000). Next, cells were washed with PBS + 0.2% Tween-20 three times for 5 minutes each, followed by incubation with a donkey anti-rabbit AlexFluor 488 secondary antibody diluted in 3% BSA and 0.2% Tween-20 in PBS for 1 hour on ice (1:1000). Cells were washed with PBS + Tween-20 three

times, incubated with a DAPI solution for 5 minutes, washed again with PBS + Tween-20 three times, and mounted onto slides with VectaShield mounting media. Slides were stored in slide boxes at 4°C.

Imaging

Stained cells were imaged on a Nikon Ti2 microscope fitted with a Yokogawa CSU-W1 SoRa spinning disk confocal scanner unit and Photometrics Prime 95B sCMOS detector controlled by NIS-Elements software. All images were processed in Fiji/ImageJ. The middle image in a Z-stack was selected for all images processed. Images were acquired using identical settings for each cell line, and the same threshold parameters were used for all images within an experiment. Regions of interest were drawn around cells, and the mean integrated fluorescence intensity was calculated as a function of the number of nuclei in the field or as a function of cell area. At least three images were taken per transfection and cell staining condition, and each experiment was repeated at least three times. As a result, cells were counted from at least nine images per transfection condition and combination of antibodies. Data were analyzed using Prism 10 (GraphPad Software).

Analysis of immunofluorescence staining

All images were processed in Fiji/ImageJ. The middle image in a Z-stack was selected for all images processed. 20uM scale bars were added to each image and the same threshold parameters were used for all images within an experiment, for each cell line. Channel colors were changed to blue (nuclei), green (plasma membrane and intracellular APP), magenta (plasma membrane PrP^{C}), and yellow (plasma membrane APP), and channels were saved both separately and as a montage. Images from the same experiment were grouped together, regions of interest were drawn around cells from each image and the mean integrated density was calculated as a function of the number of nuclei counted in an experiment and as a

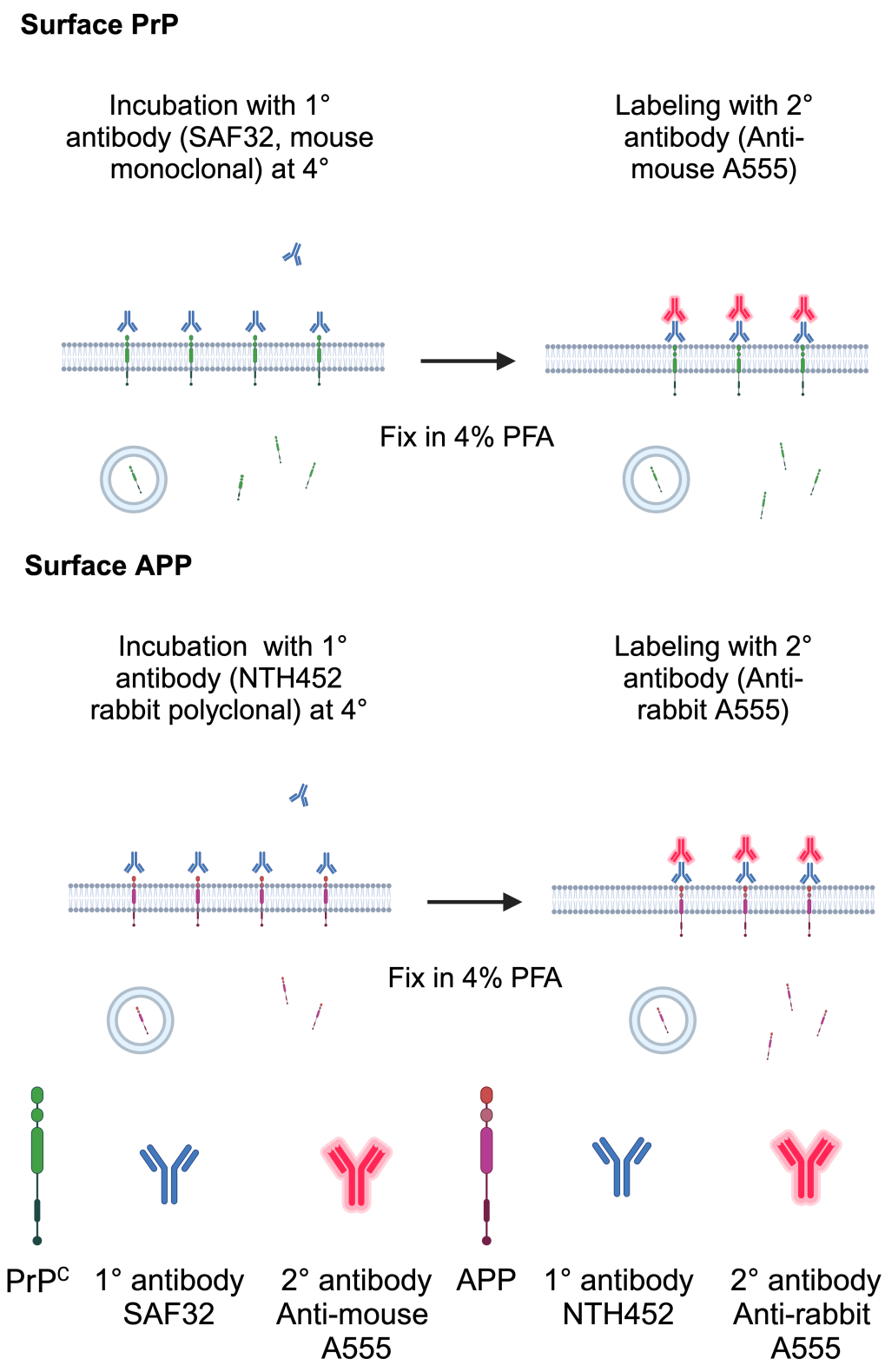

Figure 2.1: Immunolabeling of plasma membrane APP and PrP^C. Made with BioRender.com.

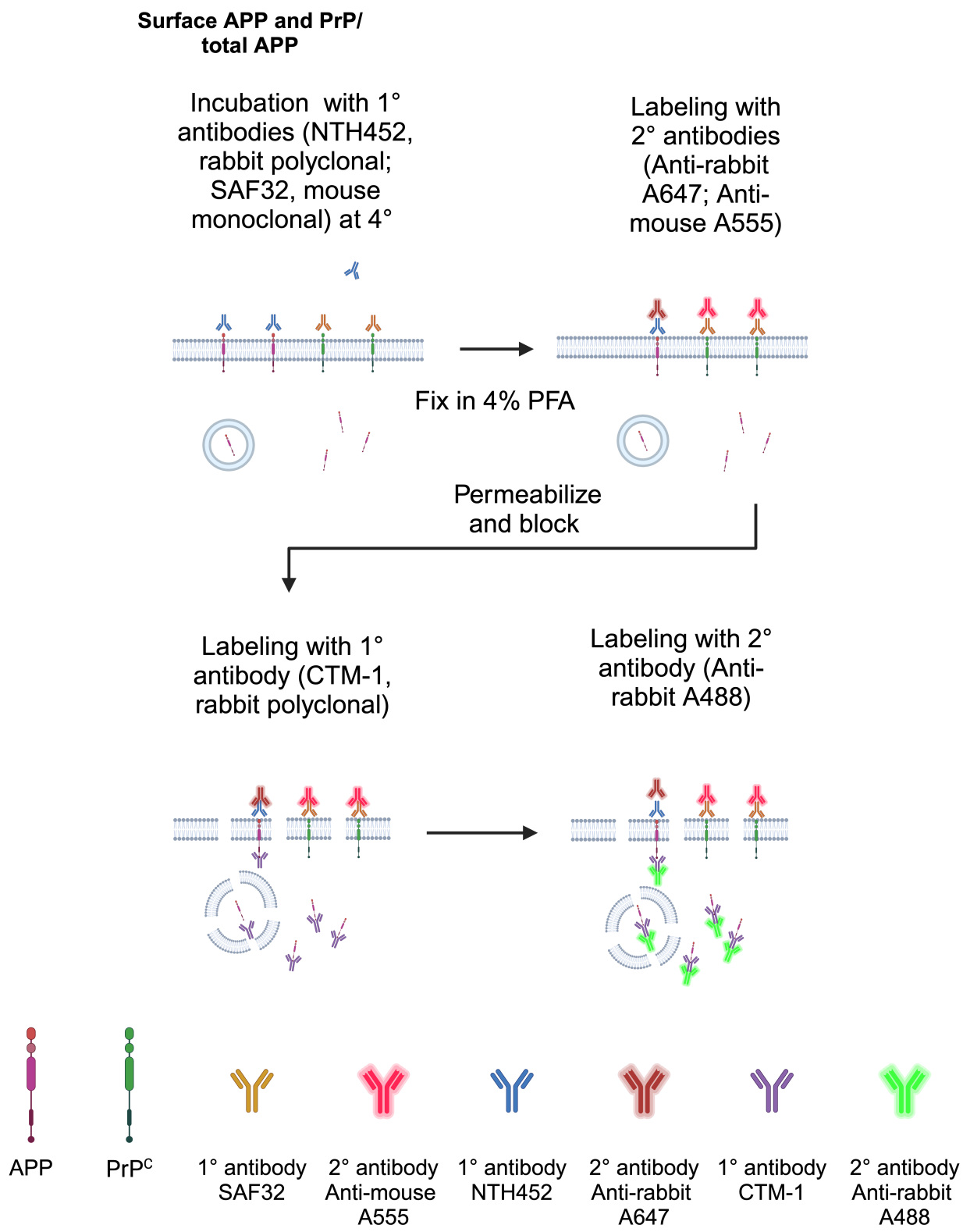

Figure 2.2: Immunolabeling of plasma membrane APP, PrP^C, and total APP. Made with BioRender.com.

function of cell area in a single Z-stack plane at the center of each cell. At least three images were taken per transfection and cell staining condition and each experiment was repeated at least three times. As a result, cells were counted from at least 9 images per transfection condition and combination of antibodies. Data were analyzed using Prism 10 (GraphPad Software).

2.2.6 Quantifications of Aβ and secreted APP

For analysis of human Aβ secreted from N2a-APPwt and N2a-APPswe cell lines, conditioned media (see above) were collected. The levels of Aβ_{38}, Aβ_{40}, and Aβ_{42} in the conditioned media were measured using V-PLEX Plus Aβ Peptide Panel 1 6E10 (K15200G). For analysis of sAPP/β-wt in the N2a-APPwt cell line, conditioned media were analyzed using MSD sAPPα/sAPPβ kit (K15120E). The plates were read on a MESO QuickPlex SQ 120. Data were analyzed using Discovery Workbench desktop analysis software (Meso Scale Discovery, Rockville, MD) and Prism 10 (GraphPad Software).

sAPPβ-sw ELISA

sAPPβ-sw secreted by N2a-APPswe cells was measured with a sAPPβ-sw solid phase sandwich ELISA kit (27733) from IBL. The plates were read at an optical density of 450 nm on the VersaMax microplate reader (Molecular Biosciences), and data were analyzed using Prism 10 (GraphPad Software).

2.2.7 Aβ Digestion Assay Using Synthetic Aβ

Extracellular degradation of Aβ in conditioned media was assessed using a previously described assay [151]. Lyophilized Aβ peptides were initially dissolved in 1% NH_4OH, followed by dilution in PBS, according to the manufacturer's instructions, and stored as 1 mg/mL aliquots. Unlike other cell experiments, the harvested conditioned media was not supple-

mented with TCM protease inhibitor. Conditioned media samples (12.5 µL) were incubated for 14 hours at 37°C with either 200 ng of synthetic hexafluoro-2-isopropanol (HFIP)-treated Aβ_{40} or Aβ_{42} (AnaSpec, Fremont, CA). After incubation, the reaction mixtures were separated on a 16.5% Tris-tricine gel and immunoblotted with mAb 6E10 to assess Aβ_{40} and Aβ_{42} degradation in the media. N2a growth media, Aβ_{40} peptide, and Aβ_{42} peptide were used as controls.

2.2.8 qRT-PCR

Total RNA was extracted from N2a-APPwt and N2a-APPswe cells transfected with control and siRNA to downregulate *Prnp* expression as previously described using the RNAqueous®-4PCR Total RNA Isolation Kit (Invitrogen, Carlsbad, CA; Thermo Fisher Scientific Inc., Waltham, MA) according to manufacturer's instructions. 200 ng RNA was reverse transcribed into cDNA and amplified using 1 M of each forward and reverse primer using the iTaq universal SYBR green one-step kit (Bio-Rad, Hercules, CA) on a Bio-Rad CFX96™Real-Time System. Actin was used as a control to normalize the levels of the target mRNA. All reactions were run in triplicate. Relative gene expression of the target genes was measured using the $2^{-\Delta\Delta CT}$ method [87]. The data were analyzed and graphed using Prism 10 (Graphpad Software).

Gene	**Forward primers (5'–3')**	**Reverse primers (5'–3')**
MoPrP	CCAAGGAGGGGGTACCCATA	CCCAGTCGTGTGCCAAAATGG
Actin	TGGAATCCTGTGGCATCCATGAAA	TAAAACGCAGCTCAGTAACCG
APP	GTAGCAGAGGAAGAAGTG	CATGACCTGGGACATCTTC

Table 2.1: Primers used for PCR amplification of genes.

2.2.9 Western Blotting

Cell lysate and conditioned media samples were prepared by adding 3X to 4X Laemmli sample buffer (Bio-Rad, Hercules, CA) in the presence or absence of 2-Mercaptoethanol was used for Tris-glycine gels, and 2X tricine sample buffer (Bio-Rad, Hercules, CA) 2-Mercaptoethanol was used for Tris-tricine gels. The proteins were solubilized and denatured by heating the samples to 95°C for 5 min. For preparation of Western Blotting with mAb P2-1, which is specific for native, non-denatured APP, the samples were incubated in 4X Laemmli buffer without 2-Mercaptoethanol and heated to 50°C for 10 minutes prior to loading.

To separate proteins ≥15kDa, 4-20% Tris-glycine gradient gels were used, whereas 16.5% Tris-tricine gels were used to separate proteins ≥15kDa. Proteins were transferred to 0.45 µm polyvinylidene difluoride (PVDF) membranes (Bio-Rad, Hercules, CA) or Immobilon™ - FL 0.45 µm PVDF membranes (Millipore) at 400 mA at 4∘C for 3 hours. Membranes were blocked in 5% milk in PBS-T or 10% BSA and 10% fish scale gelatin (FSG) in PBS-T (when using fluorescent secondary antibodies) for 1-2 hours at RT, followed by overnight incubation with primary antibodies at 4°C. Washes in between steps were in Tris-buffered saline with Tween-20 (TBS-T) or PBS-T 3X for 10 minutes, and blots were incubated in secondary antibodies at RT for 1 hour. When fluorescent secondary antibodies were used, blots were imaged on the LI-COR Odyssey near-IR imager for quantitative immunoblots immediately after washing. Otherwise, blots were incubated for 5 minutes in SuperSignal West Pico PLUS Chemiluminescent Substrate (Thermo Fisher Scientific Inc., Waltham, MA) and imaged using the ChemiDoc MP Imaging System (Bio-Rad, Hercules, CA).

2.2.10 Surface and Endocytosis Biotinylation

Surface biotinylation was performed according to established protocols [6, 90]. One hour prior to the biotinylation of proteins, 100 g/mL leupeptin was added to the cell media to inhibit lysosomal proteolysis, along with 20 µM of TAPI-2 to prevent ADAM10 cleavage of APP at the plasma membrane. Cells were then cooled to 4°C and washed twice in ice-cold PBS (supplemented with 1 mM $Ca^{(2+)}$ and 0.5 mM $Mg^{(2+)}$, used throughout the experiment), at which time they were surface-biotinylated using EZ-Link-Sulfo-NHS-SS-Biotin (Thermo Fisher Scientific Inc., Waltham, MA) at a concentration of 1mg/mL for 12 minutes. Three washes of 3-5 minutes each in PBS containing 50 mM lysine and 0.5% BSA were used to wash excess, unreacted EZ-Link-Sulfo-NHS-SS-Biotin from cells at 4°C. Cells were then washed twice in PBS for 3 minutes each, re-incubated with pre-warmed N2a growth media (supplemented with 100 g/mL leupeptin and 20 uM TAPI-2), and placed in a 37°C incubator for 15 minutes, to allow biotinylated plasma-membrane APP to internalize. Following re-internalization, cells were cooled back down to 4°C and washed once with ice-cold PBS. For wells where the remaining surface biotinylated APP was stripped, cells were treated twice with glutathione (75 mM final concentration, prepared in 75 mM NaCl, 10 mM EDTA, pH 8) at 4°C for 10–15 minutes each. Cells were washed three times in PBS to remove glutathione and lysed in ice-cold RIPA buffer. Cell lysates were centrifuged at 2000 x g for 10 minutes, and supernatants were saved (the pellet was discarded). Protein concentration was determined using the BCA assay (Pierce). Aliquots of lysates (150 g each) were incubated overnight at 4°C with 30ul of NeutrAvidin Beads (Pierce) to capture biotinylated proteins. To wash the pulldown, each Eppendorf tube was centrifuged at 400 x g for 5 minutes, following which the supernatant was discarded. The beads were resuspended in 200 uL of RIPA buffer, and each tube was placed on a nutator for 5 minutes, followed by centrifugation at 400 x g for 5 minutes. This process was repeated three times to wash the beads thoroughly. After the final wash step, the supernatant was discarded, 30 uL of 4X Laemmli sample buffer

(Bio-Rad, Hercules, CA) with 2-mercaptoethanol was added to the beads, and the beads were boiled and resolved by SDS/PAGE.

2.2.11 Statistical Analysis

Statistical analyses were performed using Prism 10 (GraphPad Software). Comparisons between two groups were performed by two-tailed unpaired t-tests (two groups), and three or more groups were analyzed by ANOVA, followed by an appropriate post-hoc multiple comparisons test.

2.3 Results

2.3.1 The Effect of PrP^C Expression on Aβ Release

We used the high-sensitivity MesoScale Discovery (MSD) assay to quantify the three major isoforms of secreted Aβ (Aβ_{42}, Aβ_{40}, and Aβ_{38}) from the conditioned media of stable N2a cell lines that stably express human wild-type (wt) APP695 (N2a-APPwt) or APP harboring the "Swedish" double mutation (N2a-APPswe) [144]. Conditioned media samples were collected from cells plated 24 hours prior to treatment with control siRNA or siRNA to PrP^C. The efficiency of PrP^C KD was $\sim$ 70% in both cell lines (Figure 2.3 A). We compared relative reductions in each Aβ isoform measured in each cell line and found an overall decrease in Aβ_{42}, Aβ_{40}, and Aβ_{38} following PrP^C KD (Figure 2.3 B-C). Concomitantly, within the conditioned media of N2a-APPwt cells, an $\sim$ 40% reduction was observed in Aβ_{40} and Aβ_{42} levels, with an $\sim$ 85% reduction in Aβ_{38} levels (Figure 2.3 B). The large apparent decrease in Aβ_{38} levels, however, was attributed to the fact that Aβ_{38} levels were below the detection limits of MSD in three samples treated with siRNA to PrP^C. Within the conditioned media of the N2a-APPswe cell line, an $\sim$ 20% reduction in all three isoforms of Aβ was observed (Figure 2.3 C). Only Aβ_{40} and Aβ_{38} isoforms were significantly reduced in N2a-APPwt cells,

whereas all three isoforms were significantly reduced in N2a-APPswe cells. This is likely a result of the extremely low steady-state levels of Aβ_{42} secreted by N2a-APPwt cells ($\sim$ 50 $\sim$ 1300 pg/mL in N2a-APPswe cells).

2.3.2 The Effect of PrP^C Expression on APP mRNA and Protein Levels

To determine whether the reduction in Aβ following PrP^C KD was due to an indirect effect on APP expression, leading to reduced overall Aβ levels, I performed qRT-PCR to quantify mRNA levels of APP. We first confirmed that PrP^C KD was effective. qRT-PCR for PrP mRNA suggested a reduction of $\sim$ 70%, consistent with my Western Blots (Figure 2.4 A). However, there was no difference in APP mRNA in either cell line after PrP^C KD compared to controls (Figure 2.4 B). Of note, this experiment also revealed significantly lower levels of APP mRNA in N2a-APPwt cells compared to N2a-APPswe cells ($\sim$ 2.5X difference)(Figure 2.4 B). We then assessed whether steady-state APP levels were altered after PrP^C KD. Immunoblotting revealed no differences in full-length (FL) APP levels following PrP^C KD in either cell line (Figure 2.4 C-D). Thus, the unchanged levels of FL APP mRNA and FL APP protein argue against a reduction in APP expression as an explanation for the decrease in steady-state levels of secreted Aβ following PrP^C KD.

2.3.3 The Effect of PrP^C Expression on Extracellular Aβ Degradation

We next considered that PrP^C might act to directly or indirectly protect Aβ from extracellular degradation, and in its absence, Aβ degradation is facilitated. To test for this possibility, I assessed the extent of degradation of synthetic Aβ incubated in conditioned media obtained from cells expressing normal or reduced PrP^C. Twenty-four hours after transfection

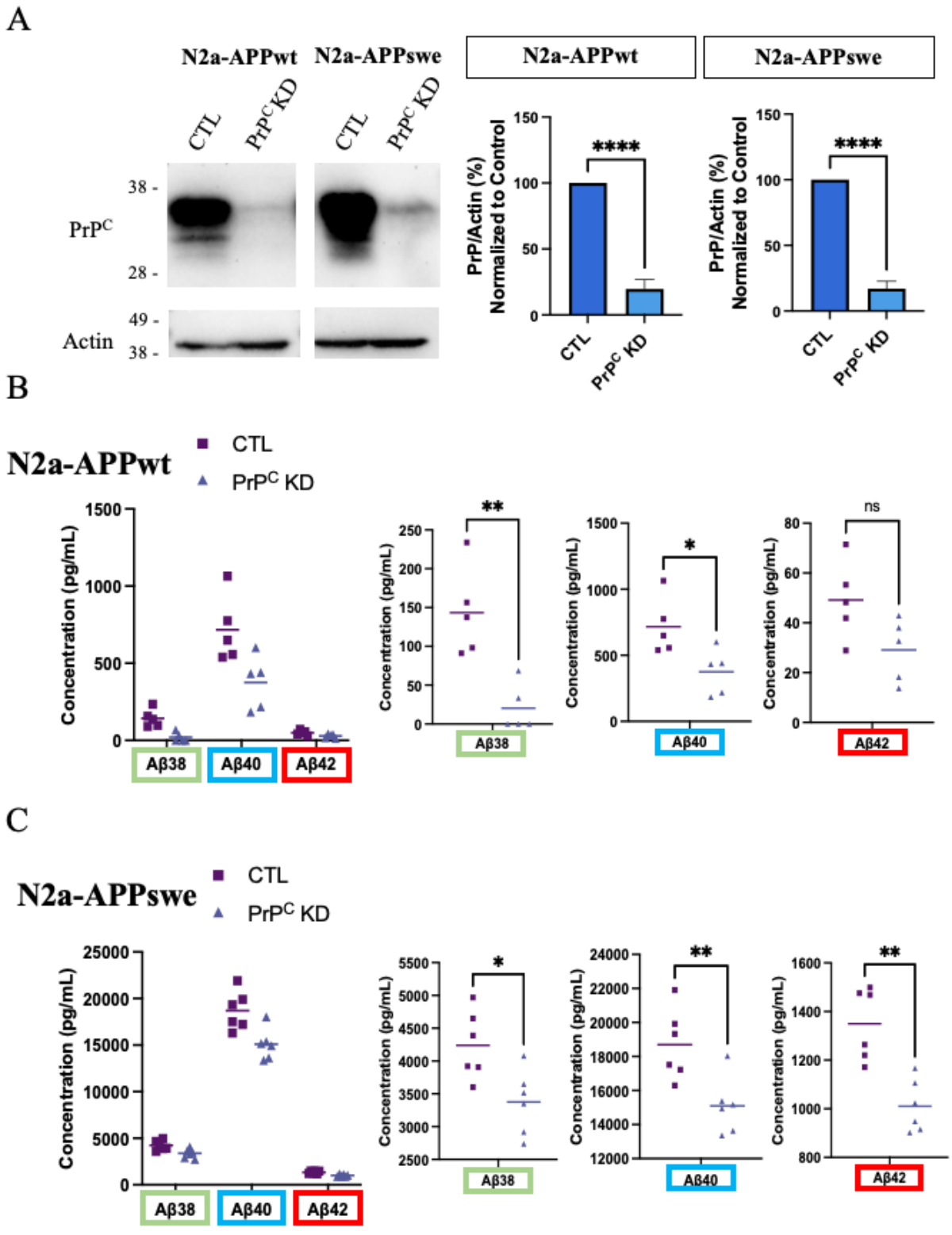

Figure 2.3: **PrP^C KD decreases the steady-state levels of secreted Aβ in N2a-APPwt and N2a-APPswe cells.**

Figure 2.3: (continued) **A.** Representative Western blots (left) and associated densitometry (right) of N2a-APPwt and N2a-APPswe cell lysates probed for PrP^C before and after siRNA-induced PrP^C KD. PrP^C signal intensities were normalized to the levels of actin. Data were analyzed by a two-tailed, unpaired t-test from three separate experiments, **** $p<0.0001$. **B-C.** MSD electrochemiluminescence quantitation of $A\beta_{38}$, $A\beta_{40}$, and $A\beta_{42}$ levels (pg/mL) in the media of N2a-APPwt (B) or N2a-APPswe (C) cells 30 hours after transfection with either scrambled (control) siRNA or anti-PrP siRNA. Data were plotted as a composite and using appropriate scales for each Aβ species. Each data point is the average of 2 technical replicates, and the data is from 5 (N2a-APPwt) or 6 (N2a-APPswe) experiments. Data were analyzed by a two-tailed, unpaired *t*-test: * $p<0.05$, ** $p<0.01$.

of N2a-APPswe and N2a-APPwt cells with control or PrP-specific siRNA, equal aliquots of conditioned media were mixed with synthetic $A\beta_{40}$ or $A\beta_{42}$ and incubated at 37°C for 14 hours at which time they were collected and resolved on 16.5% Tris-tricine gels and immunoblotted using mAb 6E10 to detect the remaining $A\beta_{40}$ and $A\beta_{42}$ peptides (Figure 2.5). The percentage of Aβ remaining, relative to the levels of Aβ peptide similarly incubated in N2a growth media, was calculated (Figure 2.5 B and D). No significant difference in degradation was observed for either $A\beta_{40}$ or $A\beta_{42}$ after 14 hours of incubation in media collected from either cell line treated with control or anti-PrP siRNA. Thus, the extracellular degradation of Aβ is not a PrP^C-dependent process, and such a process does not explain the reduction in steady-state secreted Aβ levels following PrP^C KD.

2.3.4 The Effect of PrP^C Expression on APP Processing

Based on the above findings, I considered that the reduction in Aβ secretion following PrP^C KD might result from an influence of PrP^C on the balance of APP processing by α-and β-secretases that determine whether APP follows the non-amyloidogenic or amyloidogenic pathways. The primary α-secretase, ADAM10 metalloproteinase, cleaves APP within the Aβ segment and releases soluble APPα (sAPPα into the media, thereby promoting the non-amyloidogenic pathway, whereas BACE1 cleaves APP at the amino-terminal of the Aβ

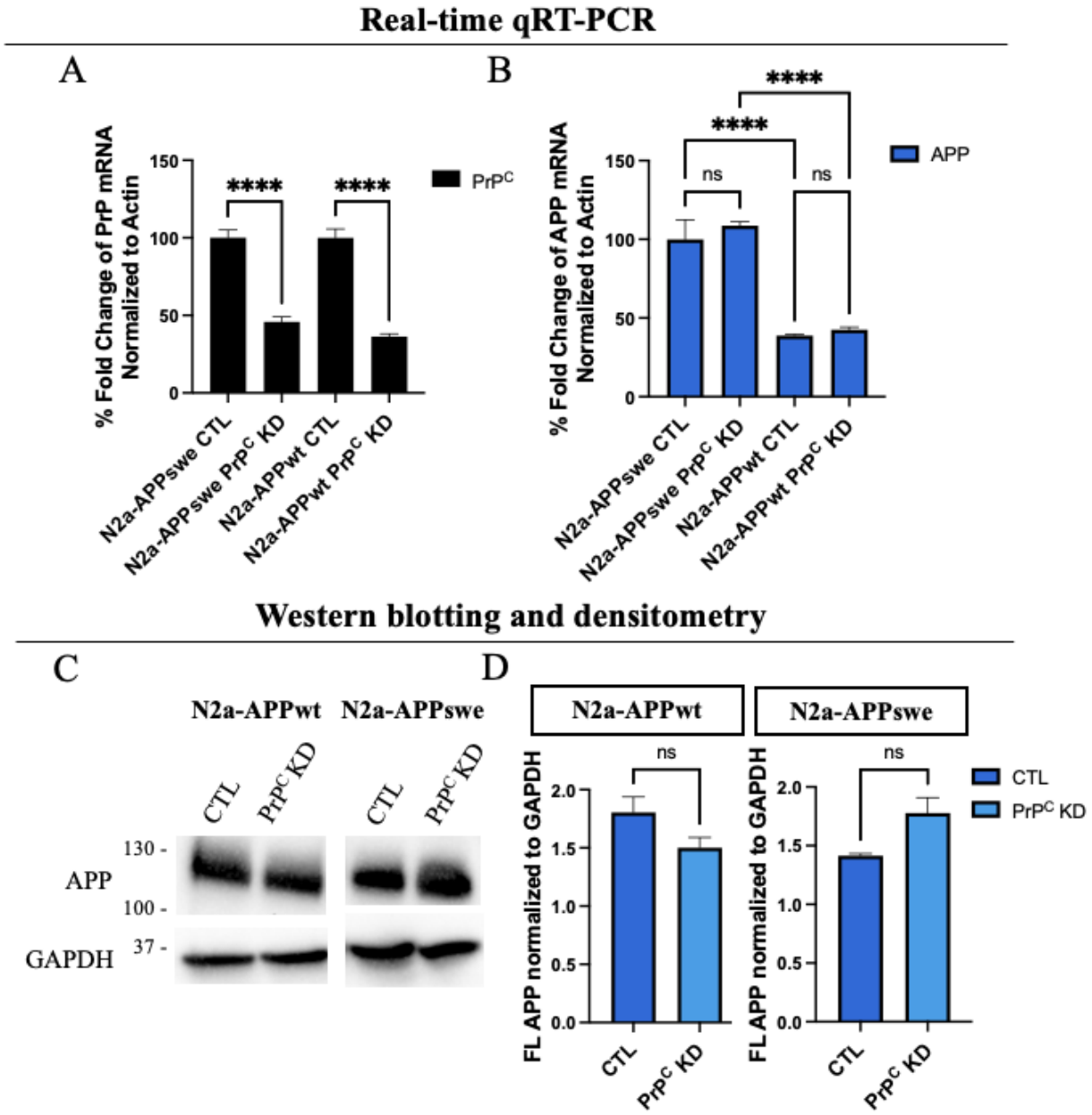

Figure 2.4: **PrP^C KD does not affect *APP* mRNA or protein levels in N2a-APPwt and N2a-APPswe cells.**

Figure 2.4: (continued). **A.** PrP^C mRNA levels are knocked down $\sim$ 50-70% by *Prnp* siRNA. Quantitative PCR analysis of PrP^C mRNA levels (control and PrP^C KD) in N2a-APPswe cells and N2a-APPwt cells as a function of $2^{-\Delta\Delta CT}$, represented by % fold change, where the control conditions are set to 100%, and normalized to Actin. **B.** APPswe mRNA levels were $\sim$ 2.5X that of APPwt mRNA levels in N2a-APPwt cells. N=4 samples per transfection condition and cell line. Data were analyzed by two-way ANOVA, **** $p<0.0001$. **C-D.** PrP^C KD does not affect full-length APP protein levels in N2a-APPwt or N2a-APPswe cells. Representative Western blots (C) and associated densitometry (D) of N2a-APPwt and N2a-APPswe cell lysates probed for APP before and after siRNA-induced PrP^C KD. Signal intensities of APP were normalized to GAPDH. N=3 Western blots. Data points were analyzed by a two-tailed, unpaired *t*-test from three separate experiments, **** $p<0.0001$, ns = not significant.

peptide, and promotes the amyloidogenic pathway, resulting in the release in sAPPβ into the media. MSD assays were designed to quantify sAPPα and sAPPβ to assess potential changes in their overall steady-state concentrations and relative ratios following PrP^C KD. A decrease in sAPPβ would confirm that impaired BACE1 cleavage of APP is, at least, partially responsible. A change in the ratio of sAPPα and sAPPβ such that sAPPα is relatively increased, would support a role for PrP^C to promote the amyloidogenic pathway and, in its absence, shift the balance to the non-amyloidogenic pathway. PrP^C KD in N2a-APPwt cells resulted in a significant decrease ($\sim$ 17%) in sAPPβ (28,996 + 499 vs. 24,370 + 611 pg/mL, N=6, $p<0.0048$) in addition to a striking increase ($\sim$ 50%) in sAPPα (19,459 + 278 vs. 29,221 + 1241 pg/mL, N=6, $p<0.0001$) (Figure 2.6 A-B). This finding supports a possible role of PrP^C to suppress the non-amyloidogenic pathway (i.e., α-secretase cleavage) or facilitate the amyloidogenic pathway, which leads to a shift to the non-amyloidogenic pathway and less Aβ production in parallel with an increase in sAPPα release in the media after PrP^C KD. Although a similar result in N2a-APPswe cells was expected, PrP^C KD effected a somewhat different outcome. As with N2a-APPwt cells, $\sim$ 15% reduction in sAPPβ was observed (2,148 + 43 vs. 1,833 + 69 ng/mL, N=12 samples, $p<0.0059$) (Figure 2.6 C), despite the much higher baseline levels of sAPPβ in N2a-APPswe cells compared to N2a-APPwt cells (2,148,000 vs 28,996 pg/mL) (Compare Figure 2.6 A and C). However, whereas sAPPα

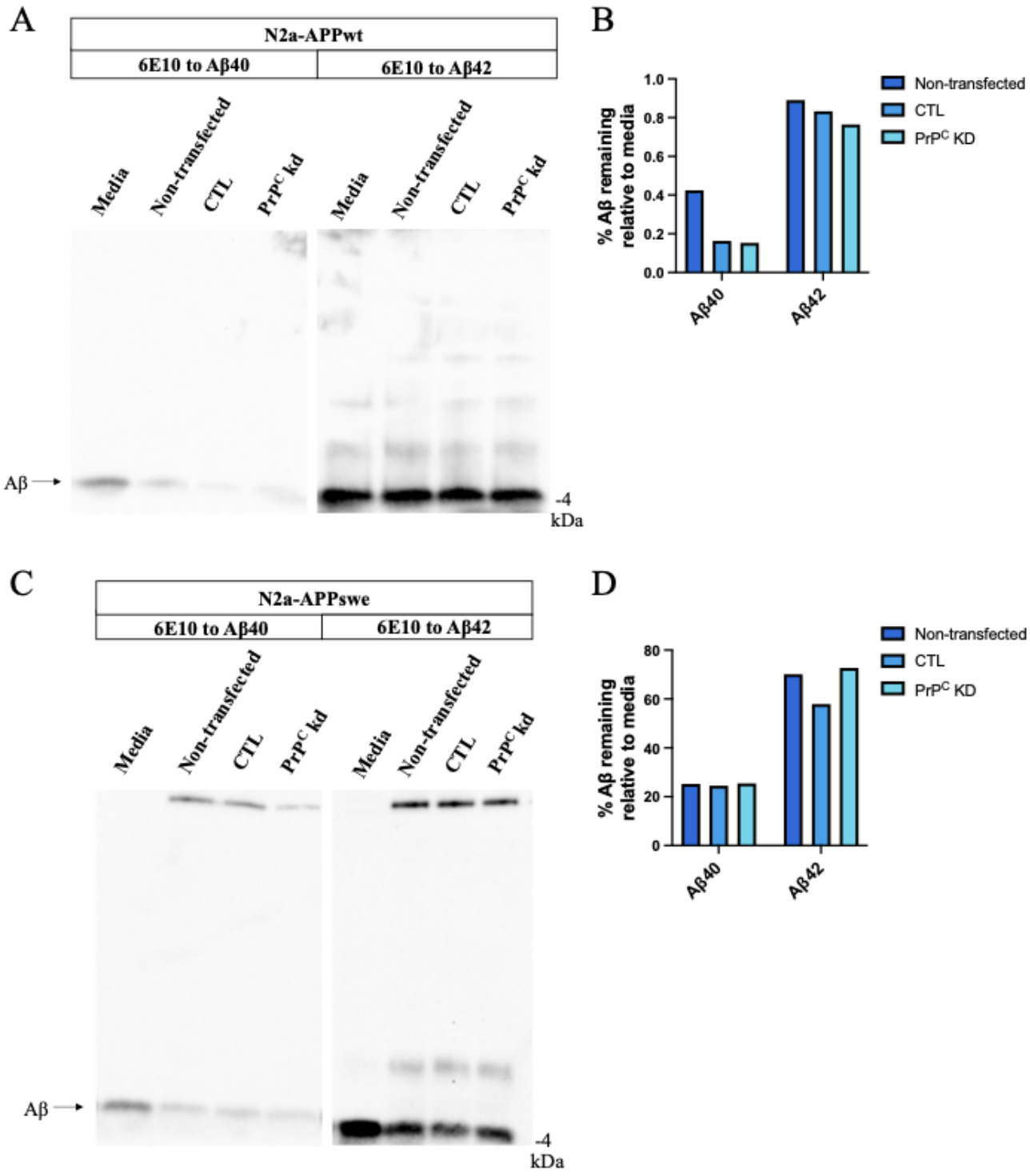

Figure 2.5: **PrP^C KD does not affect the degradation of synthetic Aβ_{40} or Aβ_{42} in conditioned media from N2a-APPwt or N2a-APPswe cells.**

Figure 2.5: (continued). **A-D.** Representative Western blots of conditioned media aliquots from N2a-APPwt or N2a-APPswe cells incubated with 200 ng of synthetic Aβ_{40} or Aβ_{42} at 37°C for 14 hours. The 6E10 antibody was used to detect Aβ_{40} or Aβ_{42} in the samples at the end of the incubation. The percent of Aβ_{40}/Aβ_{42} remaining in the media of the non-transfected, control siRNA, and *Prnp* siRNA conditions after the incubation was measured in relation to the N2a growth media condition.

significantly increased in the media of N2a-APPwt cells after PrP^C KD, it was unaffected (62,877 + 4069 vs. 67,066 + 5037 pg/mL, N=18 samples, $p<0.5269$) in N2a-APPswe cells (Figure 2.6 D). This supports the idea that APPwt and APPswe are differentially processed.

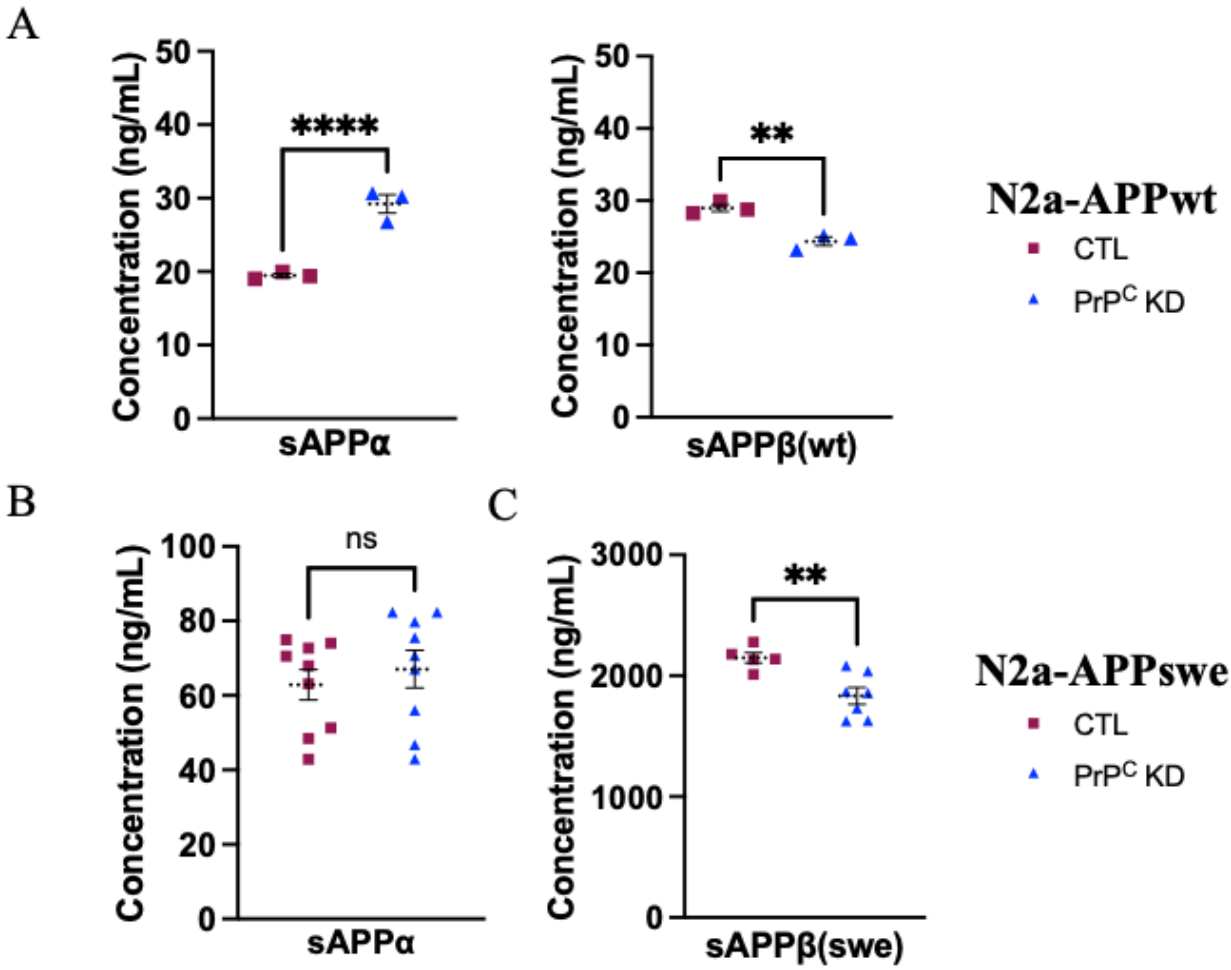

Figure 2.6: **PrP^C KD decreases steady-state levels of secreted sAPPβ in N2a-APPswe and N2a-APPwt cells, while sAPPα levels increase significantly only in N2a-APPwt cells. A.** MSD electrochemiluminescence quantitation (ng/mL) of sAPPα and sAPPβ-wt levels in the media conditioned by N2a-APPwt cells transfected with control or *Prnp* siRNA. Each data point is the average of 2 technical replicates, and 3 independent experiments were performed. Data were analyzed by two-way ANOVA, ** $p<0.01$, **** $p<0.0001$. **B.** MSD electrochemiluminescence quantitation (ng/mL) of sAPPα levels in the conditioned media of N2a-APPswe cells transfected with control or *Prnp* siRNA. Each data point is the average of 2 technical replicates, and 9 independent experiments were performed. Data was analyzed by a two-tailed, unpaired t-test. **C.** ELISA quantitation (ng/mL) of sAPPβ-swe cells transfected with control or *Prnp* siRNA. N=5 samples for the control condition and 7 for the PrP^C KD condition. Each data point is the average of 2 technical replicates. Data were analyzed by a two-tailed, unpaired *t*-test: ** $p<0.01$.

Based on these somewhat discordant findings, I explored whether APP CTFs produced

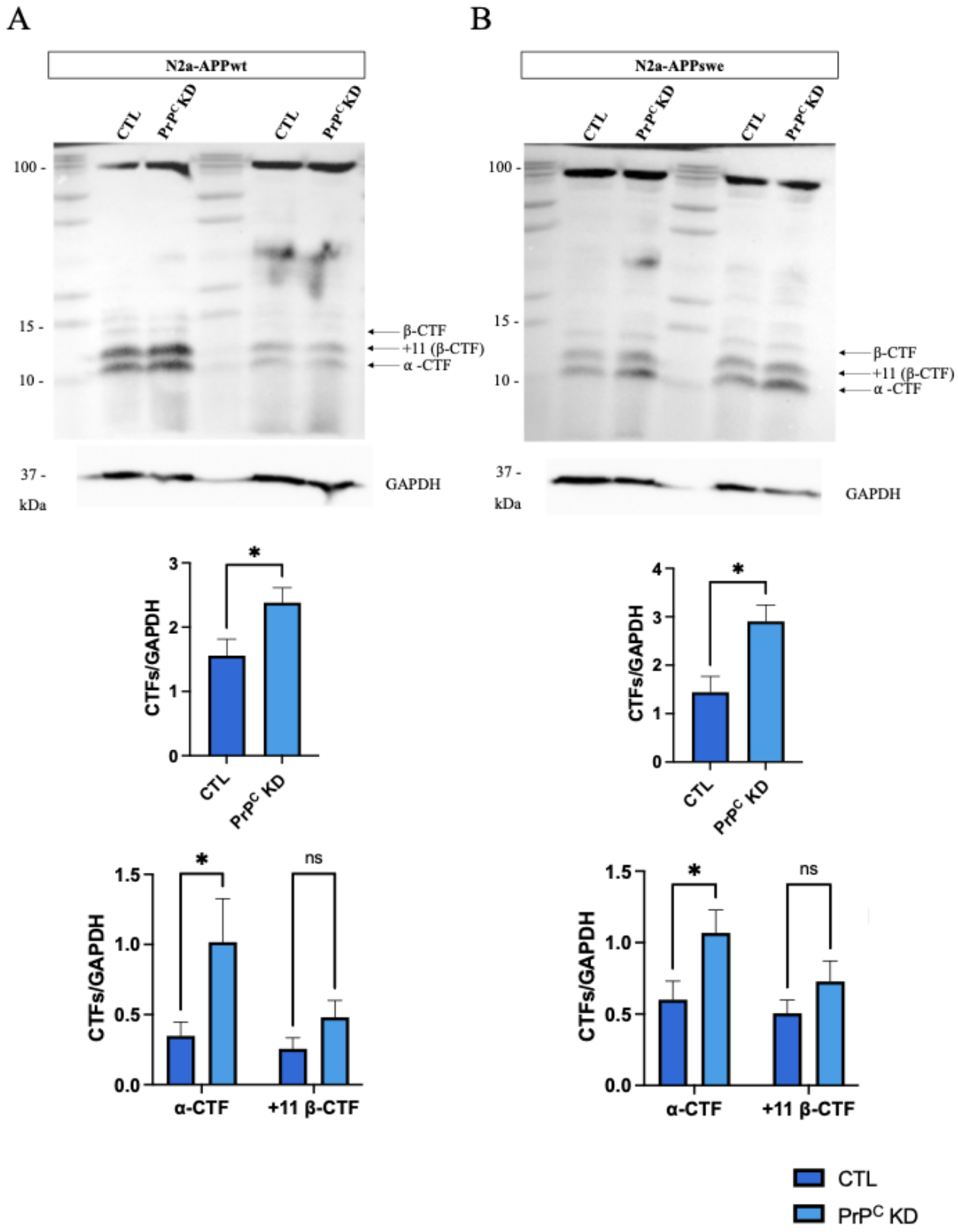

Figure 2.7: **PrP^C KD increases APP CTF levels in N2a-APPwt and N2a-APPswe cells.**

Figure 2.7: (continued). Representative Western blots (top) and associated densitometry (bottom) of N2a-APPwt and N2a-APPswe cell lysates probed with pAb Y188 to label APP and APP CTFs. Signal intensities of α-CTF, +11 β-CTF, and +1 β-CTF bands were grouped and normalized to GAPDH. CTF signals were further separated into α-CTF and +11 β-CTF bands. Data points were analyzed by a two-tailed, unpaired t-test; N=4 independent experiments, * $p<0.05$.

after α- and β- secretase cleavage mirror the observed changes in sAPPα and β. We expected an increase in α-CTF and a decrease in β-CTF in N2a-APPwt cell lysates after PrP^C KD, whereas in N2a-APPswe cells no change in α-CTF and a decrease in β-CTF were expected. Lysates of N2a-APPswe and N2a-APPwt cells were probed for CTFs using the APP C-terminal antibody Y188 (Abcam, Waltham, MA). Surprisingly, CTFs were generally increased in both cell lines after PrP KD, although the predominant fragments were β-, and the +11 β- CTF fragments (Figure 2.7). As such, these results mirrored the changes in sAPPα in N2a-APPwt cells but not in N2a-APPswe cells. Moreover, β-CTF levels did not significantly change, which is inconsistent with the sAPPβ data in both cell lines, indicating a disconnect between the steady-state levels of intracellular β-CTF and the N-terminal product released by the initial BACE1 cleavage of APP.

2.3.5 The Effect of PrP^C Expression on APP Trafficking Patterns

Because PrP^C is a substrate of ADAM10, the main α-secretase that cleaves APP, it might act by substrate competition to mitigate α-secretase cleavage of APP and promote its cleavage via the amyloidogenic pathway. However, although such an effect might explain the reduction in Aβ and sAPPβ in both cell types after PrP^C KD, and the increase in sAPPα in N2a-APPwt cells, it would not be of sufficient magnitude to explain the lack of effect of PrP^C KD on sAPPα in N2a-APPswe cells. Based on the differences in sAPPα production between the two cell lines after PrP^C KD, I asked whether the reduction in PrP^C differentially alters plasma membrane levels of APPwt or APPswe. The metabolic fates of APPswe and APPwt

are different in that APPswe is readily cleaved in the Golgi and trans-Golgi Network by BACE1 [144] whereas APPwt is trafficked to the plasma membrane where the majority of the α-secretases are localized. As a result, any alteration in these trafficking patterns by PrP^C could result in differential modifications of APP processing. We first compared signal intensities of plasma membrane-bound APP and PrP^C in non-permeabilized N2a-APPwt and N2a-APPswe cells before and after PrP^C KD. NTH452, a rabbit polyclonal antibody selective for the N-terminal of APP, was used to assess plasma membrane localized APP and the PrP^C mAb SAF32 was used to assess plasma membrane localized PrP^C. This revealed a robust qualitative increase in surface staining of APP concomitant with the reduction of PrP^C signal in both cell lines after PrP^C KD (Figure 2.8).

Similarly treated cells were then permeabilized prior to staining with CTM1, a C-terminal APP antibody that recognizes α-CTF, and β-CTF, in addition to full-length APP, to assess changes in C-terminal APP fragments after PrP^C KD (Figure 2.9). By computing the mean integrated density of each cell that was permeabilized and stained with CTM1, I assessed the full-length APP and CTF levels quantitatively. These levels reflect total intracellular APP levels at a fixed time point, in individual cells. The calculated mean integrated density of CTM1 staining in N2a-APPwt cells was significantly increased following PrP^C KD ($p<0.0001$) (Figure 2.9 Ci). Similarly, in N2a-APPswe cells, PrP^C KD increased CTM1 fluorescence per cell compared to control siRNA-transfected cells (Figure 2.9 Di). To accommodate for differences in cell size across cell lines and siRNA treatment, I also calculated mean integrated density of CTM1 fluorescence as a function of cell area in a plane, which showed a significant increase after PrP^C KD in both cell lines (Figure 2.9 Cii and Dii).

In contrast to the immunofluorescence staining results that suggest the APP signal at the

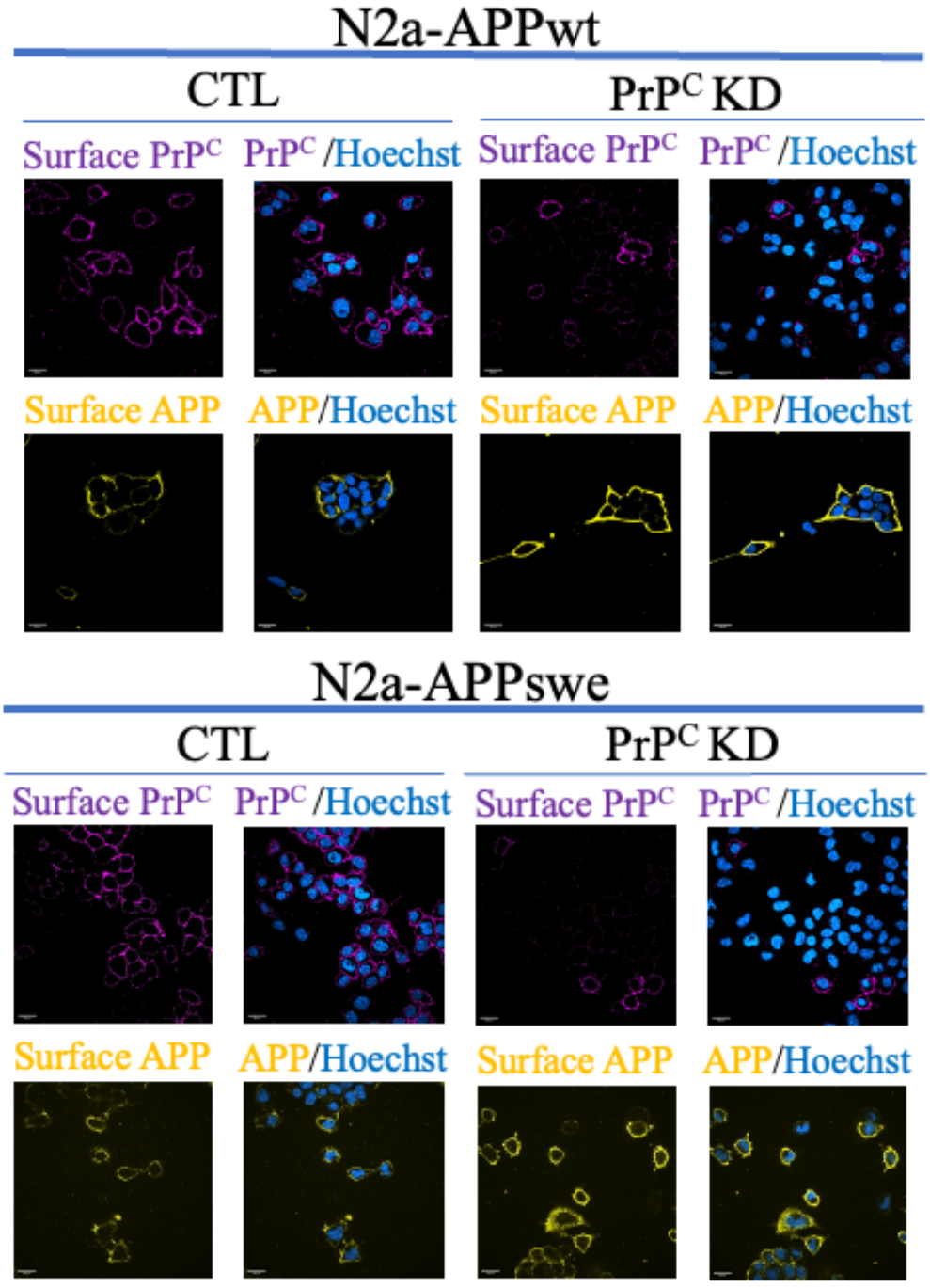

Figure 2.8: **PrP^C KD increases NTH452-labeled plasma membrane APP in N2a-APPwt and N2a-APPswe cells.** Representative images of N2a-APPwt (first two rows) and N2a-APPswe (last two rows) cells transfected with control or *Prnp* siRNA were taken from the middle plane of a Z-stack. Surface APP staining (pAb NTH452; yellow) or surface PrP^C staining (mAb SAF32; magenta) and respective composite images with Hoechst (nuclear stain) are shown. Scale bar, 20 µM.

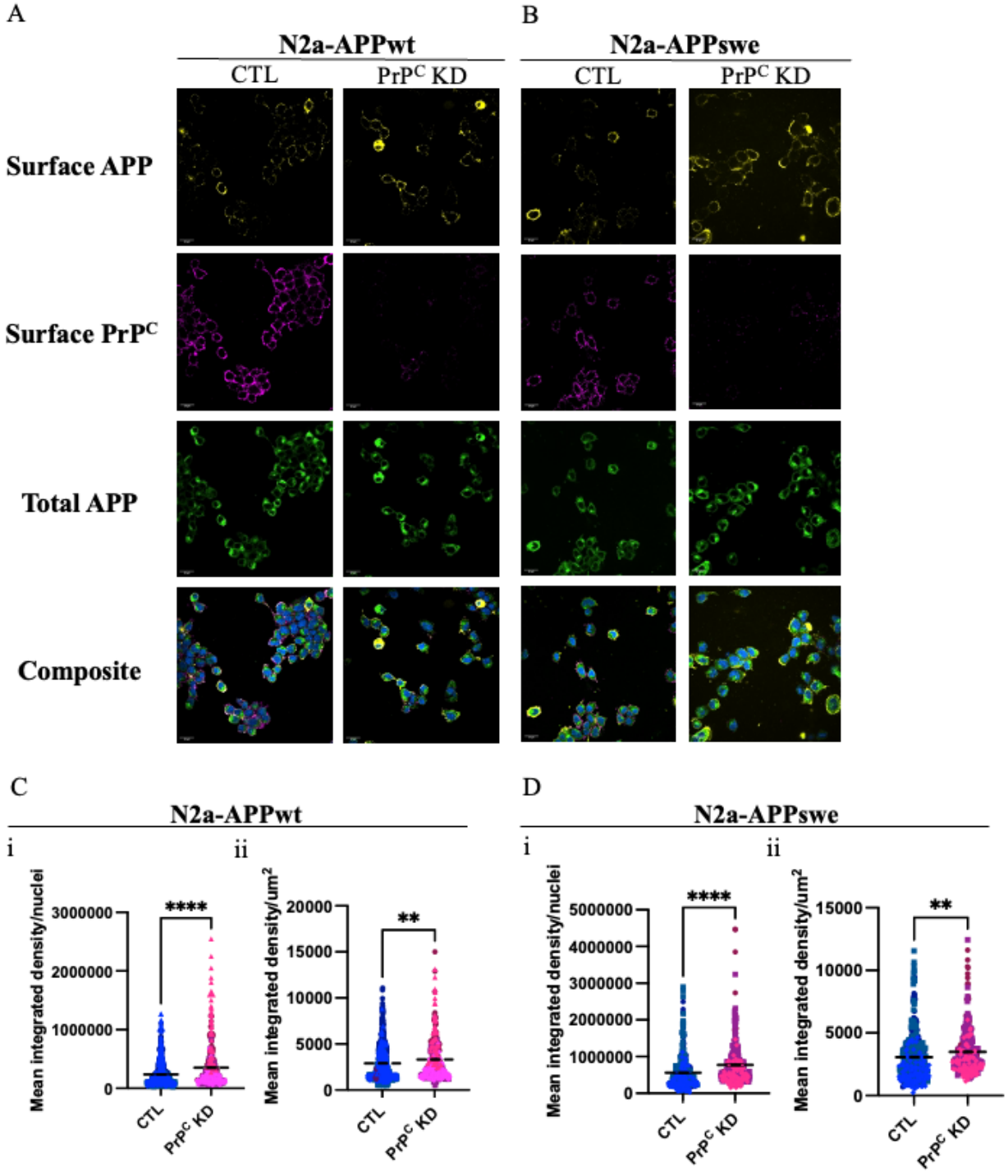

Figure 2.9: **PrP^C KD increases CTM1-labeled total APP in N2a-APPwt and N2a-APPswe cells.**

Figure 2.9: (continued). **A-B.** Representative images from the middle plane of a Z-stack taken from N2a-APPwt or N2a-APPswe cells transfected with control (left) siRNA or *Prnp* (right) siRNA. Cells were stained with pAb NTH452 to label cell surface APP (yellow) and mAb SAF32 to label cell surface PrP^C (magenta). After incubation with two secondary antibodies, the cells were permeabilized and stained with pAb CTM1 and a third secondary antibody to visualize total APP (green). The composite image includes a Hoechst nuclear stain (blue). Scale bar, 20 µM. **C-D.** Quantification of the mean integrated density of CTM1-labeled APP (green) in N2a-APPwt cells and N2a-APPswe cells. The data is taken from 16 images per condition, over four coverslips each for N2a-APPwt and N2a-APPswe cells. i. Mean integrated density of CTM1-labeled APP per cell plotted in a superplot. Each color represents one of the three/four different coverslips/experiments, and each data point is from one cell. For N2a-APPwt cells, the mean integrated density/nuclei = 467450 ± 15200 (N=712 cells) in the control condition vs. 699197 ± 37694 (N=354 cells) after PrP^C KD ($p<0.0001$). For N2a-APPswe cells, the mean integrated density/nuclei = 562,147 ± 24,677 (N=364 cells) in the control condition vs. 771,576 ± 33,159 (N=312 cells) after PrP^C KD ($p<0.0001$). ii. Quantification of the mean integrated density of CTM1-labeled APP per μm^2. The area of each cell in the middle of each Z-stack plane was measured, and the mean integrated density of CTM1-labeled APP for that cell was divided by its area in the selected plane. For N2a-APPwt cells, the mean integrated density/μm^2 = 2887 ± 70.4 (N=712 cells) in the control condition vs. 3306 ± 119.5 (N=352 cells) after PrP^C KD ($p<0.01$). For N2a-APPswe cells, the mean integrated density/μm^2 = 3073 ± 102.7 (N=364 cells) in the control condition vs. 3494 ± 103 (N=312 cells) after PrP^C KD ($p<0.01$). Data were analyzed by a two-tailed, unpaired *t*-test, ** $p<0.01$, **** $p<0.0001$.

plasma membrane and total cellular APP intensity were increased after PrP^C KD in both cell lines, my earlier Western blot data using mAb 22C11 suggested no change in full-length APP (Figure 2.4 C-D). This suggests that the increased CTM1 signal following PrP^C KD may be primarily due to an increase in the overall pool of intracellular CTFs rather than full-length APP. To ensure the lack of change in the level of full-length APP after PrP^C KD, I reassessed APP levels using the more specific APP extracellular domain conformation-specific mAb P2-1 that does not cross-react with APP homologs (amyloid precursor-like-proteins 1 and 2), which also showed no difference in APP following PrP^C KD (Figure 2.10, A.1), as did the qRT-PCR data (Figure 2.4 A). Thus, the observed increase in intracellular fluorescence of CTM1 likely reflects an increase in APP CTFs rather than full-length APP. These findings agree well with the Western blot data using the C-terminal Y188 mAb that suggested an increase in CTFs in both cell lines after PrP^C KD (Figure 2.7).

The increase in full-length APP immunofluorescence signal in non-permeabilized PrP^C KD cells combined with the lack of change in total cellular full-length APP, led us to consider that APP might be more efficiently trafficked to, or retained at, the plasma membrane. As a consequence of such retention, a greater fraction of APP would be subject either to plasma membrane, or endosome-localized, secretases if diverted to the endocytic pathway (Figure 2.7). To assess whether APP levels are increased at the plasma membrane after PrP^C KD more precisely, I biotinylated plasma membrane proteins and probed for APP in control and PrP^C siRNA treated N2a-APPwt and N2a-APPswe cells. To obtain a more accurate readout of FL APP levels, cells were pre-incubated with the ADAM10 inhibitor, TAPI-2, which prevents APP cleavage at the plasma membrane. Compared with control cells, full-length plasma membrane-resident APP was increased $\sim$ 2-fold in N2a-APPwt cells and $\sim$ 3-fold in N2a-APPswe cells after PrP^C KD (Figure 2.11 A). To assess the selectivity of this effect, I separated aliquots of biotinylated cell lysates from N2a-APPwt and N2a-APPswe

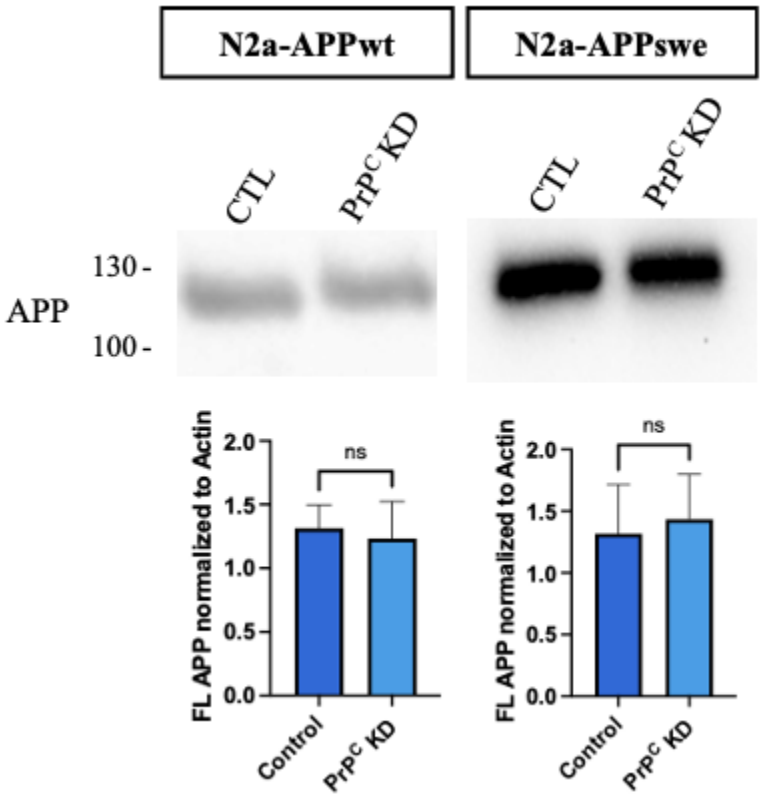

Figure 2.10: **PrP^C KD does not affect full-length APP protein levels in N2a-APPwt or N2a-APPswe cells.** Representative Western blots (top) and associated densitometry (bottom) of N2a-APPwt and N2a-APPswe cell lysates probed for APP before and after siRNA-induced PrP^C KD. APP was detected with mAb P2-1 and normalized to actin levels. Data points were analyzed by a two-tailed, unpaired t-test from three separate experiments; ns = not significant.

cells on 4-20% Tris-Glycine gels and immunoblotted to visualize the spectrum of plasma membrane-localized, biotin-labeled proteins (Figure 2.11 B). Comparison of banding patterns from control and PrP^C KD cells revealed no overall striking differences in the intensity of surface proteins labeled by biotinylation, supporting a relatively selective effect on APP following PrP^C KD.

We next asked whether the increase in plasma membrane APP after PrP^C KD results from an effect on APP turnover. To assess this, I performed surface biotinylation as described above but added a 15-minute 37°C incubation period to promote endocytosis of surface APP, after which the cells were cooled to 4°C to stop endocytosis, followed by elimination of the remaining surface biotin via glutathione-induced cleavage of the disulfide bond between biotin and plasma membrane proteins. We observed a significant increase in the fraction of endocytosed APP following PrP^C KD in both cell lines (Figure 2.11 B). This suggests that the increase in APP load to the plasma membrane leads to an increase in its endocytosis.

BACE1 cleaves APP primarily within the trans-Golgi netowrk (TGN) and endosomes. This led us to consider whether PrP^C, in some way, facilitates the effect of BACE1 to cleave APP in early secretory compartments that would act to suppress transit of full-length APP to the plasma membrane, which would explain the observed increase in full-length APP on the plasma membrane following a reduction in PrP^C. To address this possibility, I asked whether another known BACE1 substrate is similarly protected from cleavage by PrP^C KD [74] (Figure 2.11 C). NCAM1 is a glycoprotein with two major intracellular isoforms – NCAM1-140 and NCAM1-180 [74]. Similar to APP, both NCAM1-140 and NCAM1-180 are transmembrane proteins that follow the secretory pathway. Probing the fraction of biotinylated plasma membrane proteins for NCAM1 revealed no significant change in the levels of either NCAM1-140 or NCAM1-180 after PrP^C KD (Figure 2.11 C). While there are no conclusive studies on the

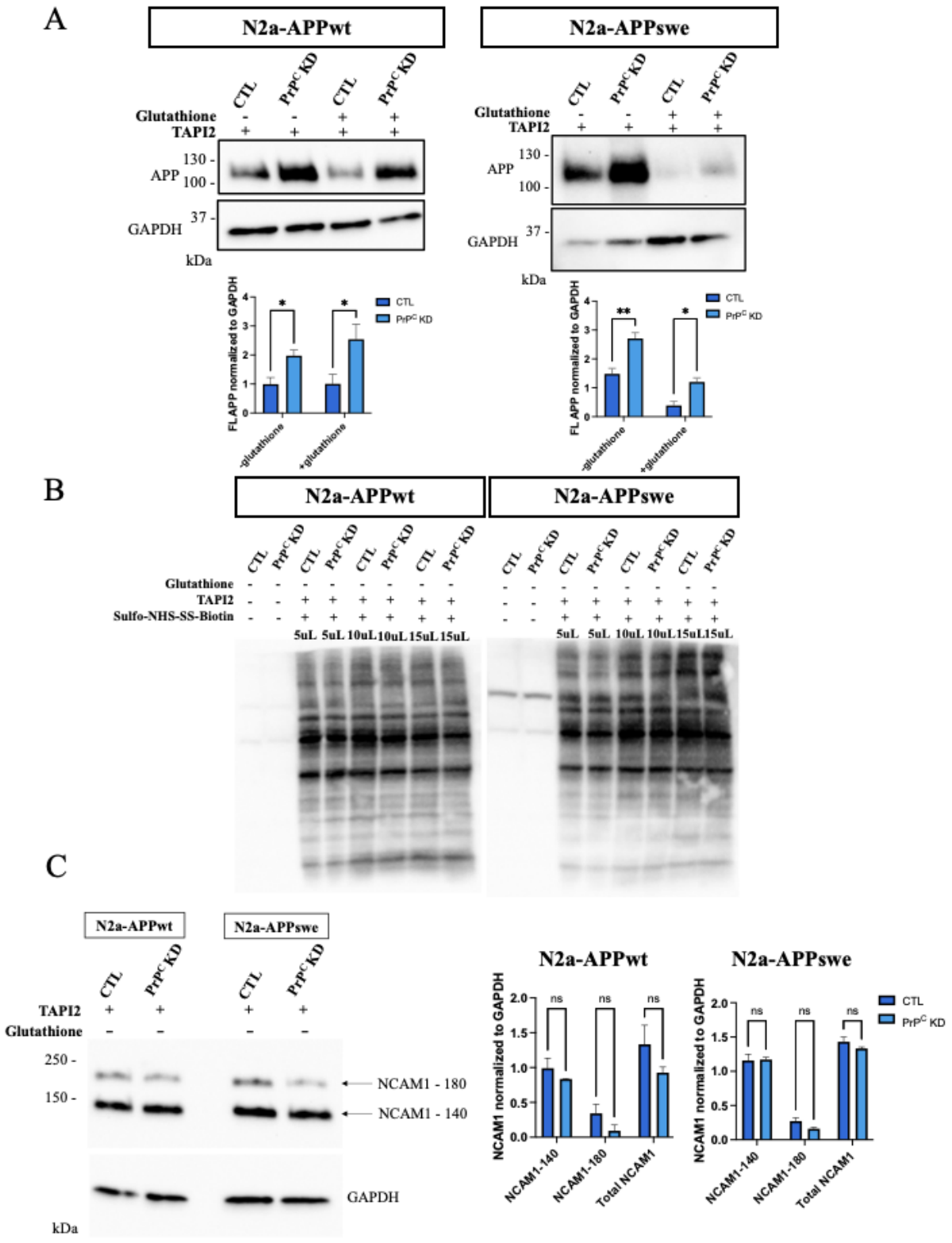

Figure 2.11: **PrP^C KD increases full-length APP at the surface in N2a-APPswe and N2a-APPwt cells.**

Figure 2.11: (continued). **A.** The levels of both full-length surface APP and APP endocytosed from the plasma membrane after a 15-minute, 37°C incubation were significantly increased in N2a-APPwt and N2a-APPswe cells following PrP^C KD. Representative Western blots and densitometry are shown. FL APP was detected using the Y188 antibody, and the signal intensities were normalized to GAPDH. **B.** PrP^C KD does not result in a global increase of biotinylated plasma membrane proteins. Cells were transfected with control or siRNA to PrP^C, and surface proteins were biotinylated with sulfo-NHS-SS-biotin. 5, 10, or 15 µL of N2a-APPwt and N2a-APPswe cell lysates were fractionated through a 4-20% Tris-Glycine gel and immunoblotted with an anti-biotin antibody.**C.** The levels of surface NCAM1, another substrate of BACE1, were not altered following PrP^C KD. NCAM1-140 and NCAM1-180 were detected using AB5032 antibody, and signal intensities were normalized to GAPDH. The data from three separate experiments were analyzed by a two-way ANOVA, * $p<0.05$, ** $p<0.01$, ns = not significant.

specific compartments in which BACE1 cleaves of NCAM1, BACE1 is assembled and trafficked through the secretory pathway and endosomal-lysosomal system [33]. The optimal pH of BACE1 activity is pH $\sim$ 4.5. BACE1 localizes to acidic intracellular compartments, such as the Golgi apparatus, TGN, and endosomes [52, 53, 76]. BACE1's pro-domain is cleaved by a serine protease in the ER, which produces a more mature form of BACE1 [155]. Even in an immature state, BACE1 can still cleave its substrates [153]. APPswe gets cleaved by BACE1 in the TGN, either because it is more conformationally accessible to BACE1 or because it is sequestered into the same compartments that BACE1 is being trafficked through [144]. Even though NCAM1 may not be predisposed to BACE1 cleavage in early secretory compartments in the way that APPswe is, my studies show that in addition to APPswe, plasma membrane levels of APPwt, which is not conformationally predisposed to BACE1 cleavage in early compartments, increase significantly in the absence of PrP^C. If PrP^C acts directly on BACE1 to similarly affect the trafficking of APPwt and APPswe, which are both potential BACE1 substrates that are processed differently, I hypothesize that the absence of PrP^C similarly affects other BACE1 substrates such as NCAM1. However, I did not observe a similar increase in NCAM1 plasma membrane levels in the absence of PrP^C in either the N2a-APPwt or N2a-APPswe cells (Figure 2.11 C). Thus, the effect of PrP^C to suppress APP

trafficking to the plasma membrane carries some degree of specificity that does not appear to be explained by a direct effect on BACE1.

2.4 Discussion

The role of PrP^C in AD, specifically in relation to Aβ, has garnered significant attention in recent research. Younan et al., 2013 identified a connection between misfolded forms of PrP^C and Aβ as key players in the pathogenesis of AD [162]. Some groups have additionally described a role for PrP^C in mediating the toxicity of Aβ species associated with AD [34, 117]. Furthermore, the presence of PrP^C traps Aβ in an oligomeric form, contributing to the neurotoxicity observed in AD [41].

PrP^C acts as a common ligand and downstream effector of neurotoxic species of various proteins involved in neurodegeneration, including Aβ, α-synuclein, and tau [34, 125]. Additionally, PrP^C facilitates the uptake and spread of Aβ oligomers, leading to neurotoxic effects [8]. Specifically, PrP^C mediates toxic signaling of β-sheet-rich conformers independently of infectious prion propagation, indicating a broader pathophysiological role beyond prion diseases [120].

Moreover, the interaction between PrP^C and Aβ is linked to synaptic impairment in AD, highlighting the significance of PrP^C in Aβ-induced neurotoxicity [10, 22, 67, 80, 104, 134]. However, several studies, including previous work from our lab, have also indicated that PrP^C may play a role in the clearance of Aβ, suggesting a potential therapeutic target for AD [60, 118].

Given the conflicting evidence in the field, clarifying the role of PrP^C in both normal and

AD conditions is of utmost importance to gain a better understanding of how we can use PrP^C as a therapeutic target and under what circumstances. In my study, I aimed to better clarify and extend previous observations from our lab in N2a-APPswe cells that supported a role for PrP^C in facilitating the release of Aβ [118]. Using the highly sensitive MSD platform, I confirmed that PrP^C expression is positively correlated with Aβ_{42} levels in the media of N2a-APPswe cells. With roughly 70% reduction in PrP^C levels following siRNA, I saw a significant $\sim$ 30% reduction in Aβ_{42}. I further showed that this correlation between PrP^C expression and Aβ release extends to Aβ_{40}, the two major secondary isoforms of Aβ. We measured a similar overall reduction after PrP^C knockdown, which supports a general effect of PrP^C on APP delivery to specific cellular compartments rather than a specific effect on its processing. Since N2a-APPswe cells generate high levels of Aβ_{42} and are known to process APPswe differently than APPwt, I questioned whether the effect of PrP^C on Aβ was unique to N2a-APPswe cells. Aβ_{40} levels were significantly reduced after PrP^C KD in N2a-APPwt cells. Aβ_{42} levels were too low to draw any conclusions. This result argues against a cell-specific effect.

We assessed whether the PrP^C-dependent Aβ release might be due, in part, to an effect on APP processing. We looked for changes in the relative levels of sAPPα and sAPPβ, which reflect the activity of α-secretase and β-secretase cleavage of APP, respectively. We show that PrP^C knockdown significantly reduced the level of sAPPβ in both cell lines, consistent with the observed reduction in Aβ. Whereas sAPPα was unchanged in N2a-APPswe cells, it was markedly increased in N2a-APPwt cells, suggesting a distinct difference in the manner in which APP is processed in these two cell lines. Prior studies [71] have suggested that PrP^C, a substrate of ADAM10 metalloproteinase and the principal α-secretase that cleaves APP, might act to mitigate α-secretase cleavage of APP by acting as a substrate competitor for this enzyme. Such competition could shift APP into the amyloidogenic path-

way. Although this might be sufficient to explain the decreases sAPPβ in both cell types, and the increase in sAPPα observed in N2a-APPwt cells, after PrP^C knockdown, it is not sufficient by itself, to explain the lack of effect on sAPPα in N2a-APPswe cells after PrP^C knockdown. Previous studies have found that the APPswe and APPwt cells are equally predisposed to cleavage by α-secretase [144]. For this reason, one might expect that an effect of PrP^C on ADAM10 cleavage of APP would effect both APPwt and APPswe substrates. This suggests some differences in how PrP^C might affect cleavage of APP in N2a-APPwt and N2a-APPswe cells.

We attempted to confirm these differences by assessing CTFs that are retained in the plasma membrane following α- and β-secretase cleavage. We hypothesized that the intracellular C-terminal fragments (CTFs) of APP produced by α- and β-secretase cleavage would mirror the observed changes in sAPPα and sAPPβ for each cell line. Thus, I predicted reduced β-CTF in both cell lines, to correspond with reduced Aβ release and sAPPβ in each line, in addition to an increase in αCTF, at least in N2a-APPwt cells. However, despite the differences in sAPP fragments between N2a-APPwt and N2a-APPswe cells, I found a significant increase in α-CTF, and therefore, of total CTFs after PrP^C KD. β-CTF levels did not change significantly. These data suggest a disconnect between the retention of CTFs and the initial cleavage of APP by either α- or α-secretases.

These findings raised two possibilities, which are not mutually exclusive: 1) APPwt and APPswe are processed differently, as previously suggested by others [144], and 2) the decrease in sAPPβ in both cell lines suggests there are shared aspects of processing and trafficking between APPwt and APPswe. Nontheless, CTF fractions were increased in both cell lines, possibly due to reduction of PrP^C, and hence, an effect on γ-secretase processing. A change in γ-secretase processing could lead to CTF accumulation in the endocytic pathway. While

it appears that α-CTF levels increase significantly in cell lysate following PrP knockdown, in line with my observations on sAPP fragment changes, alterations in the predominant β-secretase fragments (+11 and +1) were more variable from experiment to experiment. If there is β-CTF accumulation following PrP^C knockdown, the reduction in steady state levels of secreted Aβ might point towards intracellular CTF accumulation or degradation.

It is possible that PrP^C causes retention of APP within early secretory compartments, either directly or through a signaling mechanism. An absence of PrP^C might then allow more APP to be trafficked along the secretory pathway to the plasma membrane. This idea is supported by the immunofluorescent staining and biotinylation studies, which showed an increase in FL APP on the plasma membrane after PrP^C knockdown, in both cell lines. Moreover, there was an increase in the fraction of plasma membrane APP that underwent endocytosis after PrP^C knockdown. The retention of CTFs with a reduction in PrP^C could be explained by a differential effect of PrP at this stage of APP trafficking. Our prior work and that of others suggest PrP^C can bind to Aβ peptides. The presence of PrP^C at the plasma membrane may be required to promote the release of Aβ derived from β-CTFs and its absence could lead to Aβ accumulation. This possibility was not addressed in the current work.

I considered two potential explanations to explain the increased fraction of APP endocytosed following PrP^C knockdown in both cell lines. Since PrP^C is also a membrane protein and has a longer half-life and membrane residence than APP, its absence on the membrane could affect critical signaling processes that subsequently enhance the recycling of APP, leading to increased endocytic compartment cleavage of APP and intracellular CTF accumulation. Alternatively, the increase in plasma membrane APP as a result of PrP^C loss could be the driving factor for the increased endocytosis. Although various studies have established the interaction between Aβ oligomers (AβO) and the cellular prion protein

(PrP^C) [14, 117, 122, 165], the exact role of PrP^C in Alzheimer's disease (AD) pathophysiology remains debated. A significant focus has been on the N-terminal polybasic region of PrP^C, identified as a key site for AβO binding. This region was also thought to be crucial for its proposed interaction with β-secretase, an interaction believed to inhibit β-secretase activity and thus the cleavage of amyloid precursor protein (APP), potentially reducing the formation of toxic amyloid peptides. Previous research from Parkin et al. 2007 suggested that overexpressing PrP^C could inhibit BACE1 (β-secretase) activity, leading to decreased Aβ production [108]. However, my findings appear to contradict these earlier studies; I observed that reducing PrP^C levels decreases the degree to which APP is cleaved by BACE1, and as a result, lowers the steady-state levels of secreted Aβ.

This discrepancy may be explained by the use of different cell models; the earlier study used N2a cells expressing mouse APP, whereas my N2a cells express human APP and overexpress either wild-type (wt) or Swedish mutation (swe) APP variants.

The same group, Griffiths et al. 2011 [49], later extended their studies to incorporate the modifications of APP that I used, with a focus on the interaction of BACE1 with PrP^C [49, 50]. However, unlike the study of Griffiths et al. [49] that highlighted a direct interaction of PrP^C with BACE1 in the trans-Golgi network (TGN) and its differential effects on APP cleavage, my study did not specifically examine the mechanistic relationship between PrP^C and BACE1. APPwt and APPswe are processed within distinct subcellular compartments - BACE1 primarily cleaves APPswe in the TGN [53, 144], and the sAPPβ fragment produced from this cleavage is trafficked through the secretory pathway where it is released into the media [144]. APPwt is mainly cleaved by α-secretase at the plasma membrane, although some BACE1 cleavage may occur in endosomes resulting in low levels of Aβ [144]. In experiments using HEK cells engineered to express either APPwt or APPswe, Griffiths et al. [49] found

that PrP^C inhibited BACE1 activity on APPwt but did not affect its activity on APPswe21. In contrast, I found that reducing PrP^C levels decreased sAPPβ in both cell types, indicating that the absence of PrP^C somehow impairs BACE1 activity or its access to APP. Griffiths et al [49, 50] propose that PrP^C confines BACE1 to membrane subcompartments separate from those containing APP. However, my results suggest a different mechanism: PrP^C might target BACE1 to TGN compartments that do contain APP. The absence of PrP^C, therefore, likely hinders early BACE1 cleavage, resulting in a greater amount of APP being transported to the plasma membrane in both N2a cells expressing the APPwt and APPswe modifications.

From these results, I hypothesize that *in vivo*, PrP^C induces intracellular retention of APP that might increase exposure to BACE1 cleavage, and that its absence allows for APP to be transported through the secretory pathway to the membrane and be recycled into the endocytic pathway or back to the trans-golgi, which then increases the likelihood of cleavage in intracellular compartments such as the trans-golgi and endosomes. We also hypothesize that the role for PrP^C in APP retention is elevated when APP is both overexpressed and mutated. Confirmation of these hypotheses awaits further experimentation.

CHAPTER 3

CHAPTER 3: THE EFFECT OF PRP^C EXPRESSION ON Aβ LEVELS AND APP PROCESSING IN TRANSGENIC MICE

3.1 Introduction

Transgenic mouse models have been crucial in investigating the interplay between PrP^C and AD pathology [137]. To better understand the association between AD and PrD, our lab generated "Dual Disease" CeAPPswe/PS-1ΔE9/PrP-A116V or TgAD/GSS mice that develop both Alzheimer's Disease and Gerstmann-Sträussler-Scheinker disease (GSS), a type of PrD [118]. TgAD mice are derived from the CeAPPswe/PS-1ΔE9 transgenic line (Jackson Laboratory), which carries APPswe and PS1ΔE9 transgenes under the control of a mouse PrP promoter. TgAD mice produce extracellular Aβ deposits and are an established model of human familial AD. TgGSS mice carry the PrP-A116V transgene, which includes the A116V mutation allelic with 128V under the control of a mouse PrP promoter, which is homologous to the PrP-A117V/129V genotype that causes GSS in humans [118]. TgAD mice were crossed to TgPrP$^{-/-}$/FVB mice and subsequently crossed to TgGSS mice to establish the TgAD/GSS line [118]. Due to the initial TgPrP$^{-/-}$ cross, TgAD/GSS mice do not have endogenous PrP^C, only the PrP-A116V transgene. These mice experience earlier onset of progressive gait ataxia, exhibit enhanced histopathological features, and have elevated brain levels of disease-related proteins [118].

Our laboratory observed earlier onset of ataxia in TgAD/GSS mice (106.1 ± 6.0 days) compared to TgGSS (132.1 ± 12.7 days) [118]. TgGSS mice also died significantly earlier (126.0 ± 8.2 days) than their TgGSS counterparts (174.6 ± 18.4 days) [118]. Moreover, the laboratory observed a 2.5-fold increase in spongiform degeneration area, coupled with an increase in PrP plaque burden in TgAD/GSS mouse brains taken at ∼ four months when compared to age-

matched TgGSS mice [118]. Aβ plaque burden, normalized to the levels in TgAD mice, was significantly higher in the TgAD/GSS which express PrP-A116V or PrP^C at $\sim$ four times the normal expression level, compared to both TgAD and the TgAD/$PrP^{-/-}$ mice [118]. TgAD mice with human PrP (TgAD/HuPrP) were used as a control for the TgAD/GSS mice, since these mice express human PrP at $\sim$ four time the normal expression level [118]. The increased Aβ plaque burden in the lines expressing high levels of wild-type or mutated PrP suggests that 1) PrP expression augments Aβ plaque production and 2) there isn't a notable difference between PrP-A116V and PrP^C in their ability to promote Aβ plaque production [118]. Finally, levels of Aβ, immature APP (N-glycosylated) and mature APP (N-glycosylated, O-glycosylated, and tyrosol-sulfated) were all elevated in TgAD/GSS mice compared to TgAD and TgGSS mice [118]. These models have provided insights into how different forms of PrP^C lead to differences in deposition of A and formation of plaques, potentially affecting disease progression [118].

Moreover, PrP^C may have neuroprotective properties, which is of potential importance in understanding neurodegenerative diseases like AD [156]. Additionally, studies on transgenic mice overexpressing PrP^C have highlighted the importance of normal levels of PrP^C expression in maintaining brain function and preventing protein (Aβ, tau, and α-synuclein) aggregation associated with neurodegenerative disorders [70].

While PrP^C is well-known for its role in prion replication and neurotoxicity in transmissible spongiform encephalopathies, its exact physiological function remains unclear. Previous studies on Tg$Prnp^{-/-}$ mice have attributed various functions to PrP^C [132]. However, prior to the development of the Zurich-3 (ZHD) *Prnp*-ablated allele on a pure C57BL/6J genetic background, existing Tg$Prnp^{-/-}$ mouse lines were predominantly derived from 129 strain embryonic stem cells and crossed with non-129 strains, introducing genetic variability from

the mixing of two genetic backgrounds that could lead to misinterpretation of data [103]. The ZH3/ZH3 mice were the first co-isogenic Tg*Prnp*$^{-/-}$ mouse model, and revealed none of the phenotypes observed in other Tg*Prnp*$^{-/-}$ mouse lines, except for the development of chronic demyelinating peripheral neuropathy in aged mice [103].

As a continuation of my work *in vitro* described in Chapter 2, my goal was to determine whether my findings can be extended to a system *in vivo*. Using brains harvested from transgenic PrP^{C} knockout and wild-type (WT) mice, I compared levels of Aβ, full-length APP (FL APP), soluble APP (sAPP) ectodomains, and C-terminal fragments (CTFs). We also analyzed levels of soluble amyloid precursor-like proteins 1 and 2 (sAPLP1/2), which are homologs of APP and have some functional redundancy [25]. I showed that Tg*Prnp*$^{-/-}$ mice that lack PrP^{C} expression have increased levels of endogenous APP CTF compared to wild-type mice. This increase was only seen in female mice. Additionally, I did not find any significant differences in Aβ_{42} or Aβ_{40} (pg/mg of protein) between the Tg*Prnp*$^{-/-}$ and wild-type mice. Levels of sAPP fragments, sAPLP1, and sAPLP2 from Western blots were also unchanged in the Tg*Prnp*$^{-/-}$ mice compared to the wild-type mice. Our results suggest that the role of PrP^{C} in APP processing and trafficking may change based on the expression level of APP. Our Tg*Prnp*$^{-/-}$ mice express only endogenous levels of mouse APP, while the N2a-APPwt and N2a-APPswe cells both over-express human APP, albeit at different levels (Figure 2.4). However, the increase in endogenous APP CTFs in female Tg*Prnp*$^{-/-}$ mice does mirror the data from the cell-lines, pointing towards a different role for PrP in a system with endogenous APP.

3.2 Materials and Methods

3.2.1 Mice

Tg*Prnp*$^{-/-}$ mice [17, 19] were a gift from Dr. Stanley Prusiner (UCSF, San Francisco, CA). Wild-type (WT) and Tg*Prnp*$^{-/-}$ [17, 19], both of which maintained the FVB genetic background, were used in these studies. Right- and left-brain hemispheres were harvested from an equal number of male and female mice in each experiment. All procedures related to animal care and treatment conformed to the policies of the Institutional Animal Care and Use Committee at the University of Chicago.

3.2.2 Quantifications of Aβ and secreted APP

For analysis of endogenous Aβ (pg/mg of protein), hemibrains of 65 ± 5- day-old FVB (control) and Tg*Prnp*$^{-/-}$ mice (N=12 each) were homogenized in 10 volumes (wt/vol) of MSD lysis buffer (150 mM NaCl, 20 mM Tris pH 7.5, 1 mM EDTA, 1 mM EGTA, 1% Triton-X-100), supplemented with the following protease and phosphatase inhibitors: Halt™ Protease Inhibitor Cocktail, EDTA-Free (Thermo Fisher Scientific Inc., Waltham, MA), Phosphatase Inhibitor II (Sigma Aldrich, St. Louis, MO), Phosphatase Inhibitor Cocktail 3 (Sigma Aldrich, St. Louis, MO), and clarified by centrifugation. Aβ_{40} and Aβ_{42} levels were measured using a V-PLEX Plus Aβ Peptide Panel 1 4G8 (K15199G) (Meso Scale Discovery, Rockville, MD).

3.2.3 DEA and RIPA Fractionation

For separating soluble and membrane proteins by DEA and RIPA fractionation, hemibrains were harvested from 65 ± 5- day-old FVB (control) and Tg*Prnp*$^{-/-}$ mice (N=12 each) and homogenized using a polytron Tissue Tearor™ (Model 985370; BioSpec Products, Bartlesville, OK) on setting 3 for 30 seconds to 1 minute on ice as described [77] in 10 volumes

(wt/vol) of 0.2% diethylamine (DEA) in 50 mM NaCl (pH 10), supplemented with protease inhibitors (Halt™ Protease Inhibitor Cocktail) and 0.25 mM phenylmethylsulphonyl fluoride (PMSF). The resulting homogenate was clarified by ultracentrifugation at 100,000 × g for 30 min. The supernatant was neutralized by the addition of 10% 0.5 M Tris-HCl (pH 6.8) and saved as the DEA-soluble fraction containing all soluble proteins. The pellet was reconstituted and homogenized with radioimmunoprecipitation (RIPA) buffer using a Microson Ultrasonic Cell Disruptor (Model XL200; Misonix, Farmingdale, NY) for 30 seconds at amplitude 6 and then cleared by ultracentrifugation for 30 min at 100,000 × g to obtain the RIPA-soluble fraction, which contains all membrane-bound proteins. The samples were resolved by SDS/PAGE on Tris-Tricine gels and analyzed by immunoblotting. The primary antibodies used to probe Western blots are listed in the "Antibodies" section above and in the Appendix (as a table). The blots were developed with LI-COR IR800 anti-rabbit and IR680 anti-mouse secondary antibodies (NetaScientific, Marlton, NJ), and the signal intensities were quantified using the Odyssey Infrared Imaging System (LI-COR Biosciences, Lincoln, NE).

3.2.4 Western Blotting

Brain homogenate samples were prepared by adding 3X to 4X Laemmli sample buffer (Bio-Rad, Hercules, CA) in the presence or absence of 2-mercaptoethanol was used for Tris-glycine gels, and 2X tricine sample buffer (Bio-Rad, Hercules, CA) 2-mercaptoethanol was used for Tris-tricine gels. The proteins were solubilized and denatured by heating the samples to 95°C for 5 min.

To separate proteins ≥15kDa, 4-20% Tris-glycine gradient gels were used, whereas 16.5% Tris-tricine gels were used to separate proteins ≥15kDa. Proteins were transferred to 0.45 µm polyvinylidene difluoride (PVDF) membranes (Bio-Rad, Hercules, CA) or Immobilon™

- FL 0.45 µm PVDF membranes (Millipore) at 400 mA at 4∘C for 3 hours. Membranes were blocked in 5% milk in PBS-T or 10% BSA and 10% fish scale gelatin (FSG) in PBS-T (when using fluorescent secondary antibodies) for 1-2 hours at RT, followed by overnight incubation with primary antibodies at 4°C. Washes in between steps were in tris-buffered saline with Tween-20 (TBS-T) or PBS-T 3X for 10 minutes, and blots were incubated in secondary antibodies at RT for 1 hour. When fluorescent secondary antibodies were used, blots were imaged on the LI-COR Odyssey near-IR imager for quantitative immunoblots immediately after washing. Otherwise, blots were incubated for 5 minutes in SuperSignal West Pico PLUS Chemiluminescent Substrate (Thermo Fisher Scientific Inc., Waltham, MA) and imaged using the ChemiDoc MP Imaging System (Bio-Rad, Hercules, CA).

3.2.5 Statistical Analysis

Statistical analyses were performed using Prism 10 (GraphPad Software). Comparisons between two groups were performed by two-tailed unpaired t-tests (two groups), and three or more groups were analyzed by ANOVA, followed by an appropriate post-hoc multiple comparisons test.

3.3 Results

3.3.1 The In Vivo Effect of PrP^C Expression on Endogenous Aβ Levels in Transgenic Mice

To determine if the findings in the cell lines are observed in a more biologically relevant *in vivo* system that does not overexpress APP, I measured Aβ levels in mouse brains from WT and Tg$Prnp^{-/-}$ mice using the sensitive MSD platform (Figure 3.1). Brain lysates were prepared from an equal number of male and female mice between 60–70 days of age. This time point was chosen to avoid the high levels of BACE1 that are present until $\sim$ 60

days of age when they normalize [5]. The mean concentration of Aβ_{40} was 11.44 ± 0.6587 pg in WT mice and 12.54 ± 0.9743 pg in Tg*Prnp*$^{-/-}$ mice (N=10 mice per group) (Figure 3.1 A), while that of Aβ_{42} (per mg of total protein) was 1.291 ± 0.06206 pg in WT mice, compared with 1.216 ± 0.06293 pg in Tg*Prnp*$^{-/-}$ mice (N=10 mice per group) (Figure 3.1 B). We further stratified the two mouse groups by by brain hemisphere and sex (Figure 3.1 C-D). We found no significant differences in Aβ_{40} levels between the right- and left- brain hemispheres of either WT or Tg*Prnp*$^{-/-}$ mice (Figure 3.1 C). There were also no significant differences in Aβ_{40} levels between males and females in either mouse group (Figure 3.1 D). The low concentrations of Aβ_{40} and Aβ_{42} in WT mice expressing only endogenous APP are noteworthy and are likely to limit the ability to detect a further decrease (Figure 3.1).

3.3.2 The In Vivo Effect of PrP^C Expression on the Levels of Endogenous APP Fragments in Transgenic Mice

We then asked if the altered APP processing I observed in cultured cells following PrP^C KD was present in Tg*Prnp*$^{-/-}$ mice compared with WT mice. We applied a previously described method that separates cytosolic and extracellular proteins derived from brain into a diethylamine (DEA) fraction and membrane proteins into a RIPA fraction [5]. I then compared the relative distributions of sAPP fragments, full-length APP, and APP CTFs in each mouse line. As expected, full-length APP could be detected only in the RIPA fraction (Figure 3.3 A-B). Moreover, sAPP fragments were only detected in the DEA fraction (Figure 3.3 C). I found no difference in the level of sAPP fragments the Tg*Prnp*$^{-/-}$ and WT mice (Figure 3.3 A-B). We also found no difference in full-length APP within the membrane fraction of the two mouse lines (Figure 3.3 A-B).

APLP1 and APLP2 belong to the same family of membrane proteins as APP and are processed by similar secretases but lack the Aβ region (Figure 3.2).

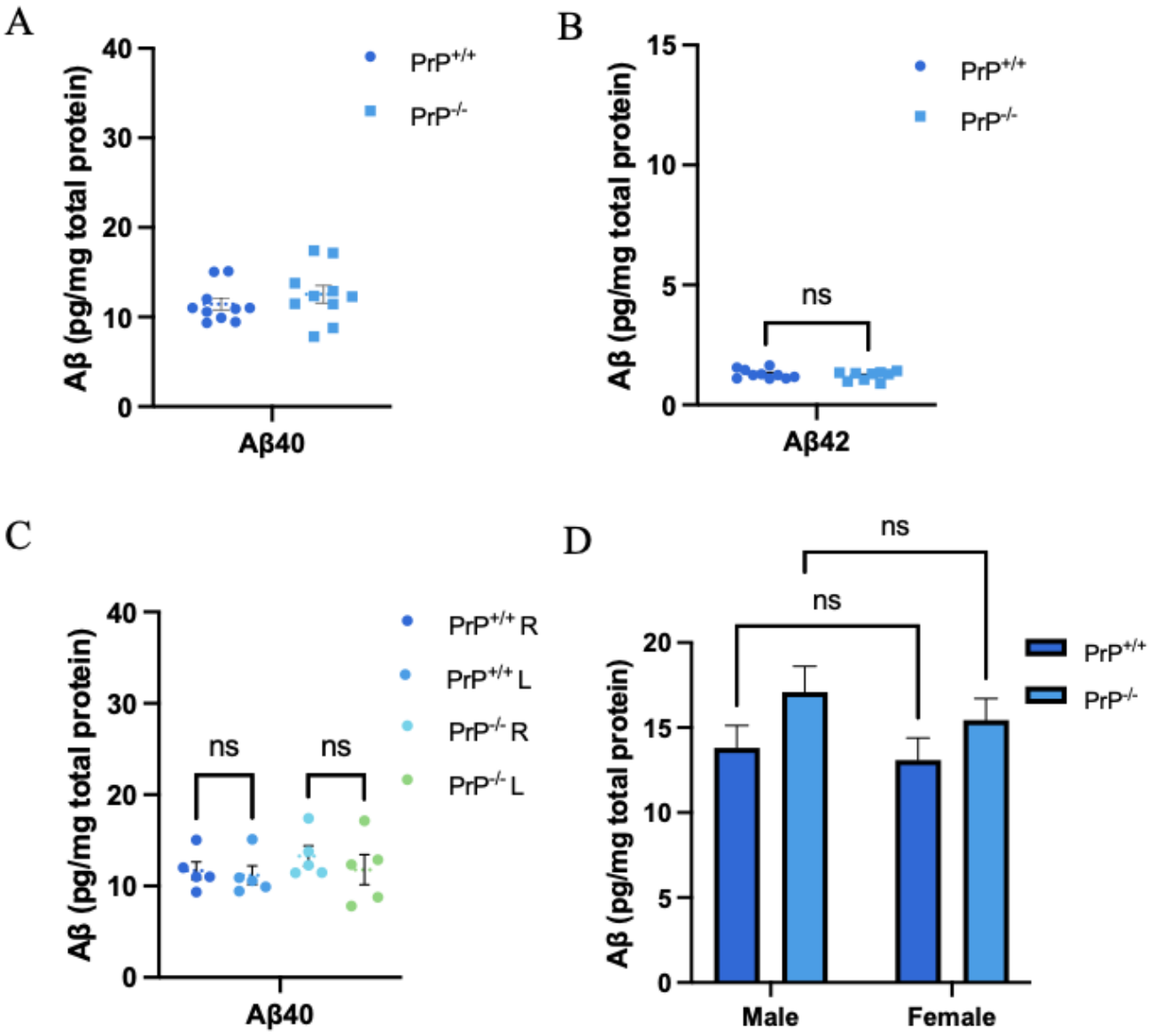

Figure 3.1: **Brain homogenates derived from Tg*Prnp*$^{-/-}$ and WT mice contain similar levels of Aβ_{40} and Aβ_{42} A-B**. MSD electrochemiluminescence quantification of Aβ_{40} and Aβ_{42} levels in brain homogenates of WT mice and Tg*Prnp*$^{-/-}$ mice (pg/mg). **C.** Aβ_{40} levels grouped by brain hemisphere. D. Aβ_{40} levels grouped by mouse sex. N=10 mice per group. Each data point is the average of 2 technical replicates. Data were analyzed by a two-tailed, unpaired *t*-test: ns = not significant.

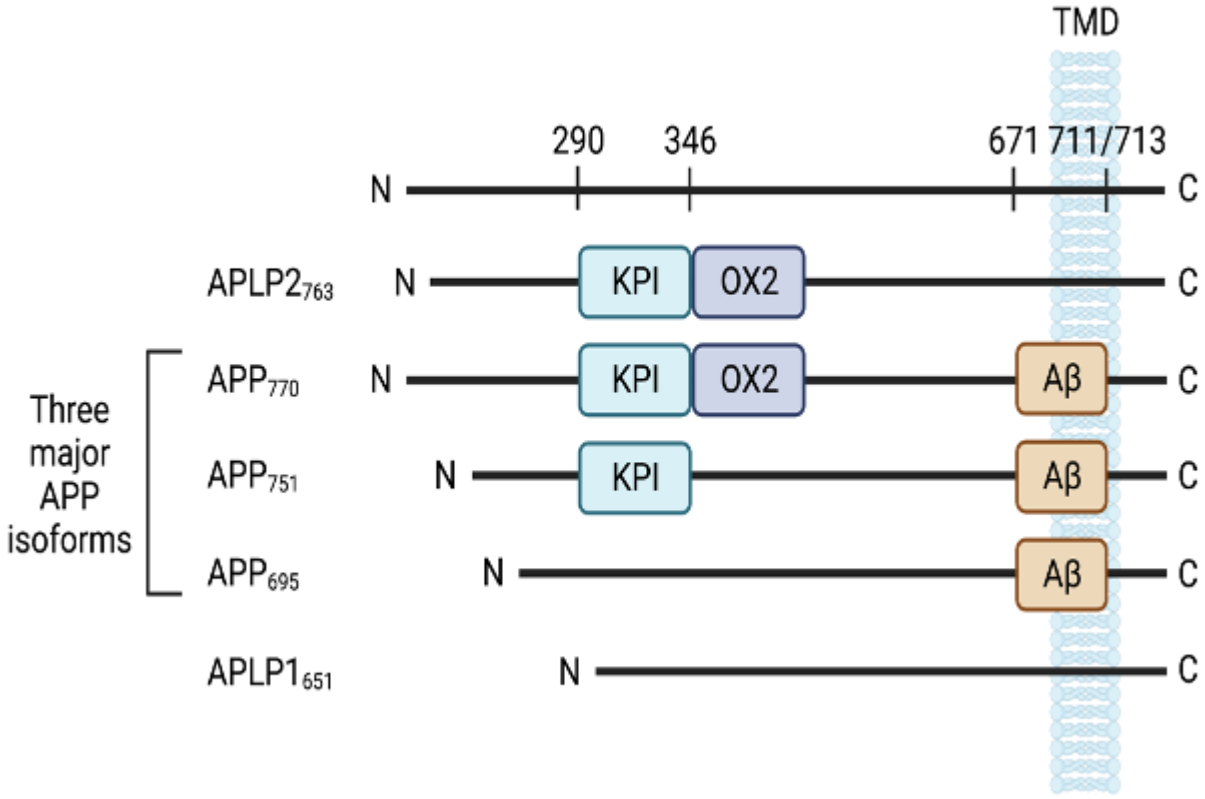

Figure 3.2: **Isoforms and homologs of APP**. APP is a large transmembrane protein with three major isoforms generated through the alternative splicing of exons 7 and 8 [9] - APP_{770}, APP_{751}, and APP_{693}. Amyloid precursor like-proteins 1 and 2 (APLP1 and APLP2) are shown for size comparison. The Aβ peptide sequence (in orange) starts within the ectodomain and ends within the transmembrane domain (TMD) of APP. APLP1 and 2 do not contain the Aβ peptide sequence.

APLP1 and 2 have shared synaptic functions and, as such, partial redundancy [25], however there were no differences in the levels of either protein between the two mouse lines (Figure 3.3 D-E). The loss of PrP^C in an endogenous APP-expressing mouse did not affect the overall levels of APP, APLP1, and APLP2 or APLP1/2 in the mice, as a group (Figure 3.3 D-E). However, when the data were analyzed according to sex, a clear and significant increase in APP CTFs, specifically α-CTF and +11 β-CTF fragments, within the RIPA fraction was observed only in female Tg$Prnp^{-/-}$ mice compared to female WT mice (Figure 3.3 B).

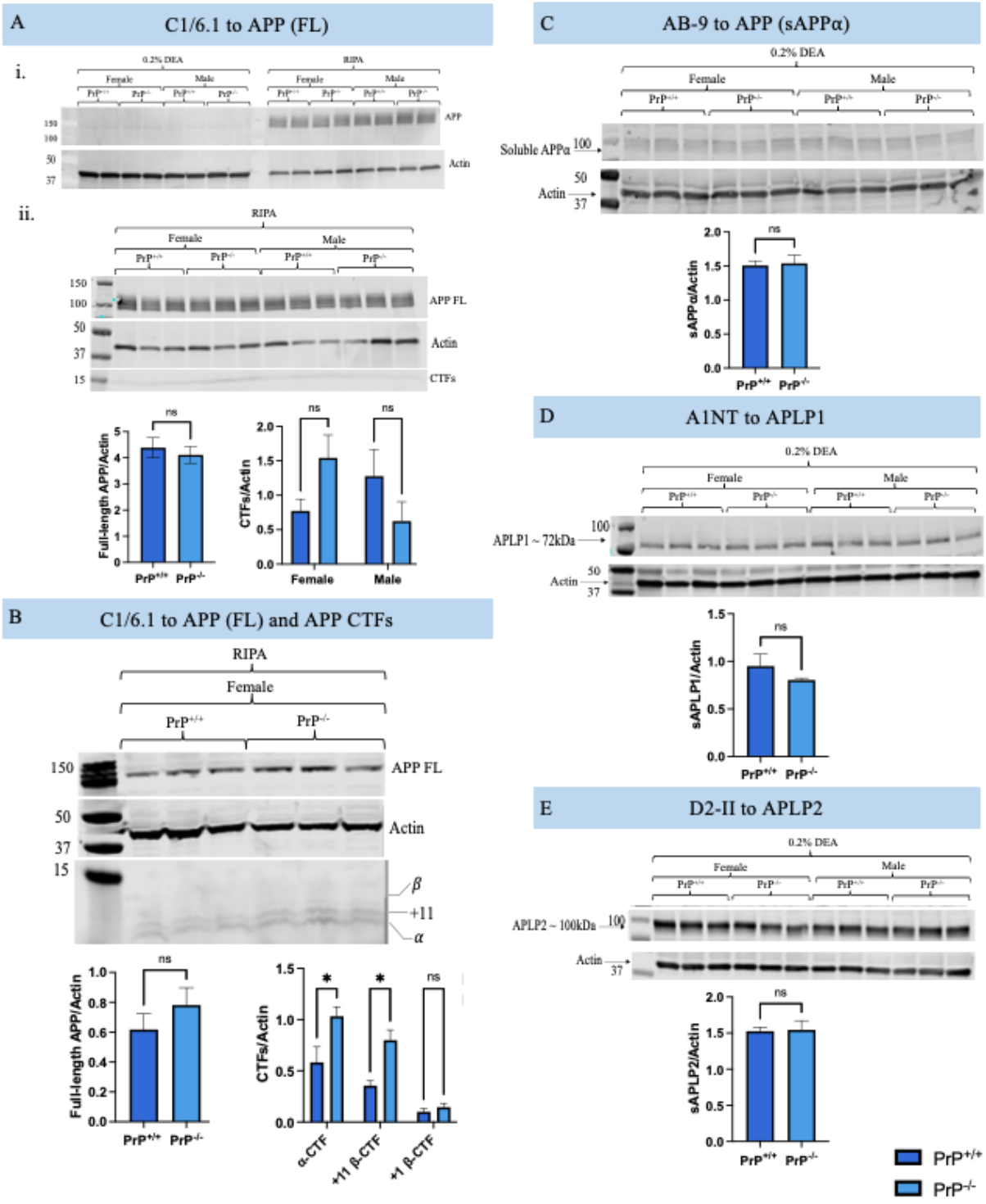

Figure 3.3: **RIPA-soluble brain homogenates show increased α-CTF and +11 β-CTF levels in Tg*Prnp*$^{-/-}$ females compared to WT mice.**

Figure 3.3: (continued). **A.** i. 65-day-old from Tg$Prnp^{-/-}$ and wild-type (FVB) mouse brains were separated into a soluble protein fraction (0.2% DEA) and a detergent-soluble membrane protein fraction (RIPA). Aliquots of each fraction were analyzed by immunoblotting with a C-terminal antibody to APP (C1/6.1) to confirm the separation of soluble and membrane-bound proteins. ii. Analysis of the RIPA fraction with a C-terminal antibody to APP (C1/6.1) confirms that there is no change in FL APP levels between Tg$Prnp^{-/-}$ and WT mice or males and females. **B.** Separation of RIPA-soluble proteins using a 16.5% Tris-tricine gel reveals an increase in α-CTF and +11 β-CTF levels in Tg$Prnp^{-/-}$ females compared to WT mice. **C.** Analysis of the DEA fractions with the AB-9 antibody to sAPP reveals no difference in sAPP between Tg$Prnp^{-/-}$ and WT mice. **D-E.** Analysis of the DEA fractions with antibodies to APLP1 or APLP2 reveals no differences in sAPLP1 or sAPLP2 between the genotypes. The results are representative blots from N=12 g$Prnp^{-/-}$ and N=12 WT mice. Protein molecular weight ladders are measured in kDa. The levels of indicated proteins in the RIPA and DEA homogenates (normalized to actin) were quantified. The data were analyzed by a two-tailed unpaired t-test, * $p<0.05$.

This finding agrees with the cell results which showed an increase in intracellular CTFs via immunofluorescence staining and Western Blotting (Figures 2.7 and 2.8), without any discernable change in total cellular levels of full-length APP (Figure 2.4) in female but not in male mice. However, this assay did not show an increase in sAPPα, a decrease in sAPPβ, or an increase in plasma membrane APP. These results should be weighed carefully, since stably transfected cells overexpress human APP at much higher relative levels than endogenous mouse APP. Nonetheless, the finding supports the idea that, in the absence of PrP^C, CTFs are generated and intracellularly retained through similar mechanisms in both female mice and the stably modified cell lines.

3.4 Discussion

Previous research from Parkin et al. 2007 [108] found that Aβ levels increased in a PrP^C knockout (KO) mouse model compared to wild-type (wt) mice [108]. In contrast, I observed that the deletion of PrP^C in mice did not change the levels of Aβ_{42} or Aβ_{40}. I have not re-examined the rate of plaque formation *in vivo*. My findings suggest the abasence of PrP^C

does not influence the accumulation of these specific Aβ peptides. These results contrast with expectations on a proposed protective role of PrP^C in sporadic Alzheimer's disease (AD) and its interaction with the APP processing pathway.

These discrepancies may be partly explained as follows. The previous study, Parkin et al. 2007 [108] noted an increase in Aβ peptides in PrP^C KO mice, but it utilized a genetically different PrP^C KO mouse strain (129OlaPrP$^{-/-}$) and examined the mice at 4 weeks of age — a time when BACE1 expression is notably high. Thus, the prior studies might not have taken a potentially important variable into account. Moreover, this previous study relied on immunoblotting for brain fraction analysis, whereas I employed the more sensitive MSD platform for my measurements.

In my examination of brain fractions expressing endogenous mouse APP and PrP^C, I found no significant changes in Aβ levels between PrP^C KO and wild-type (wt) mice at 65 days of age, although I did note increases in CTFs in female mice. These findings suggest that the impact of PrP^C on Aβ levels may be more complex than previously thought and highlights the need for further investigation into the nuanced role of PrP^C in AD pathogenesis.

In the future, I am planning to carry out similar experiments *in vivo* in transgenic AD mice that carry the APPswe modification, as well as a PS1 deletion in exon 9 (TgAD), crossed with Tg*Prnp*$^{-/-}$ mice. Based on our prior results, I expect to see a reduction in Aβ_{40} or Aβ_{42} in TgAD/Tg*Prnp*$^{-/-}$ mice, compared with just the TgAD mice. We also expect intracellular CTF accumulation in the TgAD/Tg*Prnp*$^{-/-}$, and possibly a reduction in sAPP/*beta*, which was seen in the N2a-APPswe cells. These results would confirm that the effects of PrP^C on APP processing, trafficking, and subsequent Aβ generation is heightened in an APP-overexpressing model, and perhaps more pronounced in an AD model.

CHAPTER 4

CHAPTER 4: GENERAL DISCUSSION

4.1 A Historical Overview of the Field of Neurobiology

The field of neurobiology has undergone a remarkable evolution over the centuries, significantly enhancing our understanding of the brain's functioning in health and disease. In the early days, our understanding of neurobiology came from the dissections and theoretical insights of ancient scholars like Alcmaeon of Croton, who discovered the optic nerve and suggested that the brain is the seat of thought and sensation [24]. This idea was a significant departure from earlier beliefs that attributed cognitive functions to the heart.

By the 19th century, figures like Paul Broca and Carl Wernicke had advanced the understanding of language-related brain regions, giving rise to theories of localized brain functions [16]. This era also saw the development of the theory of phrenology by Franz Joseph Gall [131]; although later debunked, it influenced the focus on the brain's anatomy for determining function. Various foundational theories and techniques have deeply influenced the field of neurobiology. Histological techniques such as the Golgi stain, introduced in the late 19th century, have been crucial for visualizing the architecture of neurons and their networks [106]. This technique was instrumental in developing the "neuron doctrine," first articulated by Santiago Ramón y Cajal, which posits that the neuron is the fundamental unit of the brain [89]. This concept has shaped our understanding of neurological function [16, 128, 129].

In the latter half of the 21st century, renowned behavioral neuroscientist Richard F. Thompson eloquently described the transition from focusing purely on behavioral aspects to a more integrated approach that included molecular, cellular, and systemic levels of neurobiology [146]. Thompson's work emphasized using model systems, ranging from invertebrates to

mammals, to elucidate the neural circuits involved in memory and learning, highlighting the cerebellum's role in motor learning and the hippocampus in memory processes [146]. Overall, the 20th and 21st centuries have been influenced heavily by technological advances in neuroimaging and molecular biology, with the goal of understanding and treating neurological conditions.

For example, the theory of the Developmental Origins of Health and Disease (DOHaD), which links early life conditions to the risk of developing various chronic conditions later in life, has broadened our perspective on how early life interventions can influence long-term health outcomes [16, 61, 139].

Furthermore, the Amyloid Cascade Hypothesis, which I have discussed previously, has been pivotal in framing our current understanding of Alzheimer's disease. Proposed by Hardy and Higgins in 2017 [56], this hypothesis suggests that the accumulation of amyloid-β peptides in the brain is the initial trigger in the pathogenesis of Alzheimer's disease, leading to tau pathology, neuronal death, and, ultimately, cognitive decline.

These concepts and tools have collectively enriched the field of neurobiology, providing insights into the normal functioning of the nervous system and the pathological bases of neurological diseases. This historical context underscores a trajectory of increasing complexity and specificity in our understanding of brain science, reflecting a field as dynamic as the organ it studies.

4.2 A Historical Overview of Fields of Neurological Disease and Molecular and Cellular Neuroscience

4.2.1 A Historical Overview of Neurological Disease

The recognition and categorization of neurological diseases have evolved significantly over the centuries. Early work focused on symptomatic observations without understanding the underlying causes. In the 19th century, figures like James Parkinson and Jean-Martin Charcot made landmark descriptions of neurological disorders like Parkinson's disease and multiple sclerosis, linking clinical symptoms with post-mortem brain pathology, establishing a foundation for modern neurology [37, 92, 109].

4.2.2 The Birth and Evolution of Neuroscience

Neuroscience emerged as a formal discipline in the mid-20th century, particularly through the efforts of pioneers like Stephen W. Kuffler [36]. Kuffler's work at Harvard laid the groundwork for the first neuroscience research program, which emphasized a holistic approach to understanding the nervous system, integrating neurophysiology, neuroanatomy, and biochemistry into a cohesive field [36].

4.2.3 Molecular and Cellular Contributions

Advances in molecular and cellular neuroscience have drastically changed our approach to neurological diseases. The use of molecular genetics in the late 20th and early 21st centuries has been crucial in identifying the specific genetic alterations associated with different forms of neurological disorders, such as mutations linked to Alzheimer's disease (AD), Huntington's disease (HD) and Parkinson's disease (PD) [119]. These advancements have improved diagnostic accuracy and opened up new avenues for targeted gene therapies. The molecular genetics aspect of neurobiology has been greatly enhanced by the use of model organisms like

flies and mice, which have facilitated significant breakthroughs in understanding the genetic bases of neurological diseases [36]. These model systems have allowed for detailed studies of gene expression and the resultant phenotypic changes associated with genetic mutations [36].

4.2.4 Molecular Genetics in Neurology

The field of molecular genetics in neurology has seen profound advancements that promise to revolutionize our understanding and treatment of neurological disorders, potentially exceeding the transformative impacts of technologies like magnetic resonance imaging (MRI) and positron emission tomography (PET), that made it possible to measure brain activity in alert patients for the first time [36]. This rapid progression in genetic analysis is poised to provide a new intellectual framework for neurology, shifting the focus from traditional symptom-based and neuropathological classifications to a more nuanced understanding based on underlying molecular and cellular mechanisms.

The Role of Molecular Genetics in Huntington's Disease (HD)

Notably, the pioneering work of Botstein and colleagues in 1980 fundamentally changed genetic research by introducing restriction fragment length polymorphism (RFLP) analysis [13]. This method allowed for a detailed mapping of genetic markers across the human genome, facilitating the localization of genes associated with inherited diseases, even in noncoding regions of the genome [13]. This was a significant step forward, making it easier to identify the genetic bases of diseases like sickle-cell anemia, as demonstrated by Kan and colleagues in the late 1970s and early 1980s [72, 73].

Anthony Monaco's and Louis Kunkel's groundbreaking work exemplifies the power of molecular genetics in neurology. Using the RFLP approach, Monaco and Kunkel identified the genetic locus for Duchenne's muscular dystrophy, an X-linked neuromuscular disease pre-

dominantly affecting young males [98]. Their discovery linked the disease to the area flanking the Xp region of chromosome 21 [98]. This finding not only pinpointed the genetic basis of Duchenne's muscular dystrophy but also paved the way for further genetic and cellular studies to understand the disease's pathophysiology.

The Role of Molecular Genetics in Channelopathies and Mitochondrial Disorders

The identification, cloning, and sequencing of genes related to channelopathies and mitochondrial disorders illustrate the significant potential of molecular genetics in neurology. Channelopathies, which involve dysfunctions in ion channel genes, and mitochondrial disorders, which affect cellular energy metabolism, represent areas where genetic insights have dramatically altered our understanding [36]. Previously, many of these conditions were indistinguishable or unrecognized until the responsible genetic mutations were identified [36]. This genetic revelation has enhanced diagnostic accuracy and opened new avenues for targeted treatments.

Drosophila Models

Research utilizing *Drosophila Melanogaster*(fruit flies) has proven invaluable, particularly in exploring the genetic influences on behavior and neurological diseases. Flies, with their simple genetic makeup and short life cycle, provided an ideal model for studying complex behaviors and their genetic underpinnings. *Drosophila* research has contributed significantly to our understanding of diseases like Huntington's. Zipursky and colleagues expressed n of an amino-terminal fragment of the human huntingtin protein with expanded polyglutamine tracts in *Drosophila*, which led to observable neurodegenerative changes that parallel HD in humans [69]. This model demonstrated that the length of polyglutamine repeats correlates with the age of onset and severity of neuronal degeneration, mimicking the human condition of HD [69].

Mouse Models

Mice have also played a critical role in studying various neurological conditions. A notable study involved expressing the first exon of the mutant human huntingtin protein in transgenic mice, which recapitulated many of the neurological phenotypes associated with HD [91]. These mice developed neurological signs, such as tremors and uncoordinated movements, and had shortened lifespans, providing a valuable model for further investigation into disease mechanisms and potential therapies [91].

4.2.5 Cellular Biology in Neurological Disorders

Cellular biology has provided critical insights into how cells and intracellular structures function and interact in the nervous system. This includes understanding the life cycle of cells, intracellular trafficking, and the role of various cellular organelles in maintaining neuronal health. For example, studies on the endoplasmic reticulum (ER) have shown how ER stress is marked by alterations in specific proteins that result in reduced translation, increased production of ER chaperones, and the elimination of misfolded proteins [86]. If ER stress is severe or prolonged, it can trigger cellular pathways that lead to cell death [86]. ER stress has been implicated in several human neurological conditions, including Parkinson's disease, Alzheimer's disease, and prion disease, among others [86]. Similarly, investigations into the role of lysosomes have elucidated their critical function in clearing cellular debris, a process that, when disrupted, leads to cellular dysfunction. In neurons, lysosomes are trafficked via dynein-mediated axonal transport of lysosomes, which is critical for synaptic functionality [85]. Unique disruptions in lysosomal trafficking across different neurodegenerative conditions lead to distinct patterns of auto/endolysosomal mistrafficking [85].

Protein Studies in Neurology

Protein studies, particularly those involving the structure and function of proteins within neural cells, have significantly advanced our understanding of neurological diseases. For instance, research into tau proteins and Aβ in Alzheimer's disease, the latter of which is the focus of my dissertation, has shown how abnormalities in protein folding and aggregation can lead to cell death and disease progression. Furthermore, the study of receptor proteins and ion channels has revealed how alterations in their structure or expression can lead to dysfunctions in neuronal signaling, as seen in various channelopathies [36].

4.2.6 Integration of Cellular Biology with Molecular Genetics

The integration of cellular biology and protein studies with molecular genetics creates a robust framework for neurology. This interdisciplinary approach allows researchers to understand the genetic blueprint of diseases and how these genetic changes manifest at the cellular and protein levels. For example, genetic mutations that lead to the production of dysfunctional proteins can now be studied in the context of how these proteins interact with cellular organelles and signaling pathways, offering a comprehensive view of disease mechanisms [36].

4.2.7 A Convergence of Neurology and Psychiatry

Discoveries in the neurobiological underpinnings of psychiatric disorders have significantly propelled the integration of neurology and psychiatry. For instance, studies on the role of neurotransmitters like serotonin and dopamine have elucidated their impact on mood disorders and schizophrenia, bridging gaps between behavioral symptoms and molecular pathways [92]. This convergence can be illustrated in modern treatments targeting these molecular pathways, such as selective serotonin reuptake inhibitors (SSRIs), which offer more effective management of psychiatric conditions [92].

4.2.8 Future Directions in Neurology

Clinicians are increasingly considering the dysfunction of specific neuronal organelles, such as lysosomes, the endoplasmic reticulum, or the cytoskeleton, and classes of molecules, including receptors, ion channels, intracellular signaling pathways, and transcription factors, in their diagnostic and therapeutic approaches [36]. This shift is underpinned by the growing ability of molecular genetics to elucidate the intricate biological pathways that underlie neurological diseases [36].

4.2.9 Implications for Therapeutic Development

As our understanding of cellular and molecular neuroscience deepens, developing new therapies will likely focus on molecular and cellular targets. The potential for creating treatments that precisely address the genetic root causes of disorders offers hope for more effective and personalized medical interventions. This evolution in neurology not only represents a shift in scientific understanding but also heralds a new era in patient care, where treatments are tailored to the specific molecular dysfunctions within each individual. We are experiencing a shift in the paradigm of broad symptomatic classifications to a more precise, mechanistic understanding of neurological diseases that aligns with their underlying cellular, molecular, and genetic causes.

4.3 My Ph.D. Thesis's Contribution to the Fields of Neurological Disease and Molecular and Cellular Neuroscience

In recent years, there has been considerable interest in the potential and somewhat varied functions of cellular prion protein (PrP^C) in Alzheimer's disease (AD) [162]. Some groups have implicated PrP^C as central to the toxicity of amyloid-β (Aβ) in AD [34, 117]. For instance, PrP^C traps Aβ in an oligomeric form, facilitating its uptake and spread via toxic

signaling of β-sheet-rich conformers, thereby contributing to the neurotoxicity observed in AD [8, 41, 120]. Research suggests that the interaction between PrP^C and Aβ has been linked to synaptic impairment in AD, highlighting the significance of PrP^C in Aβ-induced neurotoxicity [10, 22, 67, 80, 104, 134]. Moreover, PrP^C acts as a common ligand and downstream effector of neurotoxic species of various proteins involved in neurodegeneration, including Aβ, α-synuclein, and tau [34, 125].

Other research suggests that PrP^C may have a protective role in certain forms of AD through its interaction with the pro-domain of immature BACE1 [49, 50]. This interaction influences the localization of BACE1, thereby affecting amyloid precursor protein (APP) processing. Specifically, the presence of PrP^C seems to increase BACE1 localization within the trans-Golgi network (TGN), where BACE1 is more likely to cleave the Swedish mutant form of APP (APPswe) [49]. This relocalization potentially prevents BACE1 from reaching the plasma membrane and endosomes, the sites where wild-type APP (APPwt) would typically be cleaved [49]. Consequently, the expression of PrP^C should theoretically reduce the cleavage of APPwt by BACE1, while its absence would diminish the cleavage of APPswe by BACE1. However, contrasting findings from the same group have indicated that PrP^C-null mice exhibit increased levels of Aβ, which does not align with the protective role hypothesis [108].

My data add to the discussion, revealing that the absence of PrP^C reduces the cleavage of both APPswe and APPwt by BACE1 in early compartments. This results in increased levels of full-length APP (FL APP) at the plasma membrane, increased endocytosis of FL APP, and decreased levels of sAPPβ secreted into the media. To the best of my knowledge, we are the first group to trace the products of APP processing and trafficking in the presence or absence of PrP^C.

In this dissertation, I not only reaffirm our previous observations that PrP^C facilitates the release of Aβ in N2a-APPswe cells, but I also provide new evidence that PrP^C has a suppressive effect on APP trafficking to the plasma membrane which normally promotes its exposure to BACE1 cleavage within early compartments. Thus, in the absence of PrP^C, APP levels increase at the plasma membrane and less Aβ is produced. In effect, PrP^C promotes the amyloidogenic pathway by increasing the exposure of APP to BACE1 within early secretory compartments. These processing events are not direct, but are predicted to be due to the differences in cellular localization of BACE1, which is primarily localized to the acidic lumen of the Golgi apparatus, TGN, and endosomes [52, 53, 76] and α-secretase, which primarily resides on the plasma membrane [52]. My research contributes to the broader field of cellular neuroscience by delineating how cellular components like PrP^C can influence crucial pathways in neurodegenerative diseases, specifically AD. This study not only explores the pathogenic interactions involving PrP^C and APP processing but also integrates cellular trafficking mechanisms that can significantly influence disease outcomes. Through detailed cellular and molecular analyses, my work underscores the dynamic nature of protein interactions within cellular compartments that contribute to neurodegenerative pathology.

By illustrating how PrP^C influences APP's subcellular localization, and function and by exploring the subsequent alterations in APP processing dynamics that lead to Aβ generation, my thesis expands our understanding of the molecular underpinnings of AD beyond the traditional amyloid-centric view. This research highlights the complexity of intracellular protein trafficking and its regulation, providing insights into the cellular basis of proteinopathies. The findings presented offer potential new targets for therapeutic interventions that could modify the course of disease by altering protein processing pathways at the cellular level.

Furthermore, this work contributes to a nuanced understanding of neurodegenerative diseases by demonstrating that changes in the localization and function of critical proteins like PrP^C and APP can lead to significant variations in disease phenotypes. This emphasizes the importance of cellular context in the pathogenesis of neurological diseases and underscores the potential of targeting specific cellular pathways to mitigate disease progression. Such insights are vital for developing next-generation therapeutics aimed at modulating disease at the molecular and cellular levels, potentially offering more effective and targeted approaches to treatment.

4.4 My Ph.D. Thesis's Major Takeaways

I first confirmed the direct relationship between PrP^C expression and Aβ_{42} release in N2a-APPswe cells using the MSD platform. I found that a $\sim$ 70% knockdown of PrP^C led to a $\sim$ 20% reduction in Aβ_{42} release in the media. Moreover, this relationship extended beyond Aβ_{42} to involve Aβ_{40} and possibly Aβ_{38}; the other two major species of Aβ, were similarly decreased. These findings support a general effect of PrP^C on APP delivery to specific cellular compartments rather than a specific effect on its processing. Since N2a-APPswe cells generate high levels of Aβ_{42} and the subcellular locations of APPswe processing differs from that of APPwt, I questioned whether the effect of PrP^C on Aβ was unique to N2a-APPswe cells. Aβ_{42} was barely detectable in N2a-APPwt cells; prelimary results suggested reduced levels after PrP^C KD, but were not statistically significant. In contrast, Aβ_{40} and Aβ_{38}, which were present at higher levels than Aβ_{42}, were significantly reduced.These findings argue against an Aβ isoform-specific or APP modification-specific effect of PrP^C on Aβ release in N2a cells.

Based on the ability of PrP to regulate release of all major species of Aβ in both cell lines, I questioned whether PrP^C expression has an effect on APP processing. We looked

for changes in the relative levels of sAPPα and sAPPβ, which reflect the activity of α-secretase and BACE1 cleavage of APP, respectively. PrP^C KD significantly reduced the level of sAPPβ in both cell lines, consistent with the observed reduction in Aβ. In contrast, whereas sAPPα was unchanged in N2a-APPswe cells, it was markedly increased in N2a-APPwt cells, suggesting a distinct difference in the way APP is processed in these two cell lines. Both APPwt and APPswe are equally susceptible to cleavage by α-secretase [144], which would suggest that sAPPα fragments should increase in both cell lines in the absence of PrP^C. Since N2a-APPswe cells express the APPswe modification at $\sim$ 2.5 times the level of APPwt, it is possible that any moderate increase in sAPPα fragments in APPswe expressing cells is diluted by the expression level of the modification. Moreover, levels of secreted sAPPα increase significantly in N2a-APPwt cells, but not in N2a-APPswe cells. Pulse-chase experiments have demonstrated that while there was no difference between the APPswe and APPwt modifications in their rate of arrival to the plasma membrane (in FL form), $\sim$ 80% of APPswe never made it to the cell surface [144]. A large fraction of APPswe is cleaved by BACE1 on its way through the secretory pathway, and labeled CTFs resulting from this cleavage end up in the endosomes [144].

As mentioned previously, N2a-APPswe cell line, in which the "Swedish" mutation (K595N/M596L) in the amyloid precursor protein (APP) is expressed, serves as a crucial model for studying AD pathology [144]. This specific mutation significantly enhances the cleavage of APP by β-secretase, leading to an increased production of Aβ peptides, which are central to the development of AD [144]. While this cell line is an incredibly useful tool for studying Aβ release, there are some limitations in the use of this model. For example, since there is a substantial difference in the amount of APPswe and APPwt that ends up on the plasma membrane under normal conditions, it is likely that even in the absence of PrP^C, I might not see a significant change in secreted sAPPα levels in the N2a-APPswe cells.

Therefore, this result might not be reflective of AD cases that are not linked to this mutation.

I attempted to confirm these differences by assessing the levels of CTFs generated following α- and β-secretase cleavage. We hypothesized that the APP CTFs derived from α- and β-secretase cleavage of FL APP would mirror the observed changes in sAPPα and sAPPβ for each cell line. Thus, I predicted reduced β-CTF in both cell lines to correspond with reduced Aβ release and sAPPβ in each line and an increase in α-CTF, at least in N2a-APPwt cells. Despite differences in sAPPα levels in N2a-APPwt (increase) and N2a-APPswe cells (no change), I found an increase in total CTFs after PrP^C KD due to increases in α-CTF in both cell lines. This suggests a disconnect between the retention of CTFs and the initial cleavage of APP by either α- or β- secretases.

The above findings raised two possibilities that are not mutually exclusive: 1) APPwt and APPswe are processed differently, as previously suggested by others [54, 141] and 2) the decrease in sAPPβ in both cell lines suggests there are shared aspects of processing and trafficking between APPwt and APPswe. Differences in PrP^C modulation of sAPPα and sAPPβ secretion between the cell lines might be explained by differences in the potential influence of PrP^C on secretase activities (i.e., β- secretase cleaves APPswe $\sim$ 20 times more efficiently than α-secretase in my study, based on relative sAPP levels; (Figure2.6). Nevertheless, it is striking that the CTF fractions were increased in both cell lines. One possible explanation for these observations might be that the reduction of PrP^C impairs β-secretase processing, leading to CTF accumulation. While it appears that α-CTF levels increase significantly in cell lysate following PrP KD, which would be in line with the increase in sAPPα level changes, alterations in the predominant BACE1-derived fragments (+1 and +11 β-CTFs) were more variable from experiment to experiment.

One way to explain my findings is that PrP^C expression might directly or indirectly enhance retention of nascent APP within early secretory compartments, where BACE1 activity predominates. With PrP^C KD, APP may be more efficiently trafficked to the plasma membrane. Our immunofluorescence staining and biotinylation studies, which revealed an increase in FL APP on the plasma membrane after PrP^C KD in both cell lines, support this idea. This effect, with or without a direct impact on α- or β- secretase, could explain the differences I observed in APP cleavage products among the two cell lines.

I also investigated whether PrP^C KD alters either α- or β- secretase expression levels. Western Blotting of cell lysates from N2a-APPwt and N2a-APPswe cells using specific antibodies against ADAM10 and BACE1 revealed no significant changes in on α- or β- secretase expression levels after PrP^C KD (data not shown). Using secretase expression levels as a proxy for enzymatic activity, my findings suggest that the observed effects on APP processing in the absence of PrP^C are not a result of changes in secretase levels and reinforce the notion that PrP^C may modulate the trafficking of APP within the cell.

Moreover, I found an increase in the fraction of APP that underwent endocytosis at the plasma membrane following PrP^C KD. Retention of CTFs with a reduction in PrP^C could relate to a differential effect of PrP^C at this stage of APP trafficking. Based on prior work conducted in our laboratory and that of others, which suggests PrP^C can bind to Aβ, PrP^C's presence at the plasma membrane may be required to promote the release of Aβ derived from β-CTFs. Thus, PrP^C's absence could lead to accumulation. This possibility was not addressed in the current work.

We considered two scenarios to explain the increase in the fraction of plasma membrane APP that undergoes endocytosis after PrP^C KD in either cell line. Since both PrP^C and

a subset of FL APP reside in lipid rafts [136] and PrP^C has a longer half-life and membrane residence than APP, its absence on the plasma membrane could affect critical signaling processes that subsequently enhance the internalization of surface APP, leading to its processing by BACE1 and intracellular CTF accumulation. Alternatively, the increase in plasma membrane APP after PrP^C reduction might simply be sufficient to increase its endocytosis. Since my data show that similar fractions of plasma membrane APP are endocytosed from the plasma membrane in both N2a-APPwt and N2a-APPswe cells, it appears that the fraction of APP endocytosed is directly related to the amount of APP on the cell surface.

Although various studies have established the interaction between Aβ oligomers (AβO) and PrP^C [14, 117, 122, 165], the exact role of PrP^C in AD pathophysiology remains under debate. A significant focus has been on the N-terminal polybasic region of PrP^C, identified as a key site for Aβ oligomer binding. This region was also considered crucial for its proposed interaction and inhibition of BACE [108]. Parkin et al. 2007 suggested that overexpressing PrP^C could inhibit BACE1 activity, leading to decreased Aβ production [108]. However, my findings appear to contradict those findings; I observed that reducing PrP^C decreases the degree to which APP is cleaved by BACE1 and this leads to a reduction in the steady-state levels of secreted Aβ. Moreover, Parkin, et al. [108] found that Aβ levels increased in a PrP^C knockout (KO) mouse model compared to wild-type mice. We found that the deletion of PrP^C in wild-type FVB mice did not change the levels of Aβ_{42} or Aβ_{40}. This finding suggests that, in our mouse model, the absence of PrP^C does not influence the accumulation of these specific Aβ peptides, contrasting with expectations based on the proposed protective role of PrP^C in sporadic AD mediated by its direct interaction with the pro-domain of BACE1 that subsequently changes its localization and reduces Aβ peptide generation.

Moreover, I found an increase *in vivo* in intracellular CTFs in the absence of PrP^C in female

mice. This finding agrees with the data from N2a cells showing an increase in the levels of CTFs without any discernable change in total cellular levels of full-length APP (Figure 2.4 A-B), using immunofluorescence staining and Western blotting (Figure 2.7 and Figure 2.8). However, the DEA/RIPA fractionation did not show changes in sAPPα or sAPPβ, both of which were observed in the N2a cell lines. One possibility to explain my findings is that the stability of the soluble fragments of APP could be different in brains than in cell lines, such that the soluble fragments are more prone to degradation in the brain. Moreover, there is spatial separation between APP cleavage and eventual ectodomain secretion in neurons that is difficult to observe in a cell model. Specifically, APP is primarily processed in somato-dendritic compartments before its fragments are secreted from axons [102]. The spatial and temporal components involved in this process may occlude significant, observable changes in sAPP fragments and plasma membrane APP levels. Intracellularly retained CTFs, on the other hand, may be more resistant to lysosomal degradation in the brain or possibly take longer to reach the lysosomes due to the spatial separation of cellular functions, ultimately allowing for their detection in my experiments. As a result, it is possible that ectodomain secretion can be uncoupled from the fate of CTFs *in vivo*.

Despite the experimental differences described above, my examination of mouse brain fractions expressing endogenous mouse APP and PrP^C found no significant changes in Aβ levels between PrP^C KO and WT mice at 65 days of age. However, I did note increases in CTFs for female mice. To study the interaction effects of variable PrP^C levels on AD progression, other groups have crossed the APPswe/PS1ΔE9 mouse model of AD with mice overexpressing or lacking PrP^C [105]. Ordóñez-Gutiérrez et al. 2013 [105] found that Aβ deposits were, in fact, influenced by PrP^C levels, with more prion protein resulting in increased Aβ aggregation in aged mice. Moreover, there was no difference in APP or BACE1 levels among older animals of different genotypes, suggesting that the changes in Aβ deposition are not due to

variations in the expression of these proteins [105]. These findings support my data *in vitro* and suggest that I would see a more pronounced effect in Aβ deposition and APP processing in an APP-overexpressing model.

Another report focused on the direct interaction of PrP^C with BACE1 in the TGN and differential effects on APP cleavage [49]. We did not specifically examine the relationship between PrP^C and BACE1. APPwt and APPswe processing within subcellular compartments differ significantly. BACE1 cleaves nascent APPswe as early as in the TGN [53, 144], and the sAPPβ fragment released from this cleavage is trafficked through the secretory pathway where it is released into the media [144]. APPwt is mainly cleaved by α-secretase at the plasma membrane, although BACE1 cleavage of internalized APP occurs during transit through the endocytic pathway, resulting in low levels of Aβ [144]. Griffiths et al. [49] found, in stably-transfected human embryonic kidney (HEK) cells, that PrP^C inhibited BACE1 cleavage of APPwt but not APPswe [49]. In contrast, I found that reducing PrP^C levels decreased sAPPβ in both cell types, indicating that the absence of PrP^C might impair BACE1 activity or its access to APP. Griffiths et al. [49] proposed that PrP^C confines BACE1 to membrane subcompartments separate from those containing APPwt. However, my results suggest a different mechanism: PrP^C promotes BACE1 cleavage of APP in the secretory and endocytic pathways. The absence of PrP^C, therefore, likely hinders early BACE1 cleavage, resulting in a greater amount of APP being transported to the plasma membrane in both N2a cells expressing APPwt and APPswe.

Differences in cell models, the sensitivity of the assays used, and the types of experiments performed can potentially explain the discrepancies between my results and prior results from other laboratories. Our results still fit with the mechanism proposed by Griffiths et al. [49] that suggest PrP^C interacts with the pro-domain of BACE1 resulting in BACE1 local-

ization to the TGN. The primary difference is that I saw an increase in both FL APPwt and APPswe on the plasma membrane (PM) in the absence of PrP^C. This suggests, in turn, that both APPwt and APPswe trafficking is similarly affected by the absence of PrP^C, thereby suggesting both a direct and indirect influence of PrP^C on APP processing. Our data are not necessarily at odds with previous findings, but rather, indicate the complexity of PrP^C's role in APP processing and trafficking.

One consistency in my data across the experiments *in vitro* and *in vivo* is that the absence of PrP^C leads to APP CTF accumulation. Our findings point towards a new dual role for PrP^C. PrP^C may facilitate both the conversion of CTFs to Aβ and the degradation of CTFs in lysosomes. In the absence of PrP^C, CTFs are neither converted to Aβ nor degraded, leading to CTF accumulation, an effect that may be more robust *in vivo*. This suggests a possible impact on γ-secretase cleavage of APP CTFs or lysosomal degradation of CTFs by PrP^C. Previous research indicates that the use of γ-secretase chemical inhibitors, along with loss-of-function mutations and deletions in presenilin 1 (PS1), leads to significant alterations in the glycosylation and trafficking of APP [20, 28, 81]. These changes manifest by accumulating APP, C-terminal fragments (CTFs), and other membrane proteins on the plasma membrane [81]. This accumulation signals a bottleneck in endocytic trafficking due to an overload of substrates, with CTFs monopolizing essential trafficking molecules like clathrin and dynamin on the cell surface. Despite the trafficking congestion, cellular processes such as division continue; cells do not undergo apoptosis, but rather reach steady-state [81]. Considering the challenges associated with investigating γ-secretase activity—specifically, the potential for severe interference with protein trafficking and degradation pathways—we have determined that evaluating the impact of PrP^C on the γ-secretase-mediated cleavage of APP falls outside the scope of my current work.

My findings suggest that the impact of PrP^C on Aβ levels may be more complex than previously thought and highlights the need for further investigation into the nuanced role of PrP^C in AD pathogenesis.

APPENDIX A

APPENDIX: SUPPLEMENTARY

A.1 Western Blots

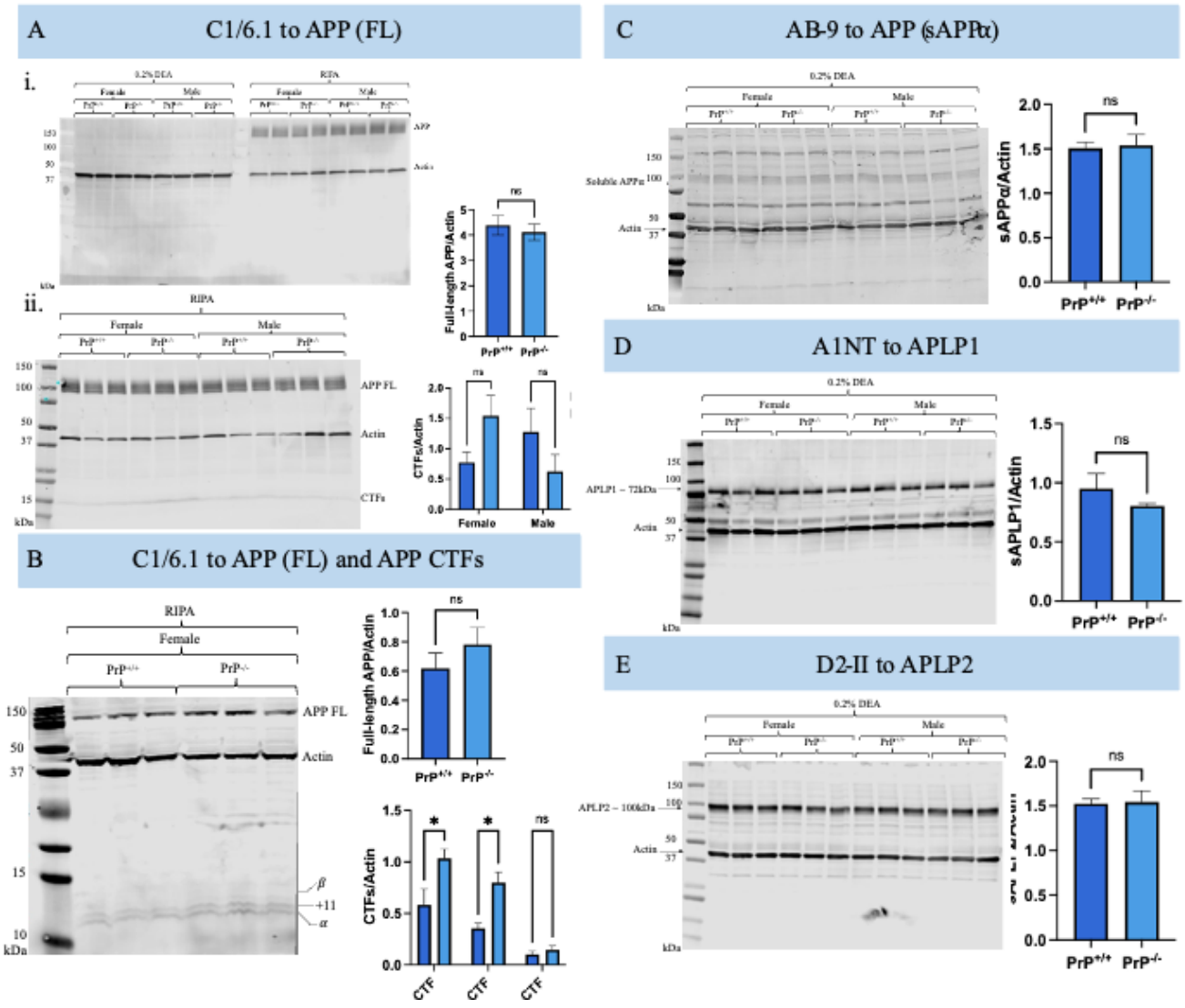

Figure A.1: **Original, uncropped Western blot images from Figure 3.3: RIPA-soluble brain homogenates show increased α-CTF and +11 β-CTF levels in Tg*Prnp*$^{-/-}$ females compared to WT mice.**

Figure A.1: (continued). **A.** i. 65-day-old from Tg$Prnp^{-/-}$ and wild-type (FVB) mouse brains were separated into a soluble protein fraction (0.2% DEA) and a detergent-soluble membrane protein fraction (RIPA). Aliquots of each fraction were analyzed by immunoblotting with a C-terminal antibody to APP (C1/6.1) to confirm the separation of soluble and membrane-bound proteins. ii. Analysis of the RIPA fraction with a C-terminal antibody to APP (C1/6.1) confirms that there is no change in FL APP levels between Tg$Prnp^{-/-}$ and WT mice or males and females. **B.** Separation of RIPA-soluble proteins using a 16.5% Tris-tricine gel reveals an increase in α-CTF and +11 β-CTF levels in Tg$Prnp^{-/-}$ females compared to WT mice. **C.** Analysis of the DEA fractions with the AB-9 antibody to sAPP reveals no difference in sAPP between Tg$Prnp^{-/-}$ and WT mice. **D-E.** Analysis of the DEA fractions with antibodies to APLP1 or APLP2 reveals no differences in sAPLP1 or sAPLP2 between the genotypes. The results are representative blots from N=12 g$Prnp^{-/-}$ and N=12 WT mice. Protein molecular weight ladders are measured in kDa. The levels of indicated proteins in the RIPA and DEA homogenates (normalized to actin) were quantified. The data were analyzed by a two-tailed unpaired t-test, * $p<0.05$.

A.2 APP Antibody Epitopes and Secretase Cleavage Sites

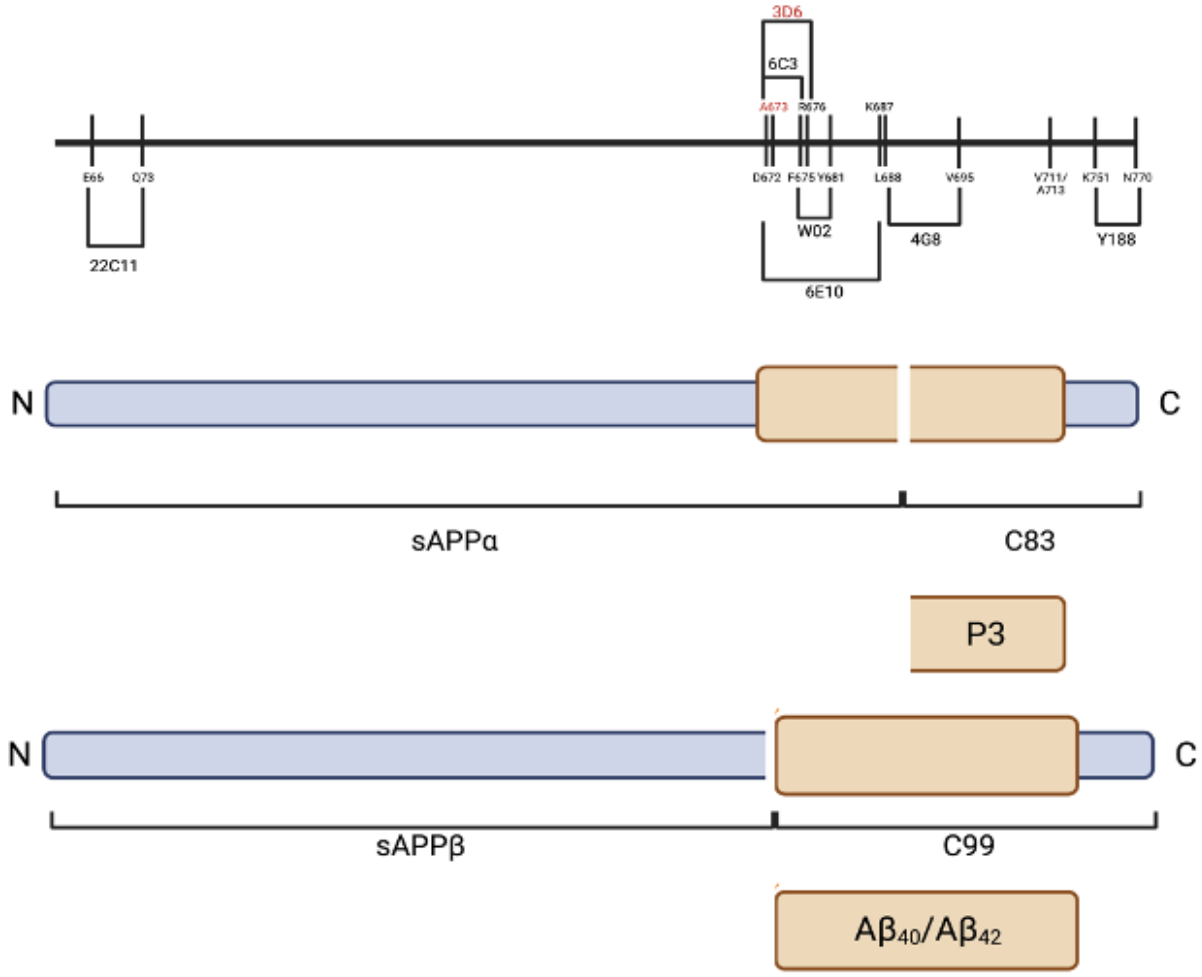

Figure A.2: **Schematic representation of APP antibody epitopes and secretase cleavage sites. Made with BioRender.com.**

A.3 List of Primary and Secondary Antibodies

Antibodies	Target	Company	Catalog Number	Concentration	Notes
Primary Antibodies					
β-Actin antibody	Actin	SantaCruz Biotechnology, Dallas, TX	sc-47778	1:1000	
Anti-GAPDH antibody (6C5)	GAPDH	Invitrogen, Carlsbad, CA	AM4300	1:10000	
anti-APP 22C11 anti-mouse mAb	APP (mature, immature, sAPP)	eBioscience, San Diego, CA	14-9749-82	1:1000	Cross reacts with APLP2
NTH452 anti-rabbit pAb [5, 28]	APP (FL and soluble)	Kindly provided by Dr. Gopal Thinakaran	-	1:1000	Generated against a fusion protein corresponding to APP ectodomain residues 45 to 265
NTG449 anti-rabbit pAb [29]	APP (FL PP and sAPP)	Kindly provided by Dr. Gopal Thinakaran	-	1:1000	Generated against human APP ectodomain residues 306 to 600
Amyloid precursor protein anti-mouse (mAbP2-1)	APP	Invitrogen, Carlsbad, CA	OMA1-03132	1:1000	Specific for native, non-denatured APP
C1/6.1, purified anti-APP C-terminal fragment antibody	APP (CTFs, FL)	BioLegend, San Diego, CA	SIG-39152	1:1000	
Recombinant anti-APP antibody, Y188	APP (CTFs, FL APP)	Abcam, Waltham, MA	ab32136	1:2000	

Table A.1: **List of primary antibodies 1**

Antibodies	Target	Company	Catalog Number	Concentration	Notes
Primary Antibodies					
Purified anti-β-amyloid, 1-16 antibody, 6E10	APP (FL APP, sAPPα, β-CTF, β-amyloid)	BioLegend, San Diego, CA	IG-39320	1:1000	
C-terminal pAb CTM1 [5, 28]	APP (CTFs, FL APP)	Kindly provided by Dr. Gopal Thinakaran	-	1:1000	
Mouse monoclonal (AB9) antibody to β-amyloid	APP, β-amyloid	BioTechne, Minneapolis, MN	NBP2-50055	1:1000	
AINT10 (GSTA1-1/ GSTA1-2) rabbit pAb [145]	APLP1	Kindly provided by Dr. Gopal Thinakaran	-	1:1000	Generated against a fusion protein corresponding to mouse APLP1 ectodomain residues 293 to 583
Ectodomain rabbit pAb D2II49	APLP1	Kindly provided by Dr. Gopal Thinakaran	-	1:1000	Generated against a fusion protein corresponding to mouse APLP1 ectodomain residues 293 to 583
C-terminal pAb CT12 [143]	APLP2	Kindly provided by Dr. Gopal Thinakaran		1:1000	
Ectodomain rabbit pAb D2II [142]	APLP1	Kindly provided by Dr. Gopal Thinakaran	-	1:1000	

Table A.2: **List of primary antibodies 2**

Antibodies	Target	Company	Catalog Number	Concentration	Notes
Primary Antibodies					
SAF-32 anti-PrP^C mouse mAb	PrP^C	Bertin Bioreagent, Montigny le Bretonneux, France	A03202	1:1000	Recognizes octarepeat region in N-terminal of PrP^C
D-13 chimeric human-mouse Ab [121]	PrP^C	Kindly provided by Dr. Stanley Prusiner	-	1:1000	Recognizes PrP^C aa 94-105
Recombinant anti-ADAM10 antibody [EPR5622]	ADAM10	Abcam, Waltham, MA	ab124695	1:1000	
Biotin Antibody (33)	Biotin	SantaCruz Biotechnology, Dallas, TX	sc-101339	1:1000	
Anti-NrCAM (N-terminal) anti-rabbit pAb	NrCAM (N-terminal)	Abcam, Waltham, MA	ab24344	1:500	
Anti-NrCAM (C-terminal) anti-rabbit pAb	NrCAM (C-terminal)	Cell Signaling Technology, Danvers, MA	55284	1:1000	
Human/mouse NCAM-1/CD56 antibody, anti-goat pAb	NCAM-1 (N-terminal)	BioTechne, Minneapolis, MN	AF2408	1:500	
Anti-neural cell adhesion molecule antibody, anti-rabbit pAb	NCAM-1 (C-terminal)	Sigma Aldrich, St. Louis, MO	AB5032	1:1000	

Table A.3: **List of primary antibodies 3**

Antibodies	Target	Company	Catalog Number	Concentration
Secondary Antibodies for Immunofluorescence				
Donkey anti-mouse AlexaFluor 555, highly cross adsorbed	-	Invitrogen, Carlsbad, CA; Thermo Fisher Scientific, Inc.	A-31570	1:1000
Donkey anti-rabbit AlexaFluor 488 - highly cross adsorbed	-	Invitrogen, Carlsbad, CA; Thermo Fisher Scientific, Inc.	A-21206	1:1000
Donkey anti-rabbit AlexaFluor 647 – highly cross adsorbed	-	Invitrogen, Carlsbad, CA; Thermo Fisher Scientific, Inc.	A-31573	1:1000

Table A.4: **List of secondary antibodies for immunofluorescence**

Antibodies	Target	Company	Catalog Number	Concentration
Secondary Antibodies for Western Blotting (Fluorescent)				
LICOR IRDye® 800CW Goat anti-Mouse IgG Secondary Antibody	-	NetaScientific, Marlton, NJ	LIC-926-32210	1:5000
LICOR IRDye® 680RD Donkey Anti-Rabbit IgG (H + L), Highly Cross-Adsorbed	-	NetaScientific, Marlton, NJ	LIC-926-68073	1:5000
LICOR IRDye® 680RD Goat anti-Mouse IgG (H + L) Highly Cross-Adsorbed	-	NetaScientific, Marlton, NJ	LIC-926-68070	1:5000
Secondary Antibodies for Western Blotting (HRP)				
Goat anti-Mouse IgG (H+L) Secondary Antibody, HRP	-	Invitrogen, Carlsbad, CA; Thermo Fisher Scientific, Inc.	31430	1:10000
Goat anti-Rabbit IgG (H+L) Secondary Antibody, HRP	-	Invitrogen, Carlsbad, CA; Thermo Fisher Scientific, Inc.	31460	1:10000
Mouse anti-Human IgG (H+L) Secondary Antibody, HRP	-	Invitrogen, Carlsbad, CA; Thermo Fisher Scientific, Inc.	31420	1:10000
Donkey anti-Goat IgG-HRP	-	SantaCruz	sc-2020	1:1000

Table A.5: **List of secondary antibodies for Western Blotting**

A.4 Abbreviations

Aβ: Amyloid-β protein

AD: Alzheimer's disease

ADAM10: A disintegrin and metalloproteinase 10 (one of the α-secretases)

AICD: APP intracellular domain

APP CTFs: Amyloid precursor protein C-terminal fragments

APP: Amyloid precursor protein

BACE1: β-site APP-cleaving enzyme 1 (β-secretase)

CSF: Cerebrospinal fluid

FAD: Familial Alzheimer's disease

FL APP: Full-length amyloid precursor protein

LTP: Long-term potentiation

NFTs: Neurofibrillary tangles

PM: Plasma membrane

PrP^{C}: Cellular prion protein

PrP^{Sc}: Scrapie form of prion protein

PS1/2: Presenilin 1/2 (components of γ secretase)

RIPA: Radioimmunoprecipitation

sAPPα: Soluble α-secretase-generated amyloid precursor protein ectodomain

sAPPβ: Soluble BACE1-generated amyloid precursor protein ectodomain

sAPP: Soluble APP fragment

SDS-PAGE: Sodium dodecyl sulfate polyacrylamide gel electrophoresis

siRNA: Short/small interfering ribonucleic acid

BIBLIOGRAPHY

[1] A. Aguzzi. The toxicity of antiprion antibodies is mediated by the flexible tail of the prion protein. *Nature*, 501(7465):102–106, 2013.

[2] A. Aguzzi and T. O'Connor. Protein aggregation diseases: pathogenicity and therapeutic perspectives. *Nature Reviews Drug Discovery*, 9(3):237–248, 3 2010. ISSN 1474-1784. doi:10.1038/nrd3050. number: 3 publisher: Nature Publishing Group.

[3] J. Alshaikh, K. Qin, L. Zhao, and J. Mastrianni. A novel prnp-g131r variant associated with familial prion disease. *Neurology Genetics*, 6(4), 2020.

[4] R. N. Alves, R. P. Iglesia, M. B. Prado, M. I. Melo Escobar, J. M. Boccacino, C. F. d. L. Fernandes, B. P. Coelho, A. C. Fortes, and M. H. Lopes. A new take on prion protein dynamics in cellular trafficking. *International Journal of Molecular Sciences*, 21(20):7763, 10 2020. ISSN 1422-0067. doi:10.3390/ijms21207763. PMID: 33092231 PMCID: PMC7589859.

[5] R. J. Andrew, C. G. Fernandez, M. Stanley, H. Jiang, P. Nguyen, R. C. Rice, V. Buggia-Prévot, P. De Rossi, K. S. Vetrivel, R. Lamb, A. Argemi, E. S. Allaert, E. M. Rathbun, S. V. Krause, S. L. Wagner, A. T. Parent, D. M. Holtzman, and G. Thinakaran. Lack of bace1 s-palmitoylation reduces amyloid burden and mitigates memory deficits in transgenic mouse models of alzheimer's disease. *Proceedings of the National Academy of Sciences of the United States of America*, 114(45):E9665–E9674, 11 2017. ISSN 1091-6490. doi:10.1073/pnas.1708568114. PMID: 29078331 PMCID: PMC5692556.

[6] J. Aow, T.-R. Huang, Y. T. Goh, A. X. Sun, G. Thinakaran, and E. H. Koo. Evidence for a clathrin-independent endocytic pathway for app internalization in the neuronal somatodendritic compartment. *Cell reports*, 42(7):112774, 7 2023. ISSN 2211-1247. doi:10.1016/j.celrep.2023.112774. PMID: 37450368 PMCID: PMC10449584.

[7] P. V. Arriagada, J. H. Growdon, E. T. Hedley-Whyte, and B. T. Hyman. Neurofibrillary tangles but not senile plaques parallel duration and severity of alzheimer's disease. *Neurology*, 42(3 Pt 1):631–639, 3 1992. ISSN 0028-3878. doi:10.1212/wnl.42.3.631. PMID: 1549228.

[8] S. Aulić, L. Masperone, J. Narkiewicz, E. Isopi, E. Bistaffa, E. Ambrosetti, B. Pastore, E. De Cecco, D. Scaini, P. Zago, F. Moda, F. Tagliavini, and G. Legname. -synuclein amyloids hijack prion protein to gain cell entry, facilitate cell-to-cell spreading and block prion replication. *Scientific Reports*, 7(1):10050, 8 2017. ISSN 2045-2322. doi:10.1038/s41598-017-10236-x. publisher: Nature Publishing Group.

[9] N. D. Belyaev, K. A. Kellett, C. Beckett, N. Z. Makova, T. J. Revett, N. N. Nalivaeva, N. M. Hooper, and A. J. Turner. The transcriptionally active amyloid precursor protein (app) intracellular domain is preferentially produced from the 695 isoform of app in a β-secretase-dependent pathway*. *Journal of Biological Chemistry*, 285(53):41443–41454, 2010.

[10] I. Benilova and B. De Strooper. Prion protein in alzheimer's pathogenesis: a hot and controversial issue. *EMBO Molecular Medicine*, 2(8):289–290, 8 2010. ISSN 1757-4676. doi:10.1002/emmm.201000088. number-of-pages: 290 publisher: Springer Nature.

[11] D. C. Bolton, M. P. McKinley, and S. B. Prusiner. Identification of a protein that purifies with the scrapie prion. *Science (New York, N.Y.)*, 218(4579):1309–1311, 12 1982. ISSN 0036-8075. doi:10.1126/science.6815801. PMID: 6815801.

[12] E. Bossy-Wetzel, R. Schwarzenbacher, and S. A. Lipton. Molecular pathways to neurodegeneration. *Nature medicine*, 10(Suppl 7):S2–S9, 2004.

[13] D. Botstein, R. L. White, M. Skolnick, and R. W. Davis. Construction of a genetic link-

age map in man using restriction fragment length polymorphisms. *American journal of human genetics*, 32(3):314, 1980.

[14] A. Brody and S. M. Strittmatter. Synaptotoxic signaling by amyloid beta oligomers in alzheimer's disease through prion protein and mglur5. *Advances in pharmacology (San Diego, Calif.)*, 82:293–323, 2018. ISSN 1054-3589. doi:10.1016/bs.apha.2017.09.007. PMID: 29413525 PMCID: PMC5835229.

[15] D. R. Brown, K. Qin, J. W. Herms, A. Madlung, J. Manson, R. Strome, P. E. Fraser, T. Kruck, A. von Bohlen, W. Schulz-Schaeffer, A. Giese, D. Westaway, and H. Kretzschmar. The cellular prion protein binds copper in vivo. *Nature*, 390(6661):684–687, 12 1997. ISSN 0028-0836. doi:10.1038/37783. PMID: 9414160.

[16] R. E. Brown. Why study the history of neuroscience? *Frontiers in Behavioral Neuroscience*, 13:82, 2019.

[17] H. Büeler, M. Fischer, Y. Lang, H. Bluethmann, H.-P. Lipp, S. J. DeArmond, S. B. Prusiner, M. Aguet, and C. Weissmann. Normal development and behaviour of mice lacking the neuronal cell-surface prp protein. *Nature*, 356(6370):577–582, 1992.

[18] M. Béland and X. Roucou. The prion protein unstructured n-terminal region is a broad-spectrum molecular sensor with diverse and contrasting potential functions. *Journal of neurochemistry*, 120(6):853–868, 2012.

[19] H. Büeler, A. Aguzzi, A. Sailer, R. A. Greiner, P. Autenried, M. Aguet, and C. Weissmann. Mice devoid of prp are resistant to scrapie. *Cell*, 73(7):1339–1347, 7 1993. ISSN 0092-8674. doi:10.1016/0092-8674(93)90360-3. PMID: 8100741.

[20] D. Cai, J. Y. Leem, J. P. Greenfield, P. Wang, B. S. Kim, R. Wang, K. O. Lopes, S.-H. Kim, H. Zheng, P. Greengard, et al. Presenilin-1 regulates intracellular trafficking and

cell surface delivery of β-amyloid precursor protein. *Journal of Biological Chemistry*, 278(5):3446–3454, 2003.

[21] H. Cai, Y. Wang, D. McCarthy, H. Wen, D. R. Borchelt, D. L. Price, and P. C. Wong. Bace1 is the major β-secretase for generation of aβ peptides by neurons. *Nature neuroscience*, 4(3):233–234, 2001.

[22] A. M. Calella, M. Farinelli, M. Nuvolone, O. Mirante, R. Moos, J. Falsig, I. M. Mansuy, and A. Aguzzi. Prion protein and a-related synaptic toxicity impairment. *EMBO Molecular Medicine*, 2(8):306–314, 8 2010. ISSN 1757-4676. doi:10.1002/emmm.201000082. PMID: 20665634 PMCID: PMC2962809.

[23] V. Campana, D. Sarnataro, and C. Zurzolo. The highways and byways of prion protein trafficking. *Trends in Cell Biology*, 15(2):102–111, 2 2005. ISSN 0962-8924. doi:10.1016/j.tcb.2004.12.002. PMID: 15695097.

[24] G. G. Celesia. Alcmaeon of croton's observations on health, brain, mind, and soul. *Journal of the History of the Neurosciences*, 21(4):409–426, 2012.

[25] H. J. Cha, J. Shen, and J. Kang. Regulation of gene expression by the app family in the adult cerebral cortex. *Scientific reports*, 12(1):66, 2022.

[26] C. Chen and X.-P. Dong. Epidemiological characteristics of human prion diseases. *Infectious diseases of poverty*, 5:1–10, 2016.

[27] S. Chen, S. P. Yadav, and W. K. Surewicz. Interaction between human prion protein and amyloid-beta (abeta) oligomers: role of n-terminal residues. *The Journal of Biological Chemistry*, 285(34):26377–26383, 8 2010. ISSN 1083-351X. doi:10.1074/jbc.M110.145516. PMID: 20576610 PMCID: PMC2924066.

[28] H. Cheng, K. S. Vetrivel, R. C. Drisdel, X. Meckler, P. Gong, J. Y. Leem, T. Li, M. Carter, Y. Chen, P. Nguyen, T. Iwatsubo, T. Tomita, P. C. Wong, W. N. Green,

M. Z. Kounnas, and G. Thinakaran. S-palmitoylation of -secretase subunits nicastrin and aph-1. *The Journal of Biological Chemistry*, 284(3):1373–1384, 1 2009. ISSN 0021-9258. doi:10.1074/jbc.M806380200. PMID: 19028695 PMCID: PMC2615504.

[29] J. Chung, G. Phukan, D. Vergote, A. Mohamed, M. Maulik, M. Stahn, R. J. Andrew, G. Thinakaran, E. Posse de Chaves, and S. Kar. Endosomal-lysosomal cholesterol sequestration by u18666a differentially regulates amyloid precursor protein (app) metabolism in normal and app-overexpressing cells. *Molecular and Cellular Biology*, 38(11):e00529–17, 6 2018. ISSN null. doi:10.1128/MCB.00529-17. Publisher: Taylor Francis.

[30] D. Ciric and H. Rezaei. Biochemical insight into the prion protein family. *Frontiers in cell and developmental biology*, 3:5, 2015.

[31] J. P. Cleary, D. M. Walsh, J. J. Hofmeister, G. M. Shankar, M. A. Kuskowski, D. J. Selkoe, and K. H. Ashe. Natural oligomers of the amyloid-beta protein specifically disrupt cognitive function. *Nature Neuroscience*, 8(1):79–84, 1 2005. ISSN 1097-6256. doi:10.1038/nn1372. PMID: 15608634.

[32] N. J. Cobb and W. K. Surewicz. Prion diseases and their biochemical mechanisms. *Biochemistry*, 48(12):2574–2585, 3 2009. ISSN 0006-2960. doi:10.1021/bi900108v. PMID: 19239250 PMCID: PMC2805067.

[33] S. L. Cole and R. Vassar. The alzheimer's disease -secretase enzyme, bace1. *Molecular Neurodegeneration*, 2:22, 11 2007. ISSN 1750-1326. doi:10.1186/1750-1326-2-22. PMID: 18005427 PMCID: PMC2211305.

[34] G. T. Corbett, Z. Wang, W. Hong, M. Colom-Cadena, J. Rose, M. Liao, A. Asfaw, T. C. Hall, L. Ding, A. DeSousa, M. P. Frosch, J. Collinge, D. A. Harris, M. S. Perkinton, T. L. Spires-Jones, T. L. Young-Pearse, A. Billinton, and D. M. Walsh. Prp

is a central player in toxicity mediated by soluble aggregates of neurodegeneration-causing proteins. *Acta Neuropathologica*, 139(3):503–526, 3 2020. ISSN 1432-0533. doi:10.1007/s00401-019-02114-9. PMID: 31853635 PMCID: PMC7035229.

[35] C. J. Cortes, K. Qin, E. M. Norstrom, W. N. Green, V. P. Bindokas, and J. A. Mastrianni. Early delivery of misfolded prp from er to lysosomes by autophagy. *International Journal of Cell Biology*, 2013:560421, 2013. ISSN 1687-8876. doi:10.1155/2013/560421. PMID: 24454378 PMCID: PMC3877647.

[36] W. M. Cowan, D. H. Harter, and E. R. Kandel. The emergence of modern neuroscience: some implications for neurology and psychiatry. *Annual review of neuroscience*, 23(1): 343–391, 2000.

[37] G. de La Tourette. Étude sur une affection nerveuse caractérisée par l'incoordination motrice accompagnée d'écholalie et de copralalie. *Arch Neurol*, 9:19–42, 1885.

[38] B. De Strooper, T. Iwatsubo, and M. S. Wolfe. Presenilins and γ-secretase: structure, function, and role in alzheimer disease. *Cold Spring Harbor perspectives in medicine*, 2(1):a006304, 2012.

[39] C. M. Dobson. Protein misfolding, evolution and disease. *Trends in Biochemical Sciences*, 24(9):329–332, 9 1999. ISSN 0968-0004. doi:10.1016/s0968-0004(99)01445-0. PMID: 10470028.

[40] F. Dohler, D. Sepulveda-Falla, S. Krasemann, H. Altmeppen, H. Schlüter, D. Hildebrand, I. Zerr, J. Matschke, and M. Glatzel. High molecular mass assemblies of amyloid-β oligomers bind prion protein in patients with alzheimer's disease. *Brain*, 137(3):873–886, 2014.

[41] V. D'Argenio and D. Sarnataro. Microbiome influence in the pathogenesis of prion and

alzheimer's diseases. *International Journal of Molecular Sciences*, 20(19):4704, 9 2019. ISSN 1422-0067. doi:10.3390/ijms20194704. PMID: 31547531 PMCID: PMC6801937.

[42] S. E. Encalada, L. Szpankowski, C.-h. Xia, and L. S. B. Goldstein. Stable kinesin and dynein assemblies drive the axonal transport of mammalian prion protein vesicles. *Cell*, 144(4):551–565, 2 2011. ISSN 0092-8674. doi:10.1016/j.cell.2011.01.021.

[43] C. Falker, A. Hartmann, I. Guett, F. Dohler, H. Altmeppen, C. Betzel, R. Schubert, D. Thurm, F. Wegwitz, P. Joshi, C. Verderio, S. Krasemann, and M. Glatzel. Exosomal cellular prion protein drives fibrillization of amyloid beta and counteracts amyloid beta-mediated neurotoxicity. *Journal of Neurochemistry*, 137(1):88–100, 4 2016. ISSN 1471-4159. doi:10.1111/jnc.13514. PMID: 26710111.

[44] R. Francis, G. McGrath, J. Zhang, D. A. Ruddy, M. Sym, J. Apfeld, M. Nicoll, M. Maxwell, B. Hai, M. C. Ellis, et al. aph-1 and pen-2 are required for notch pathway signaling, γ-secretase cleavage of βapp, and presenilin protein accumulation. *Developmental cell*, 3(1):85–97, 2002.

[45] D. B. Freir, A. J. Nicoll, I. Klyubin, S. Panico, J. M. Mc Donald, E. Risse, E. A. Asante, M. A. Farrow, R. B. Sessions, H. R. Saibil, A. R. Clarke, M. J. Rowan, D. M. Walsh, and J. Collinge. Interaction between prion protein and toxic amyloid assemblies can be therapeutically targeted at multiple sites. *Nature Communications*, 2(1):336, 6 2011. ISSN 2041-1723. doi:10.1038/ncomms1341. number: 1 publisher: Nature Publishing Group.

[46] C. Gajate and F. Mollinedo. Isolation of lipid rafts through discontinuous sucrose gradient centrifugation and fas/cd95 death receptor localization in raft fractions. *Methods in Molecular Biology (Clifton, N.J.)*, 1557:125–138, 2017. ISSN 1940-6029. doi:10.1007/978-1-4939-6780-3_13. PMID: 28078589.

[47] G. K. Gouras, K. Willén, and M. Faideau. The inside-out amyloid hypothesis and synapse pathology in alzheimer's disease. *Neurodegenerative Diseases*, 13(2-3):142–146, 2014.

[48] B. M. Greenberg and R. T. Johnson. Transmissible spongiform encephalopathies. In *Cerebrospinal Fluid in Clinical Practice*, pages 191–194. Elsevier Inc., 2009.

[49] H. H. Griffiths, I. J. Whitehouse, H. Baybutt, D. Brown, K. A. B. Kellett, C. D. Jackson, A. J. Turner, P. Piccardo, J. C. Manson, and N. M. Hooper. Prion protein interacts with bace1 protein and differentially regulates its activity toward wild type and swedish mutant amyloid precursor protein. *The Journal of Biological Chemistry*, 286(38):33489–33500, 9 2011. ISSN 1083-351X. doi:10.1074/jbc.M111.278556. PMID: 21795680 PMCID: PMC3190950.

[50] H. H. Griffiths, I. J. Whitehouse, and N. M. Hooper. Regulation of amyloid-production by the prion protein. *Prion*, 6(3):217–222, 7 2012. ISSN 1933-6896. doi:10.4161/pri.18988. PMID: 22449984 PMCID: PMC3399542.

[51] T. Gómez-Isla, R. Hollister, H. West, S. Mui, J. Growdon, R. Petersen, and B. Hyman. Neuronal loss correlates with but exceeds neurofibrillary tangles in alzheimer's disease. *Annals of Neurology: Official Journal of the American Neurological Association and the Child Neurology Society*, 41(1):17–24, 1997.

[52] C. Haass, A. Y. Hung, M. G. Schlossmacher, D. B. Teplow, and D. J. Selkoe. beta-amyloid peptide and a 3-kda fragment are derived by distinct cellular mechanisms. *Journal of Biological Chemistry*, 268(5):3021–3024, 1993.

[53] C. Haass, C. A. Lemere, A. Capell, M. Citron, P. Seubert, D. Schenk, L. Lannfelt, and D. J. Selkoe. The swedish mutation causes early-onset alzheimer's disease by beta-

secretase cleavage within the secretory pathway. *Nature Medicine*, 1(12):1291–1296, 12 1995. ISSN 1078-8956. doi:10.1038/nm1295-1291. PMID: 7489411.

[54] C. Haass, C. Kaether, G. Thinakaran, and S. Sisodia. Trafficking and proteolytic processing of app. *Cold Spring Harbor Perspectives in Medicine*, 2(5):a006270, 5 2012. ISSN 2157-1422. doi:10.1101/cshperspect.a006270. PMID: 22553493 PMCID: PMC3331683.

[55] H. Hampel, R. Vassar, B. De Strooper, J. Hardy, M. Willem, N. Singh, J. Zhou, R. Yan, E. Vanmechelen, A. De Vos, et al. The β-secretase bace1 in alzheimer's disease. *Biological psychiatry*, 89(8):745–756, 2021.

[56] J. A. Hardy and G. A. Higgins. Alzheimer's disease: the amyloid cascade hypothesis. *Science (New York, N.Y.)*, 256(5054):184–185, 4 1992. ISSN 0036-8075. doi:10.1126/science.1566067. PMID: 1566067.

[57] D. A. Harris. Trafficking, turnover and membrane topology of prp: Protein function in prion disease. *British Medical Bulletin*, 66(1):71–85, 6 2003. ISSN 0007-1420. doi:10.1093/bmb/66.1.71.

[58] D. A. Harris, M. T. Huber, P. van Dijken, S. L. Shyng, B. T. Chait, and R. Wang. Processing of a cellular prion protein: identification of n- and c-terminal cleavage sites. *Biochemistry*, 32(4):1009–1016, 2 1993. ISSN 0006-2960. doi:10.1021/bi00055a003. PMID: 8093841.

[59] A. Hartmann, C. Muth, O. Dabrowski, S. Krasemann, and M. Glatzel. Exosomes and the prion protein: More than one truth. *Frontiers in Neuroscience*, 11, 2017. ISSN 1662-453X. URL `https://www.frontiersin.org/articles/10.3389/fnins.2017.00194`. [Online; accessed 2024-01-21].

[60] J. Hernandez-Rapp, S. Martin-Lannerée, T. Hirsch, J.-M. Launay, and S. Mouillet-Richard. Hijacking prpc-dependent signal transduction: when prions impair a clearance. *Frontiers in Aging Neuroscience*, 6, 2014. ISSN 1663-4365. URL `https://www.frontiersin.org/articles/10.3389/fnagi.2014.00025`. [Online; accessed 2024-03-04].

[61] D. J. Hoffman, R. M. Reynolds, and D. B. Hardy. Developmental origins of health and disease: current knowledge and potential mechanisms. *Nutrition reviews*, 75(12): 951–970, 2017.

[62] D. M. Holtzman. Alzheimer's disease: Moving towards a vaccine. *Nature*, 454(7203): 418–420, 7 2008. ISSN 1476-4687. doi:10.1038/454418a. PMID: 18650906.

[63] J.-Y. Hur. γ-secretase in alzheimer's disease. *Experimental & molecular medicine*, 54 (4):433–446, 2022.

[64] I. Hussain, D. Powell, D. R. Howlett, D. G. Tew, T. D. Meek, C. Chapman, I. S. Gloger, K. E. Murphy, C. D. Southan, D. M. Ryan, et al. Identification of a novel aspartic protease (asp 2) as β-secretase. *Molecular and Cellular Neuroscience*, 14(6): 419–427, 1999.

[65] B. T. Hyman, K. Marzloff, and P. V. Arriagada. The lack of accumulation of senile plaques or amyloid burden in alzheimer's disease suggests a dynamic balance between amyloid deposition and resolution. *Journal of Neuropathology and Experimental Neurology*, 52(6):594–600, 11 1993. ISSN 0022-3069. doi:10.1097/00005072-199311000-00006. PMID: 8229078.

[66] M. Imran and S. Mahmood. An overview of human prion diseases. *Virology journal*, 8:1–9, 2011.

[67] M. Ingelsson, H. Fukumoto, K. L. Newell, J. H. Growdon, E. T. Hedley-Whyte, M. P. Frosch, M. S. Albert, B. T. Hyman, and M. C. Irizarry. Early abeta accumulation and progressive synaptic loss, gliosis, and tangle formation in ad brain. *Neurology*, 62(6): 925–931, 3 2004. ISSN 1526-632X. doi:10.1212/01.wnl.0000115115.98960.37. PMID: 15037694.

[68] J. Ironside and M. Head. Neuropathology and molecular biology of variant creutzfeldt-jakob disease. *Mad Cow Disease and Related Spongiform Encephalopathies*, pages 133–159, 2004.

[69] G. R. Jackson, I. Salecker, X. Dong, X. Yao, N. Arnheim, P. W. Faber, M. E. MacDonald, and S. L. Zipursky. Polyglutamine-expanded human huntingtin transgenes induce degeneration of drosophila photoreceptor neurons. *Neuron*, 21(3):633–642, 1998.

[70] B. S. A. E. W. J. C. J. Jackson GS, Linehan J. Overexpression of mouse prion protein in transgenic mice causes a non-transmissible spongiform encephalopathy. *Journal of Neuroscience*, 45(3):345–356, 2023. URL `https://www.ncbi.nlm.nih.gov/pmc/articles/PMC9562354/`.

[71] H. H. Jarosz-Griffiths, N. J. Corbett, H. A. Rowland, K. Fisher, A. C. Jones, J. Baron, G. J. Howell, S. A. Cowley, S. Chintawar, M. Z. Cader, et al. Proteolytic shedding of the prion protein via activation of metallopeptidase adam10 reduces cellular binding and toxicity of amyloid-β oligomers. *Journal of Biological Chemistry*, 294(17):7085–7097, 2019.

[72] Y. W. Kan and A. M. Dozy. Polymorphism of dna sequence adjacent to human beta-globin structural gene: relationship to sickle mutation. *Proceedings of the National Academy of Sciences*, 75(11):5631–5635, 1978.

[73] Y. W. Kan, K. Y. Lee, M. Furbetta, A. Angius, and A. Cao. Polymorphism of dna se-

quence in the β-globin gene region: application to prenatal diagnosis of β0 thalassemia in sardinia. *New England Journal of Medicine*, 302(4):185–188, 1980.

[74] W. Kim, H. Watanabe, S. Lomoio, and G. Tesco. Spatiotemporal processing of neural cell adhesion molecules 1 and 2 by bace1 in vivo. *Journal of Biological Chemistry*, 296, 2021.

[75] S. Kins, N. Lauther, A. Szodorai, and K. Beyreuther. Subcellular trafficking of the amyloid precursor protein gene family and its pathogenic role in alzheimer's disease. *Neuro-Degenerative Diseases*, 3(4-5):218–226, 2006. ISSN 1660-2854. doi:10.1159/000095259. PMID: 17047360.

[76] E. H. Koo and S. L. Squazzo. Evidence that production and release of amyloid beta-protein involves the endocytic pathway. *Journal of Biological Chemistry*, 269(26): 17386–17389, 1994.

[77] P.-H. Kuhn, K. Koroniak, S. Hogl, A. Colombo, U. Zeitschel, M. Willem, C. Volbracht, U. Schepers, A. Imhof, A. Hoffmeister, C. Haass, S. Roßner, S. Bräse, and S. F. Lichtenthaler. Secretome protein enrichment identifies physiological bace1 protease substrates in neurons. *The EMBO journal*, 31(14):3157–3168, 6 2012. ISSN 1460-2075. doi:10.1038/emboj.2012.173. PMID: 22728825 PMCID: PMC3400020.

[78] P. N. Lacor, M. C. Buniel, P. W. Furlow, A. S. Clemente, P. T. Velasco, M. Wood, K. L. Viola, and W. L. Klein. Abeta oligomer-induced aberrations in synapse composition, shape, and density provide a molecular basis for loss of connectivity in alzheimer's disease. *The Journal of Neuroscience: The Official Journal of the Society for Neuroscience*, 27(4):796–807, 1 2007. ISSN 1529-2401. doi:10.1523/JNEUROSCI.3501-06.2007. PMID: 17251419 PMCID: PMC6672917.

[79] F. M. LaFerla, K. N. Green, and S. Oddo. Intracellular amyloid- in alzheimer's

disease. *Nature Reviews Neuroscience*, 8(7):499–509, 7 2007. ISSN 1471-0048. doi:10.1038/nrn2168. number: 7 publisher: Nature Publishing Group.

[80] J. Laurén, D. Gimbel, H. Nygaard, J. Gilbert, and S. Strittmatter. Cellular prion protein mediates impairment of synaptic plasticity by amyloid- oligomers. *Nature*, 457 (7233):1128–1132, 2009.

[81] J. Y. Leem, C. A. Saura, C. Pietrzik, J. Christianson, C. Wanamaker, L. T. King, M. L. Veselits, T. Tomita, L. Gasparini, T. Iwatsubo, et al. A role for presenilin 1 in regulating the delivery of amyloid precursor protein to the cell surface. *Neurobiology of disease*, 11(1):64–82, 2002.

[82] S. Lesné, M. T. Koh, L. Kotilinek, R. Kayed, C. G. Glabe, A. Yang, M. Gallagher, and K. H. Ashe. A specific amyloid- protein assembly in the brain impairs memory. *Nature*, 440(7082):352–357, 3 2006. ISSN 1476-4687. doi:10.1038/nature04533. number: 7082 publisher: Nature Publishing Group.

[83] D. Levitan, J. Lee, L. Song, R. Manning, G. Wong, E. Parker, and L. Zhang. Ps1 n- and c-terminal fragments form a complex that functions in app processing and notch signaling. *Proceedings of the National Academy of Sciences*, 98(21):12186–12190, 2001.

[84] Y.-C. Liao, R. V. Lebo, G. A. Clawson, and E. A. Smuckler. Human prion protein cdna: molecular cloning, chromosomal mapping, and biological implications. *Science*, 233(4761):364–367, 1986.

[85] P. P. Lie and R. A. Nixon. Lysosome trafficking and signaling in health and neurodegenerative diseases. *Neurobiology of disease*, 122:94–105, 2019.

[86] D. Lindholm, H. Wootz, and L. Korhonen. Er stress and neurodegenerative diseases. *Cell Death & Differentiation*, 13(3):385–392, 2006.

[87] K. J. Livak and T. D. Schmittgen. Analysis of relative gene expression data using real-time quantitative pcr and the 2- $\delta\delta$ct method. *methods*, 25(4):402–408, 2001.

[88] A. C. Lo, C. Haass, S. L. Wagner, D. B. Teplow, and S. S. Sisodia. Metabolism of the "swedish" amyloid precursor protein variant in madin-darby canine kidney cells. *The Journal of Biological Chemistry*, 269(49):30966–30973, 12 1994. ISSN 0021-9258. PMID: 7983032.

[89] F. López-Muñoz, J. Boya, and C. Alamo. Neuron theory, the cornerstone of neuroscience, on the centenary of the nobel prize award to santiago ramón y cajal. *Brain research bulletin*, 70(4-6):391–405, 2006.

[90] A. L. Mammen, R. L. Huganir, and R. J. O'Brien. Redistribution and stabilization of cell surface glutamate receptors during synapse formation. *Journal of Neuroscience*, 17(19):7351–7358, 10 1997. ISSN 0270-6474, 1529-2401. doi:10.1523/JNEUROSCI.17-19-07351.1997. publisher: Society for Neuroscience section: Articles PMID: 9295381.

[91] L. Mangiarini, K. Sathasivam, M. Seller, B. Cozens, A. Harper, C. Hetherington, M. Lawton, Y. Trottier, H. Lehrach, S. W. Davies, et al. Exon 1 of the hd gene with an expanded cag repeat is sufficient to cause a progressive neurological phenotype in transgenic mice. *Cell*, 87(3):493–506, 1996.

[92] J. B. Martin. The integration of neurology, psychiatry, and neuroscience in the 21st century. *American Journal of Psychiatry*, 159(5):695–704, 2002.

[93] A. Matamoros-Angles, A. Hervera, J. Soriano, E. Martí, P. Carulla, F. Llorens, M. Nuvolone, A. Aguzzi, I. Ferrer, A. Gruart, J. M. Delgado-García, and J. A. Del Río. Analysis of co-isogenic prion protein deficient mice reveals behavioral deficits, learning impairment, and enhanced hippocampal excitability. *BMC biology*, 20(1):17, 1

2022. ISSN 1741-7007. doi:10.1186/s12915-021-01203-0. PMID: 35027047 PMCID: PMC8759182.

[94] P. C. McHugh, J. A. Wright, R. J. Williams, and D. R. Brown. Prion protein expression alters app cleavage without interaction with bace-1. *Neurochemistry international*, 61 (5):672–680, 2012.

[95] R. Meyer, M. KA, B. M. Barry, R.A., and P. SB. Separation and properties of cellular and scrapie prion proteins. *Proc. Natl. Acad. Sci. USA*, 83:2310–2314, 1986.

[96] H. Miranzadeh Mahabadi and C. Taghibiglou. Cellular prion protein (prpc): Putative interacting partners and consequences of the interaction. *International Journal of Molecular Sciences*, 21(19):7058, 9 2020. ISSN 1422-0067. doi:10.3390/ijms21197058. PMID: 32992764 PMCID: PMC7583789.

[97] R. Mishra, M. Elgland, A. Begum, T. Fyrner, P. Konradsson, S. Nyström, and P. Hammarström. Impact of n-glycosylation site variants during human prp aggregation and fibril nucleation. *Biochimica et Biophysica Acta (BBA)-Proteins and Proteomics*, 1867 (10):909–921, 2019.

[98] A. P. Monaco, R. L. Neve, C. Colletti-Feener, C. J. Bertelson, D. M. Kurnit, and L. M. Kunkel. Isolation of candidate cdnas for portions of the duchenne muscular dystrophy gene. *Nature*, 323(6089):646–650, 1986.

[99] E. Monsellier, M. Ramazzotti, N. Taddei, and F. Chiti. Aggregation propensity of the human proteome. *PLOS Computational Biology*, 4(10):e1000199, 10 2008. ISSN 1553-7358. doi:10.1371/journal.pcbi.1000199. publisher: Public Library of Science.

[100] R. Morales, K. M. Green, and C. Soto. Cross currents in protein misfolding disorders: interactions and therapy. *CNS neurological disorders drug targets*, 8(5):363–371, 11

2009. ISSN 1996-3181. doi:10.2174/187152709789541998. PMID: 19702573 PMCID: PMC2804467.

[101] M. P. Murphy and H. LeVine. Alzheimer's disease and the -amyloid peptide. *Journal of Alzheimer's disease : JAD*, 19(1):311, 1 2010. ISSN 1387-2877. doi:10.3233/JAD-2010-1221. PMID: 20061647 PMCID: PMC2813509.

[102] E. D. Niederst, S. M. Reyna, and L. S. Goldstein. Axonal amyloid precursor protein and its fragments undergo somatodendritic endocytosis and processing. *Molecular biology of the cell*, 26(2):205–217, 2015.

[103] M. Nuvolone, M. Hermann, S. Sorce, G. Russo, C. Tiberi, P. Schwarz, E. Minikel, D. Sanoudou, P. Pelczar, and A. Aguzzi. Strictly co-isogenic c57bl/6j-prnp-/- mice: A rigorous resource for prion science. *Journal of Experimental Medicine*, 213(3):313–327, 2016.

[104] S. Oddo, A. Caccamo, J. D. Shepherd, M. P. Murphy, T. E. Golde, R. Kayed, R. Metherate, M. P. Mattson, Y. Akbari, and F. M. LaFerla. Triple-transgenic model of alzheimer's disease with plaques and tangles: intracellular abeta and synaptic dysfunction. *Neuron*, 39(3):409–421, 7 2003. ISSN 0896-6273. doi:10.1016/s0896-6273(03)00434-3. PMID: 12895417.

[105] L. Ordóñez-Gutiérrez, J. M. Torres, R. Gavín, M. Antón, A. I. Arroba-Espinosa, J.-C. Espinosa, C. Vergara, J. A. Del Río, and F. Wandosell. Cellular prion protein modulates β-amyloid deposition in aged app/ps1 transgenic mice. *Neurobiology of aging*, 34(12):2793–2804, 2013.

[106] E. Pannese. The golgi stain: invention, diffusion and impact on neurosciences. *Journal of the History of the Neurosciences*, 8(2):132–140, 1999.

[107] E. T. Parkin, N. T. Watt, A. J. Turner, and N. M. Hooper. Dual mechanisms for shedding of the cellular prion protein*. *Journal of Biological Chemistry*, 279(12): 11170–11178, 3 2004. ISSN 0021-9258. doi:10.1074/jbc.M312105200.

[108] E. T. Parkin, N. T. Watt, I. Hussain, E. A. Eckman, C. B. Eckman, J. C. Manson, H. N. Baybutt, A. J. Turner, and N. M. Hooper. Cellular prion protein regulates -secretase cleavage of the alzheimer's amyloid precursor protein. *Proceedings of the National Academy of Sciences*, 104(26):11062–11067, 6 2007. doi:10.1073/pnas.0609621104. publisher: Proceedings of the National Academy of Sciences.

[109] J. Parkinson. An essay on the shaking palsy. *The Journal of neuropsychiatry and clinical neurosciences*, 14(2):223–236, 2002.

[110] P. C. Pauly and D. A. Harris. Copper stimulates endocytosis of the prion protein. *The Journal of Biological Chemistry*, 273(50):33107–33110, 12 1998. ISSN 0021-9258. doi:10.1074/jbc.273.50.33107. PMID: 9837873.

[111] A. Pelchen-Matthews, G. Raposo, and M. Marsh. Endosomes, exosomes and trojan viruses. *Trends in Microbiology*, 12(7):310–316, 7 2004. ISSN 0966-842X. doi:10.1016/j.tim.2004.05.004. PMID: 15223058.

[112] A. Pensalfini, R. Albay III, S. Rasool, J. W. Wu, A. Hatami, H. Arai, L. Margol, S. Milton, W. W. Poon, M. M. Corrada, et al. Intracellular amyloid and the neuronal origin of alzheimer neuritic plaques. *Neurobiology of disease*, 71:53–61, 2014.

[113] S. Prusiner. The priori diseases. *Brain pathology*, 8(3):499–513, 1998.

[114] S. B. Prusiner. Novel proteinaceous infectious particles cause scrapie. *Science (New York, N.Y.)*, 216(4542):136–144, 4 1982. ISSN 0036-8075. doi:10.1126/science.6801762. PMID: 6801762.

[115] S. B. Prusiner and S. J. DeArmond. Molecular biology and pathology of scrapie and the prion diseases of humans. *Brain Pathology (Zurich, Switzerland)*, 1(4):297–310, 7 1991. ISSN 1015-6305. doi:10.1111/j.1750-3639.1991.tb00673.x. PMID: 1669719.

[116] S. Przedborski, M. Vila, V. Jackson-Lewis, et al. Series introduction: Neurodegeneration: What is it and where are we? *The Journal of clinical investigation*, 111(1):3–10, 2003.

[117] S. A. Purro, A. J. Nicoll, and J. Collinge. Prion protein as a toxic acceptor of amyloid- oligomers. *Biological Psychiatry*, 83(4):358–368, 2 2018. ISSN 1873-2402. doi:10.1016/j.biopsych.2017.11.020. PMID: 29331212.

[118] K. Qin, L. Zhao, C. Gregory, A. Solanki, and J. Mastrianni. Dual disease" tgad/gss mice exhibit enhanced alzheimer's disease pathology and reveal prp c-dependent secretion of a. *Scientific reports*, 9(1):1–18, 2019.

[119] V. K. Ramanan and A. J. Saykin. Pathways to neurodegeneration: mechanistic insights from gwas in alzheimer's disease, parkinson's disease, and related disorders. *American journal of neurodegenerative disease*, 2(3):145, 2013.

[120] U. K. Resenberger, A. Harmeier, A. C. Woerner, J. L. Goodman, V. Müller, R. Krishnan, R. M. Vabulas, H. A. Kretzschmar, S. Lindquist, F. U. Hartl, G. Multhaup, K. F. Winklhofer, and J. Tatzelt. The cellular prion protein mediates neurotoxic signalling of -sheet-rich conformers independent of prion replication. *The EMBO Journal*, 30(10): 2057–2070, 5 2011. ISSN 0261-4189. doi:10.1038/emboj.2011.86. number-of-pages: 2070 publisher: John Wiley Sons, Ltd.

[121] C. Ryou, G. Legname, D. Peretz, J. C. Craig, M. A. Baldwin, and S. B. Prusiner. Differential inhibition of prion propagation by enantiomers of quinacrine. *Laboratory Investigation*, 83(6):837–843, 6 2003. ISSN 1530-0307.

doi:10.1097/01.LAB.0000074919.08232.A2. number: 6 publisher: Nature Publishing Group.

[122] S. V. Salazar and S. M. Strittmatter. Cellular prion protein as a receptor for amyloid-oligomers in alzheimer's disease. *Biochemical and Biophysical Research Communications*, 483(4):1143–1147, 2 2017. ISSN 1090-2104. doi:10.1016/j.bbrc.2016.09.062. PMID: 27639648 PMCID: PMC5303667.

[123] M. R. Sawaya, S. Sambashivan, R. Nelson, M. I. Ivanova, S. A. Sievers, M. I. Apostol, M. J. Thompson, M. Balbirnie, J. J. W. Wiltzius, H. T. McFarlane, A. Madsen, C. Riekel, and D. Eisenberg. Atomic structures of amyloid cross-beta spines reveal varied steric zippers. *Nature*, 447(7143):453–457, 5 2007. ISSN 1476-4687. doi:10.1038/nature05695. PMID: 17468747.

[124] C. Scheckel and A. Aguzzi. Prions, prionoids and protein misfolding disorders. *Nature Reviews. Genetics*, 19(7):405–418, 7 2018. ISSN 1471-0064. doi:10.1038/s41576-018-0011-4. PMID: 29713012.

[125] C. Scialò, L. Celauro, M. Zattoni, T. H. Tran, E. Bistaffa, F. Moda, R. Kammerer, E. Buratti, and G. Legname. The cellular prion protein increases the uptake and toxicity of tdp-43 fibrils. *Viruses*, 13(8):1625, 8 2021. ISSN 1999-4915. doi:10.3390/v13081625. number: 8 publisher: Multidisciplinary Digital Publishing Institute.

[126] D. J. Selkoe and J. Hardy. The amyloid hypothesis of alzheimer's disease at 25 years. *EMBO molecular medicine*, 8(6):595–608, 6 2016. ISSN 1757-4684. doi:10.15252/emmm.201606210. PMID: 27025652 PMCID: PMC4888851.

[127] A. Serrano-Pozo, M. P. Frosch, E. Masliah, and B. T. Hyman. Neuropathological alterations in alzheimer disease. *Cold Spring Harbor Perspectives in Medicine*, 1(1):

a006189, 9 2011. ISSN 2157-1422. doi:10.1101/cshperspect.a006189. PMID: 22229116 PMCID: PMC3234452.

[128] G. M. Shepherd. *Foundations of the neuron doctrine*. Oxford University Press, 2015.

[129] G. M. Shepherd, C. A. Greer, P. Mazzarello, and M. Sassoè-Pognetto. The first images of nerve cells: Golgi on the olfactory bulb 1875. *Brain research reviews*, 66(1-2):92–105, 2011.

[130] S. L. Shyng, M. T. Huber, and D. A. Harris. A prion protein cycles between the cell surface and an endocytic compartment in cultured neuroblastoma cells. *The Journal of Biological Chemistry*, 268(21):15922–15928, 7 1993. ISSN 0021-9258. PMID: 8101844.

[131] D. Simpson. Phrenology and the neurosciences: contributions of fj gall and jg spurzheim. *ANZ journal of surgery*, 75(6):475–482, 2005.

[132] A. Singh, Q. Kong, X. Luo, R. B. Petersen, H. Meyerson, and N. Singh. Prion protein (prp) knock-out mice show altered iron metabolism: a functional role for prp in iron uptake and transport. *PLoS One*, 4(7):e6115, 2009.

[133] S. Sinha, J. P. Anderson, R. Barbour, G. S. Basi, R. Caccavello, D. Davis, M. Doan, H. F. Dovey, N. Frigon, J. Hong, et al. Purification and cloning of amyloid precursor protein β-secretase from human brain. *Nature*, 402(6761):537–540, 1999.

[134] L. M. Smith and S. M. Strittmatter. Binding sites for amyloid- oligomers and synaptic toxicity. *Cold Spring Harbor Perspectives in Medicine*, 7(5):a024075, 5 2017. ISSN 2157-1422. doi:10.1101/cshperspect.a024075. PMID: 27940601 PMCID: PMC5411685.

[135] G. Sofianidis, V. Psychas, C. Billinis, V. Spyrou, S. Argyroudis, N. Papaioannou, and I. Vlemmas. Histopathological and immunohistochemical features of natural goat scrapie. *Journal of comparative pathology*, 135(2-3):116–129, 2006.

[136] S. Sonnino, M. Aureli, S. Grassi, L. Mauri, S. Prioni, and A. Prinetti. Lipid rafts in neurodegeneration and neuroprotection. *Molecular neurobiology*, 50:130–148, 2014.

[137] A. A. Steele AD, Lindquist S. The prion protein knockout mouse: a phenotype under challenge. *Prion*, 1(2):83–93, 2007.

[138] H. Steiner, E. Winkler, D. Edbauer, S. Prokop, G. Basset, A. Yamasaki, M. Kostka, and C. Haass. Pen-2 is an integral component of the γ-secretase complex required for coordinated expression of presenilin and nicastrin. *Journal of Biological Chemistry*, 277(42):39062–39065, 2002.

[139] K. Suzuki. The developing world of dohad. *Journal of developmental origins of health and disease*, 9(3):266–269, 2018.

[140] D. R. Taylor, N. T. Watt, W. S. S. Perera, and N. M. Hooper. Assigning functions to distinct regions of the n-terminus of the prion protein that are involved in its copper-stimulated, clathrin-dependent endocytosis. *Journal of Cell Science*, 118(Pt 21):5141–5153, 11 2005. ISSN 0021-9533. doi:10.1242/jcs.02627. PMID: 16254249.

[141] G. Thinakaran and E. H. Koo. Amyloid precursor protein trafficking, processing, and function. *The Journal of Biological Chemistry*, 283(44):29615–29619, 10 2008. ISSN 0021-9258. doi:10.1074/jbc.R800019200. PMID: 18650430 PMCID: PMC2573065.

[142] G. Thinakaran and S. S. Sisodia. Amyloid precursor-like protein 2 (aplp2) is modified by the addition of chondroitin sulfate glycosaminoglycan at a single site. *The Journal of Biological Chemistry*, 269(35):22099–22104, 9 1994. ISSN 0021-9258. PMID: 8071334.

[143] G. Thinakaran, C. A. Kitt, A. J. Roskams, H. H. Slunt, E. Masliah, v. C. Koch, S. D. Ginsberg, G. V. Ronnett, R. R. Reed, and D. L. Price. Distribution of an app homolog, aplp2, in the mouse olfactory system: a potential role for aplp2 in

axogenesis. *Journal of Neuroscience*, 15(10):6314–6326, 10 1995. ISSN 0270-6474, 1529-2401. doi:10.1523/JNEUROSCI.15-10-06314.1995. publisher: Society for Neuroscience section: Articles PMID: 7472397.

[144] G. Thinakaran, D. B. Teplow, R. Siman, B. Greenberg, and S. S. Sisodia. Metabolism of the "swedish" amyloid precursor protein variant in neuro2a (n2a) cells: Evidence that cleavage at the "-secretase" site occurs in the golgi apparatus (). *Journal of Biological Chemistry*, 271(16):9390–9397, 4 1996. ISSN 0021-9258, 1083-351X. doi:10.1074/jbc.271.16.9390. publisher: Elsevier PMID: 8621605.

[145] G. Thinakaran, J. B. Regard, C. M. Bouton, C. L. Harris, D. L. Price, D. R. Borchelt, and S. S. Sisodia. Stable association of presenilin derivatives and absence of presenilin interactions with app. *Neurobiology of Disease*, 4(6):438–453, 4 1998. ISSN 0969-9961. doi:10.1006/nbdi.1998.0171. PMID: 9666482.

[146] R. F. Thompson. The neurobiology of learning and memory. *Science*, 233(4767): 941–947, 1986.

[147] L. Urrea, I. Ferrer, R. Gavín, and J. A. Del Río. The cellular prion protein (prpc) as neuronal receptor for α-synuclein. *Prion*, 11(4):226–233, 2017.

[148] N. Vassallo and J. Herms. Cellular prion protein function in copper homeostasis and redox signalling at the synapse. *Journal of Neurochemistry*, 86(3):538–544, 8 2003. ISSN 0022-3042. doi:10.1046/j.1471-4159.2003.01882.x. PMID: 12859667.

[149] R. Vassar, B. D. Bennett, S. Babu-Khan, S. Kahn, E. A. Mendiaz, P. Denis, D. B. Teplow, S. Ross, P. Amarante, R. Loeloff, et al. β-secretase cleavage of alzheimer's amyloid precursor protein by the transmembrane aspartic protease bace. *science*, 286 (5440):735–741, 1999.

[150] K. S. Vetrivel, Y.-w. Zhang, H. Xu, and G. Thinakaran. Pathological and physiological functions of presenilins. *Molecular neurodegeneration*, 1:1–12, 2006.

[151] K. S. Vetrivel, X. Zhang, X. Meckler, H. Cheng, S. Lee, P. Gong, K. O. Lopes, Y. Chen, N. Iwata, K.-J. Yin, J.-M. Lee, A. T. Parent, T. C. Saido, Y.-M. Li, S. S. Sisodia, and G. Thinakaran. Evidence that cd147 modulation of -amyloid (a) levels is mediated by extracellular degradation of secreted a. *The Journal of Biological Chemistry*, 283(28): 19489–19498, 7 2008. ISSN 0021-9258. doi:10.1074/jbc.M801037200. PMID: 18456655 PMCID: PMC2443668.

[152] G. S. Victoria and C. Zurzolo. Trafficking and degradation pathways in pathogenic conversion of prions and prion-like proteins in neurodegenerative diseases. *Virus Research*, 207:146–154, 9 2015. ISSN 1872-7492. doi:10.1016/j.virusres.2015.01.019. PMID: 25645281.

[153] C. A. von Arnim, R. Spoelgen, I. D. Peltan, M. Deng, S. Courchesne, M. Koker, T. Matsui, H. Kowa, S. F. Lichtenthaler, M. C. Irizarry, et al. Gga1 acts as a spatial switch altering amyloid precursor protein trafficking and processing. *Journal of Neuroscience*, 26(39):9913–9922, 2006.

[154] K. P. Walsh, L. S. Minamide, S. J. Kane, A. E. Shaw, D. R. Brown, B. Pulford, M. D. Zabel, J. D. Lambeth, T. B. Kuhn, and J. R. Bamburg. Amyloid- and proinflammatory cytokines utilize a prion protein-dependent pathway to activate nadph oxidase and induce cofilin-actin rods in hippocampal neurons. *PLOS ONE*, 9(4):e95995, 4 2014. ISSN 1932-6203. doi:10.1371/journal.pone.0095995. publisher: Public Library of Science.

[155] H. Wang, R. Li, and Y. Shen. β-secretase: its biology as a therapeutic target in diseases. *Trends in pharmacological sciences*, 34(4):215–225, 2013.

[156] C. Weissmann and E. Flechsig. Prp knock-out and prp transgenic mice in prion research. *British medical bulletin*, 66(1):43–60, 2003.

[157] D. Westaway and J. H. Jhamandas. The p's and q's of cellular prp-a interactions. *Prion*, 6(4):359–363, 9 2012. ISSN 1933-6896. doi:10.4161/pri.20675. PMID: 22874673 PMCID: PMC3609064.

[158] B. R. Whatley, L. Li, and L.-S. Chin. The ubiquitin–proteasome system in spongiform degenerative disorders. *Biochimica et Biophysica Acta (BBA)-Molecular Basis of Disease*, 1782(12):700–712, 2008.

[159] R. G. Will, J. Ironside, M. Zeidler, K. Estibeiro, S. Cousens, P. Smith, A. Alperovitch, S. Poser, M. Pocchiari, and A. Hofman. A new variant of creutzfeldt-jakob disease in the uk. *The Lancet*, 347(9006):921–925, 1996.

[160] D. M. Wilson, M. R. Cookson, L. Van Den Bosch, H. Zetterberg, D. M. Holtzman, and I. Dewachter. Hallmarks of neurodegenerative diseases. *Cell*, 186(4):693–714, 2023.

[161] M. S. Wolfe, W. Xia, B. L. Ostaszewski, T. S. Diehl, W. T. Kimberly, and D. J. Selkoe. Two transmembrane aspartates in presenilin-1 required for presenilin endoproteolysis and γ-secretase activity. *Nature*, 398(6727):513–517, 1999.

[162] N. D. Younan, C. J. Sarell, P. Davies, D. R. Brown, and J. H. Viles. The cellular prion protein traps alzheimer's a in an oligomeric form and disassembles amyloid fibers. *The FASEB Journal*, 27(5), 2013. doi:10.1096/fj.12-222588. URL `https://doi.org/10.1096/fj.12-222588`. [Online; accessed 2024-03-04].

[163] G. Yu, M. Nishimura, S. Arawaka, D. Levitan, L. Zhang, A. Tandon, Y.-Q. Song, E. Rogaeva, F. Chen, T. Kawarai, et al. Nicastrin modulates presenilin-mediated notch/glp-1 signal transduction and βapp processing. *Nature*, 407(6800):48–54, 2000.

[164] X. Zhang, Y. Li, H. Xu, and Y.-w. Zhang. The γ-secretase complex: from structure to function. *Frontiers in cellular neuroscience*, 8:427, 2014.

[165] Y. Zhang, Y. Zhao, L. Zhang, W. Yu, Y. Wang, and W. Chang. Cellular prion protein as a receptor of toxic amyloid-42 oligomers is important for alzheimer's disease. *Frontiers in Cellular Neuroscience*, 13, 2019. ISSN 1662-5102. URL `https://www.frontiersin.org/articles/10.3389/fncel.2019.00339`. [Online; accessed 2024-01-21].